THEORETICAL CONSIDERATIONS OF DRAWING A ROJND TUBE THROUGH A CCNICAL DIE AND A POLYGONAL PLUG

By

STEPHEN PHARES ^NG'ANG'A

B.Sc. Mechanical Engineering

A thesis submitted in partial fulfilment for the award of the degree of Master of Science in Engineering in the University of Nairobi

Mechanical Engineering Department

1988

This thesis is my original work and has not been presented for a degree in any other University.

Stephen Phares Ng'ang

This thesis has been submitted for examination with my approval as University Supervisor

Dr. S.M. Maranga

CONTENTS

APPENDICES

ACKNOWLEDGEMENTS

I express my appreciation to my supervisor Dr. S.M. Maranga who has given me valuable guidance, advice and encouragement in the preparation of the thesis. Prof J.K Musuva deserves special thanks for the encouragement he has given me during the preparation of the thesis.

I thank the staff of the mechanical engineering workshops and particularly the chief technician Mr. Paul Ndegwa for the assistance he has given during the final stages of the project.

I wish to thank the DAAD Secretariat for the financial assistance they gave throughout the research period.

Finally, special thanks go to Ms F. Kollikho for typing the manuscript to very high standards.

ABSTRACT

Theoretical and practical investigations in the drawing of the following sections directly from an entirely round stock have been reported: polygonal bars, polygonal tubes with the outside and bore surfaces geometrically similar, and tubes with the outside polygonal surface and circular bore. The derived theoretical solutions enabled the industrialists to design tools to manufacture tubing or bar stocks directly from round with minimum amount of energy being dissipated in the drawing process; the resulting optimal tools also produced relatively superior polygonal stocks. This thesis extends the theoretical analysis to the manufacture of a polygonal tube by drawing an entirely round stock through a deformation passage formed by a conical die and a polygonal plug.

Using a prescribed shape of the plug and a regular conical die, two solutions of the drawing loads were derived: the lower bound and the upper bound. The lower bound load considered the homogeneous deformation and the friction work and thus ignored the redundant work. The upper bound value of the drawing force was derived from the minimum energy associated with the velocity pattern obtained by conformal napping. Unlike the axisynmetric drawing on a mandrel, the

plug profile was corrplex; an equivalent plug semi-angle was therefore used to enable comparisons to be made between deformation passages formed by a known die profile and the polygonal plugs and also to facilitate the optimization of the process parameters.

The graphs of the drawing forces drawn against the various parameterrs such as the die angle, the equivalent plug angle, the reduction of area as well as friction snowed trends similar to those tried practically and reported in the literature of polygonal tube drawing directly from round stock.

NOTATION

	Diameter of the inlet circular section
$D_{0a}(=2R_a)$	Diameter of the outlet circular section
H_a	Diagonal length of the drawing plug equal to the diameter circumscribing the polygon
L	Die length measured along the draw axis
N_s	Nurrber of sides of the drawn polygonal tube
t.	Inlet tube wall thickness
$d\hat{}(=2r_b)$	Plug diameter equal to the bore of input stock
Ak .	Cross-sectional area at entry
A_a	Cross-sectional area at exit
A_f	Ratio of cross-sectional area at entry to that at the exit
red, 'r'	Reduction of area
t_a	Minimum tube wall thickness along the diagonal of the drawn tube
K	Factor (0«<i) expressing the tube wall thickness at the diagonals in terms of D_a i.e. t_a = <D_a
d_e	Diameter of an equivalent circular section of the plug at the exit
a	Die semi-angle of the conical surface
ct	The equivalent plug semi-angle; it is the semi-angle of a conical plug corresponding to the polygonal tube drawing plug through a conical die for the same

	reduction of area and the same die length
$^{a}{}_{c}$	Plug semi-angle of the conical surface of a polygonal section drawing plug
a_s	Plug semi-angle of the flat surface of a polygaial section drawing plug
X_c	Angle subtended by the conical surface of a symmetric section of the plug at the draw axis
A_3	Angle subtended by the flat surface of a symnetric section of the plug at the draw axis
3	Included angle of a syrrmetric section of the plug
p,9,<p	General spherical co-ordinates
p	Radial distance frcm the virtual apex of the conical surface of die to the centroid of the assumed shape element at the inlet section
9	Inclination of the radius to the tube axis
4>	Inclination of a particle measured in a plane perpendicular to the draw axis
f	Relative angular deflection of an element measured in the p-Q plane
n	Relative lateral displacement of the assumed shape element referred to the inlet
$u_{P\ O\ \Phi}$	Velocities in the p, 9 and 4> directions
u_{m}, u	The mean coefficient of friction at the die-tube and plug-tube interfaces

p , p	Mean pressure at the die-tube and the plug tube interfaces
a_{za}	Mean draw stress
k	Mean yield stress in shear
Y_m	Mean yield stress in tension
W	Work dene per unit volume of material
VOL	Volumetric rate
J*	Actual externally supplied power
V	Volume of deforming material
i_{ij}	Strain rate
T	Shear stress at the sliding surface
|Au|	Velocity discontinuities along the sliding surfaces
Sp	Surface of velocity discontinuities
TV	Predetermined body tractions
S	Surfaoe area subjected to pre-determined body tractions
S^	Surface of prescribed velocity
u^	Velocity at entry and exit surfaces having predetermined body tractions
a_{ij}	Stress tensor component
a	Generalised stress or t^rta. .a. .}*
i	Generalised strsiin or $\overset{2}{\hat{}}\, e'_{j}\ e'_{j}\ \}^{i}$
t	Factor (-l<t<l) selected to cptlmise the inlet and exit shear surfaces by minimizing the plastic work

dene

N Nunber of hyperbolic curves banding the exit section

M Nianber of sectors into which the inlet section is divided.

General subscripts

a exit parameter

b entry parameter

p plug surface

d die surface

c conical

s straight or flat

m mean

5_{ij} Kronecker delta

V Poisson's ratio

1. A GENERAL INTOCDUCTICN

The prevailing economic factors such as manpower, equipment and energy facing the world today force industry to be en the look-out for alternative ways of manufacturing products for exajrple the manufacture of polygonal products by drawing or extrusion.

Hie project undertook to investigate the mechanics of drawing polygonal tube from round through a cylindrical die on a polygonal plug. This is a process whereby the bore of the tube changes from round to the polygonal shape whilst the external surface remains circular. The process would be Important to industry in for exanple the manufacture of spanners and locking devioes. Such a process would bring significant savings in the cost of raw materials, tooling, pcwer and labour. In addition the process would inpart improved mechanical properties on the final product.

The aim of the investigation was to establish a theore solution. The solution provides an estimate of the forces on the drawing tools, the optimum design of the tools and an understanding of the flow of the deforming metal. This leads to an efficient utilization of material and selection of a draw bench.

The project is an extension of the work in polygonal-bar and -tube drawing. The drawing of regular polygonal bars was investigated experimentally and theoretically by Basily {3}; the drawing of regular polygonal tube from round through a polygonal die on a polygonal plug by Kariyawasam {4}; and the drawing of regular polygonal tube from round on a cylindrical plug by Muriuki {5}. In each of the forementicned drawing processes, the theoretical predictions agreed reasonably with the actual data. There is havever, no known literature on the drawing of regular polygonal tube from round through a cylindrical die on a polygonal plug. This project therefore undertakes to study the drawing process and establish a theoretical model to predict the drawing- and plug- forces for a range of the process parameters.

In the works of the three forementioned authors (3, 4 & 5) on polygonal drawing, the workpiece of initially circular section had to transform to a polygonal section in a single pass. The passage through which the workpiece deformed into the final product combined both conical and plane surfaces of different inclinations to the draw axis to allow for gradual deformation. The shapes of the dies and the plugs in case of tubing included the pyramidical plane surfaces, the elliptical plane/conical surfaces, the triangular plane/conical surfaces and the inverted parabolic plane/conical surfaces. In this project, the elliptical plane/conical surface profile of the plug and a straight conical surface for the die were selected for the theoretical analysis.

In chapter (2), a review of the drawing theories is presented. Unlike the case of axisyrrmetf'ic drawing, in the polygonal drawing processes, the flow pattern is very complicated and the resulting theoretical models are solved numerically using a computer. Two solutions are established in this project: the first is based on the equilibrium of forces and predicts a lcwer bound solution; and the second predicts an upper bound solution and is based on a velocity field that minimises the energy required for the process and incorporates an apparent strain method and Coulomb friction. The actual draw load is bracketed by the two solutions.

The corresponding axisyrrmetric tube drawing solutions are also analysed with the aid of a computer to facilitate comparison between polygonal tube drawing and axisyrrmetric tube drawing.

Details of the derivations are in chapters (3) and the appendix. The oamputer programs developed to solve the solutions are in the appendix.

2. REVIEW OF THE LITERATURE

2.1 INTRODUCTION

Drawing of metal is an ancient craft, dating back to ancient Egypt where the process was used to draw ornamental wires. Today, large quantities of rods, tubes, wires and special sections are finished by cold drawing {6}.

Cold drawing gives a good dimensional control, a good surface finish and irrproved strength of the drawn metal {6}.

However, a limit on the reduction of area possible in a single pass is determined by the condition that the longitudinal stress at tte exit cannot exceed the strength of the drawn metal. It is important, therefore to have the tensile stress on the drawn metal as lew as possible.

A lot of literature, both theoretical and experimental has been published on the drawing process. The factors considered in the various theories include the die geometry, mechanical properties of the work material, the coefficient of friction, etc. A wide review of the drawing process is given by Wistreich {1}.

Recently, investigators have been mainly working on the drawing of non-circular sections e.g. polygonal rods and tubes, channels, etc. which had not received attention in the past. In these cases, the flow is either syirmetric or asynmetric as opposed to plane strain deformation for drawing sheets or axisyrrmetric drawing of bars and tubes. Among recent investigators on polygonal drawing include Juneja and Prakash {2}, Basily {3}, Kariyawasam {4} and Muriuki {5}. There is however, no known literature, experimental or theoretical on the direct drawing of round tube to a tubular section having an external circular surface and a polygonal bore inspite of the importance of this type of shape in engineering works such as manufacture of spanners and locking devices. This project therefore undertakes to establish a general theoretical solution on the direct drawing of such a tube.

Metal working theories can be grouped broadly under the following headings:-

(i) equilibrium approach,

(ii) slipline field approach/

(iii) upper and lower bound solution,

(iv) energy approach where the total work consists of homogeneous, redundant and friction components,

(v) visioplasticity, and

(vi) finite element method.

A comprehensive review for the equilibrium approach is presented in the next section and that for the upper and lower bound solution in section 2.3. These two theories formed the basis of the theoretical analysis presented in chapter (3).

2.2 EQUILIBRIUM APPROACH IN DRAWING

This method is based on the equilibrium of forces. It therefore takes into account only that distorsion necessary for the shape change and neglects any redundant deformation. When using the theoretical models derived by this method, the errors involved for exairple in the drawing forces may be large especially for large die angles with small reductions. However, the loads determined by this method have been found to agree closely with experimental results in seme processes especially wire drawing {1}.

2.2.1 AXISYMMFIBIC BAR DRAWING

One of the first useful equations in wire drawing was proposed by Sachs {6} in 1927. It was assumed that plane cross-sections of the workpiece remain plane as they pass through the die; the stress distribution on such planes is uniform;

the die surface is a principal plane; the mean yield stress (Y_m) is a constant; Coulomb friction applies and that this friction does not affect the stress distribution. By considering the equilibrium of forces and applying Tresca's yield criterion, the following expression for the drawing stress was obtained:-

$$a_{za} = Y_m \left(\frac{1+B}{B}\right) 1 - \left(\frac{D_a}{D_b}\right)^{2B} \qquad (2.1)$$

where B = u cot a,

U is the mean coefficient of friction

a is the mean die semi-angle

Y_m is the mean yield stress

D_a is the diameter at exit and

D^ is the diameter at entry.

Several papers on drawing processes using Sach's approach have been published; a comprehensive review is presented by Blazynski {7}.

2.2.2 AXI5YV1METRIC TUBE DRAWING

The methods of deforming tubes by cold drawing are based on three fundamental processes, viz. sinking, plug drawing and mandrel drawing. In the sinking process, the tube is drawn without any internal support resulting in a decrease in tube diameter with ideally no change in wall thickness. Wall thickening may take place but it rarely exoeeds 7%. In the plug drawing process, the tube is drawn over a fixed or floating plug positioned in the die throat. In practice, a small amount of sinking is present in the process using a plug; there is a reduction in both the diameter and the wall thickness. In the mandrel drawing process, the internal tool moves with respect to both the tube and the die.

In 1946, Sachs and Baldwin {11} derived a formula for the draw stress in the sinking of thin walled-tubing: -

$$\sigma_{za} = Y'_m \left(\frac{1+B}{B}\right) \left| 1 - \left(\frac{D_a}{D_b}\right)^B \right. \qquad (2.2)$$

where B = u cot oi

D_a and D^ are the mean diameters at exit and entry respectively and

Y'_m ^1-1_m Y is the modified mean yield stress from the von Mises yield criterion.

The solution was based on the following assumptions: -

A pressure normal to the working tool-metal interface exists on the interface of tube and die and is a principal stress; a shear stress exists on the interface because of fricticn; transverse sections are free of shear stresses; the normal stress acting on the transverse sections is uniformly distributed over the cross-section and is a principal stress; the wall thickness is small in corrparison to the tube diameter; the wall thickness of the tube remains constant throughout the process.

Oie of the limitations on the application of the equilibrium solutions is that they only account for homogeneous work and friction work and no account is taken for the redundant work. Hcwever, various investigators have proposed the incorporation of a redundancy factor in the theories and a carprehensive review is presented by Blazynski {7}. A more general method of accounting for the effect of redundancy on the parameters and mechanics of various processes was proposed by Blazynski and Cole {11}. The authors extended Baldwin and Sachs {17} theory to account for redundant work by obtaining the difference between the loads of the total and useful deformation. An upper bound solution for the sinking process incorporating the effect of redundancy has been extensively treated by Avitzur {12}. Avitzur assumed the deforming zone to be bounded by spherical shear surfaoes with their centres at the virtual apex of the die. The flew through the die was thus expressed by kinematically admissible velocity field.

2.3 UPPER AND LOWER BOUND SOLUTIONS

Prager and Hodge (16) formulated the upper bound theorem for a rigid perfectly plastic material. The theorem states that among all kinematically admissible strain rate fields, the actual one minimises the power required to effect a given process. With the additional assumption that the material is a von Mises material {12}, the final upper bound expression beccmes:-

$$J^* = 2k \int_V \sqrt{\tfrac{1}{2}\dot{\varepsilon}_{ij}\dot{\varepsilon}_{ij}}\; dv + \int_{S_\Gamma} \tau|\Delta\dot{u}|ds - \int_{S_t} T_i\dot{u}_i ds \qquad (2.3)$$

The actual externally supplied power J is never higher than that carputed by using equation (2.3). The first term expresses the power for internal deformation over the volume of deforming body. The second term includes shear power over the surfaces of velocity discontinuities including the boundaries between the tool and material. The last term includes power supplied by predetermined body tractions e.g. the back tension in wire drawing.

The normal component of velocity across a shear boundary between two zones must be continuous because of volume constancy. Parallel to the shear surface, a velocity discontinuity may exist. Also since the velocity of the tool is prescribed, the normal ccmpcnent of the postulated velocity field for the deforming material should be equal to the normal caipcnent of the velocity of the tool over the surface of contact. When the postulated velocity field satisfies the relaxed continuity requirements, i.e. permitting velocity discontinuities parallel to the shear boundary, it is called a kinematically adnissible velocity field {12}.

Kinematically actnissible solutions are useful in that in addition to predicting the loads required for a certain process, it is also possible to optimise the process taking into consideration the effects of various parameters. Also the proportion of the redundant deformation and the defects such as shaving, central burst, dead metal zone, etc. can be predicted. The approach also unveils information to eliminate the various defects.

The lower bound theorem states that among all statically admissible stress fields, the actual one maximizes the expression

$$I = \int_v T_i u_i ds \qquad (2.4)$$

where I is the computed power supplied by the tool over surfaces over which the velocity is prescribed, T^ is the normal component of traction over the prescribed surfaces and

ii_i is the relative velocity between the tool and workpiece.

The stress field describing the stress distribution within the deforming zone should satisfy the following requirements:- It should be a smooth function; it should obey the equilibrium equations; it should satisfy the surface conditions when surface tractions are prescribed and the state of stress does not violate the yield criterion. Such a stress field is called a statically admissible stress field.

Different kinematically admissible velocity fields can be assumed to determine a value of J*. For the lowest value of J*, it is presumed that the velocity field that led to it is approaching the actual velocity field.

Several statically admissible stress fields can be assumed with a view to obtaining a value for I. For the highest value of I, it is presumed that the stress field that led to it is closer to the actual stress field. For actual stress and strain rate fields, J* = I = actual power.

A number of investigators have developed the upper bound technique and applied it to specific problems. A brief recount of the more recent work relevant to the current research is presented in the next two subsections.

2.3.1 DRAWING OF SECTION RODS

In 1975, Juneja and Prakash {2} obtained an upper bound solution for the symmetric drawing of polygonal sections. The solution predicted the cptimum convergent angles of the die surfaces for the minimum drawing stress and the critical convergent angles for the formation of a dead metal zone. The draw stress was observed to decrease rapidly to that of the axi-symnetric solution by Avitzur {12} as the nunber of sides of section increases.

Concurrently but independently, Basily {3} obtained an upper and lover bound solution for the asynmetric drawing of regular polygonal bars from round bar. It was shown that the equivalent die angle can be optimised for every relevant combination of the coefficient of friction and reduction of area. It was further shewn that as the number of sides of the drawn section rod increases, results of both the upper and lower bound solutions approach those of the corresponding axisyrrmetric case.

2.3.2 TUBE DRAWING

A general upper bound solution was derived for axi-symnetric contained plastic flow occuring in processes like drawing and extrusion of tubes and wires by Juneja and Prakash {13}. The solution was extended to particular cases for instance plastic flow through conical dies using a plug or a mandrel.

Kariyawasam & Sansome {4} investigated the process of direct drawing of round tube to any regular polygonal shape both experimentally and theoretically. In addition to designing draw tools optimised to give the least work of deformation, the effect of diameter to thickness ratio of the undrawn tube and the effect of reduction of area on the draw force was also investigated.

wa Muriuki {5} investigated the direct drawing of regular polygonal tube from round on a cylindrical plug both experimentally and theoretically. The derived theoretical solutions were based on a method of conformally mapping triangular elements in the inlet plane to corresponding triangular elements in the exit plane. Several sets of the die profiles shown in Figure 3.2 on page (20) were tested experimentally. The elliptical plane/conical surface die produced results which agreed fairly well with the predicted values. Hie reports by Basily & Sansome {3} and Kariyawasam & Sansome {4} also recommended this type of the die profile to be the optimal

This project therefore selected the elliptical plane/ surfaces to be the profile of the plug to be investigated.

3 DERIVATION OF'THEORY FOR *THE* UPPER AND LOWER BOUND SOLUTION

3.1 INTRODUCTION

Equations for the upper and lower bound solution in the drawing of regular polygonal tube from round through a cylindrical die on a polygonal plug are developed in this chapter (See Figure 3.1). Close pass drawing is assumed in the derivations.

The deformation passage is complex and numerical integration was used to obtain the solutions for any given set of drawing parameters. The deformation pattern was selected such that the difference between the two bounding loads is as small as possible since the actual load lies between the two limits.

The upper bound solution was obtained by equating the total power derived for the prescribed deformation pattern to the applied power. The development of the velocity field for the upper bound solution is described in section 3.4 and Coulomb friction was incorporated by an apparent strain method presented in section 3.6.3.1 on page (43).

Figure 3.1 ISCMmiC DRAWING OF THE DEFORMATION PltOCESS IN THE DRAWING OF POLYQDNAI TOI3E FRCM ROUND ON A POLYGONAL PLUG

The derivation for the lcwer bound solution was based on the equilibrium of forces and Tresca's yield criterion. The solution was developed for the elliptical plane/conical surface plug (Figure 3.2) and a cylindrical die.

Equations for the lower and upper bound solution for axisyrrmetric drawing are presented in appendix A-5 on page (A72)

The computer programmes presented in Section 3.3 provides the results for the upper and lower bound solution for polygonal drawing and also for axisyrrmetric irawing for the purpose of comparison.

3.2 UPPER BOUND SOLUTION

In the upper bound solution, the minimum energy required to deform the material is calculated. In addition to the homogenous deformation, relative shearing at the inlet and outlet regions of the deformation zone is considered. FUrther relative shearing of the material elonents in the deformation zone is also considered and finally, friction between the deforming metal and the tools is accounted for using Coulomb's relationship.

(a) Shape 'A' (b) Shape 'B

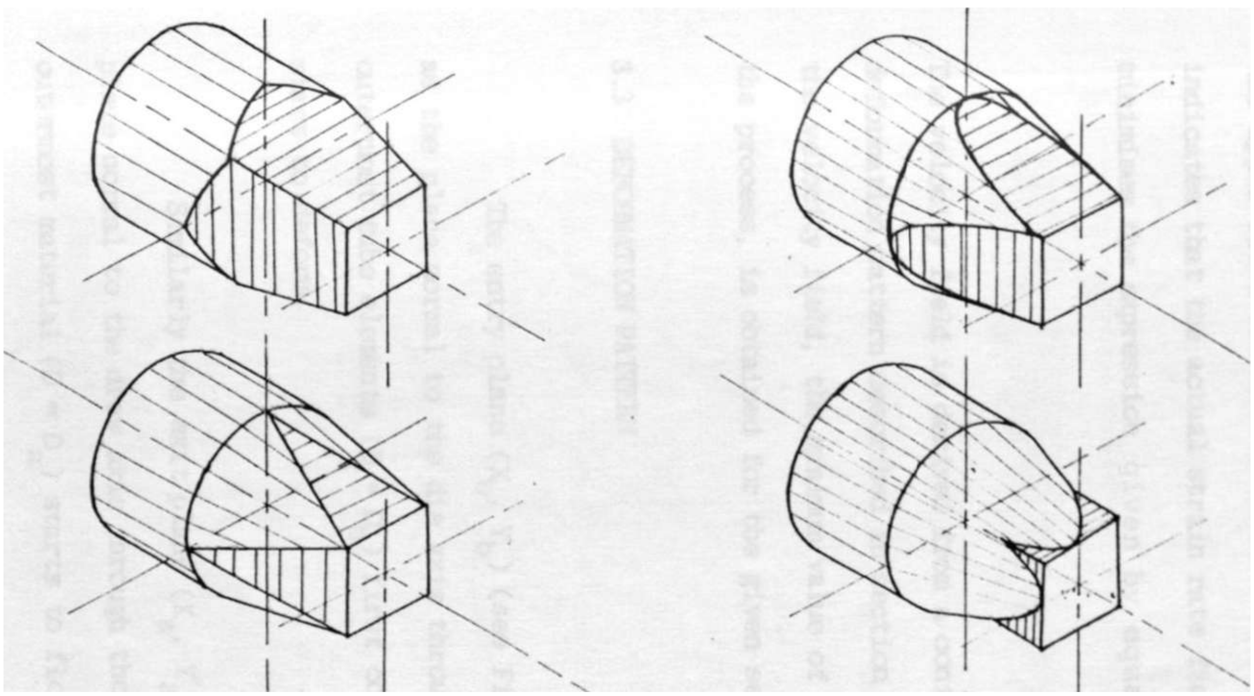

(c) Shape 'C' (d) Shiipe 'D'

Figure 3.2 ISOMETRIC DRAWING CF THE GENERAL FEATURES OF THE FOUR BASIC SHAPES OF THE PLUG, SIMILAR TO DIE SHAPES INVESTIGATED IN REFERiiNOES 3, 4 AND 5.

(a) Pyramidical plane surface

(b) Elliptical plane/conical surface

(c) Triangular plane/conical surface

(d) Inverted parabolic plime/conical surface

A velocity field is assumed and if the deforming metal obeys von Mises yield criterion and the Levy-Mises flow rule, the upper bound solution described in section 2.3 of Chapter 2 indicates that the actual strain rate field e^ is the one that minimises the expression given by equation (2.3) on page 11

The velocity field is derived from a ccnformally mapped deformation pattern described in section 3.3. Having derived the velocity field, the minimum value of J*, the power to effect the process, is obtained for the given set of drawing parameters.

3.3 DEFORMATION PATTERN

The entry plane (X^ (see Figure 3.3) is defined as the plane normal to the die axis through the point where the outermost tube elements (D = D^) first contact the die and start to deform.

Similarly the exit plane (X_{cl}, Y_{2L}) (Figure 3.3) is the plane normal to the draw axis through the point where the outermost material ($D = D_a$) starts to flew parallel to the draw axis and deformation ceases.

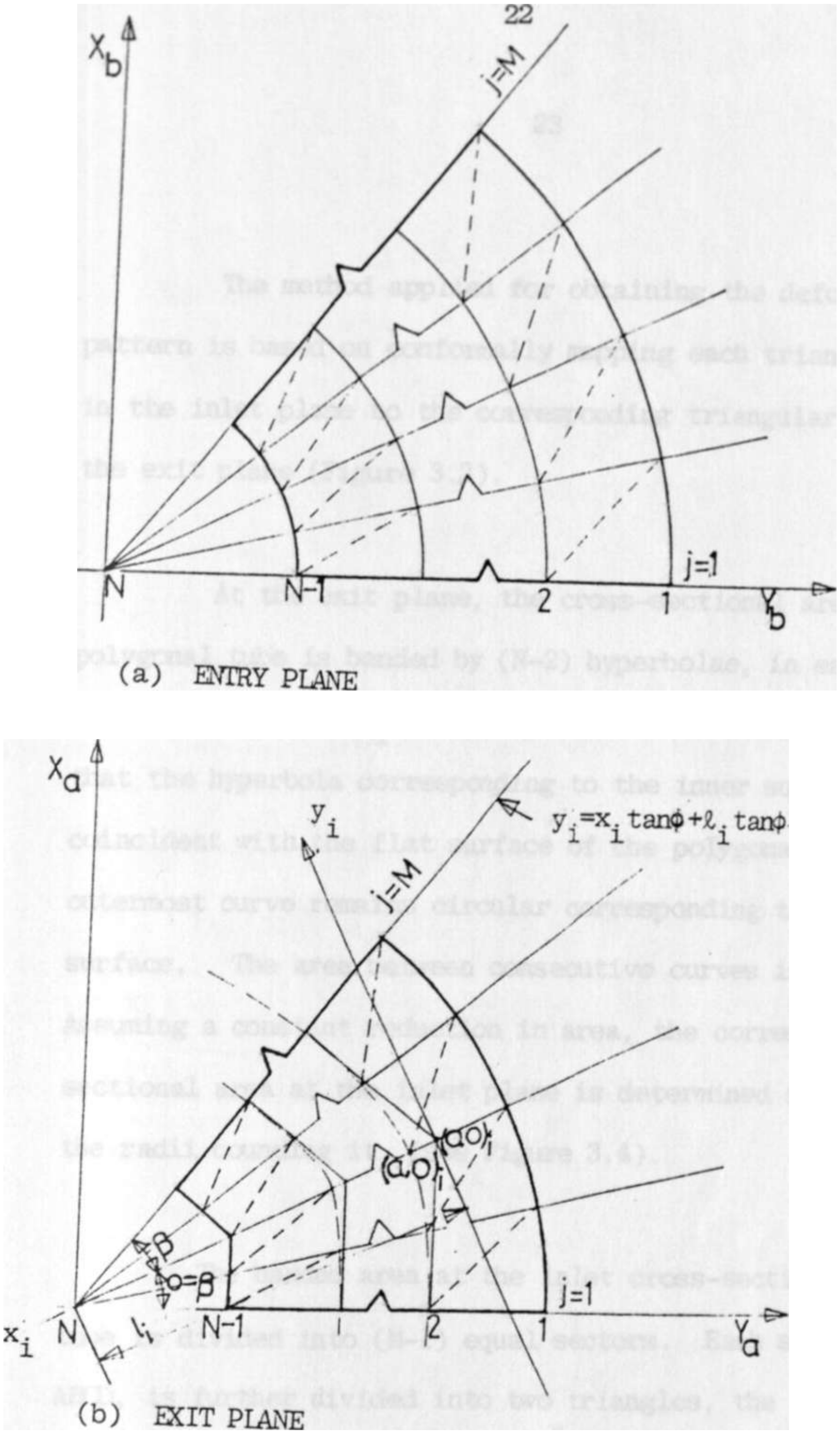

FIOTRE 3.3 DEFORMATION PATITSRN TOR THE DRAWING OF REGUUR
POLYGONAL TUBE FRCM ROUND

The method applied for obtaining the deformation pattern is based on conformally mapping each triangular element in the inlet plane to the corresponding triangular element at the exit plane (Figure 3.3).

At the exit plane, the cross-sectional area of the polygonal tube is banded by (N—2) hyperbolae, in each of which the focal distance a^ is adjusted to suit the asymptotes such that the hyperbola corresponding to the inner surface is almost coincident with the flat surface of the polygonal tube. The outermost curve remains circular corresponding to the die surface. The area between consecutive curves is calculated. Assuming a constant reduction in area, the corresponding cross-sectional area at the inlet plane is determined and hence the radii bounding it (see Figure 3.4).

The banded area at the inlet cross-section of the tube is divided into (M-1) equal sectors. Each sector, say ABCD, is further divided into two triangles, the large triangle ADB and the small triangle DCB. The area of each triangle can be determined and frcm the known co-ordinates of the vertices, the centroid is located.

Assuming a constant reduction in area of the large triangle ADB on the inlet plane, the corresponding area of the

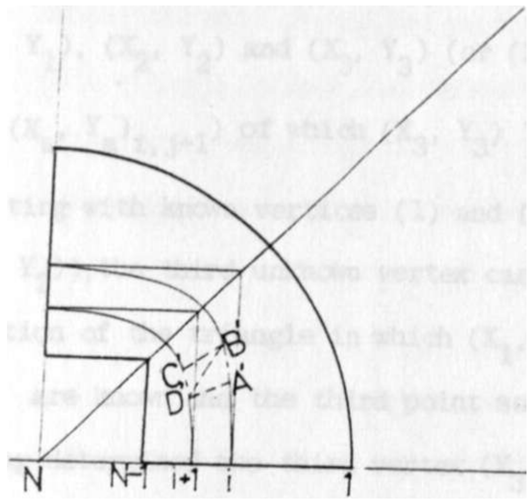

(a) EXIT PLANE

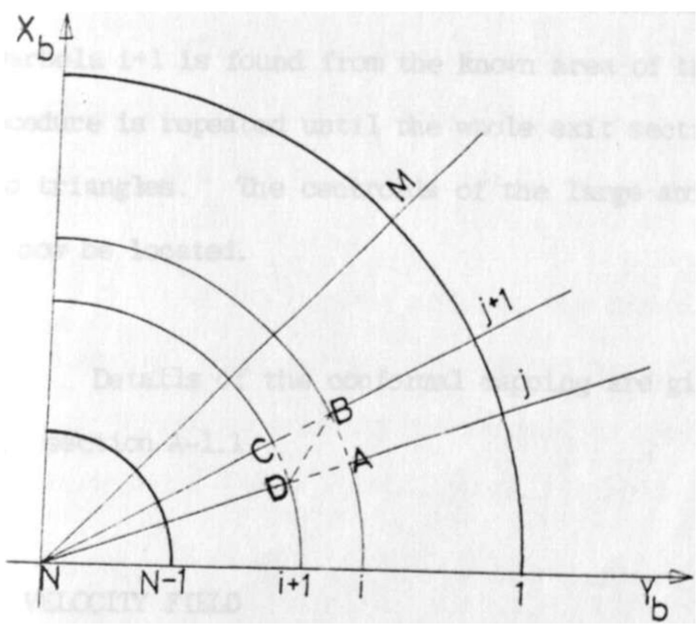

(b) ENTRY PLANE

FIGURE 3.4 MAPPING THE ENTOY PLANE TO THE
EXIT PLANE

l*irge triangle A'D'B' on the exit plane can be determined. Let this triangle at the exit plane be defined by the co-ordinates (X_r Y_x). (Xg, Y_2) and (X3, Y3) (or ($X_{a>}$ Y J ^ and (X_a, $Y_{\&}$)$_i$ j_{+1}) of which (X^, Y^) lies on the hyperbola i. Starting with kncwn vertices (1) and (2) (or (X^, Y^) and (X_2, Y_2)),the third unknown vertex can be found by solving the equation of the triangle in which (X^, Y^), ($X_{2>}$ Y_2) and the area are kncwn and the third point satifies the hyperbola i. Having determined the third vertex (X„, YJ (or (X , Y). .,)» d o a a i,j+i the point is then substituted for (X_2, Y_9) of the small triangle D'C'B' and the third unknown vertex which satifies the hyperbola i+1 is found from the known area of triangle. The procedure is repeated until the whole exit section is mapped into triangles. The centroids of the large and small triangles can now be located.

Details of the conformal mapping are given in Appendix A-1, section A-1.1.

3.4 VELOCITY FIELD

It is assumed that before meeting the die, all particles of the tube material travel parallel to the draw axis towards the die entry. Within the die, the velocity of a particle is expressed 3-dimensionally by a spherical co-ordinate system, li = u(u_p, u_Q, u^) and changes as the deformation proceeds. Beyond the exit plane, the particle travels parallel to the draw axis without further plastic deformation. A boundary therefore exists which separates the undeformed metal zone to the zone where relative deformation occurs. A particle cn reaching this surface shears and changes direction.

A similar distortion occurs at the exit except that the particles pass through the boundary from the deforming zone into a region subject to elastic distortion cnly.

There is no general theoretical method to determine the shape and position of these boundaries. It is usual to assume that the boundaries are plane, spherical or conical.

In the current problem, the deformation mode is ccmplex. A general shear surface was defined such that a particle on any streamline cn entry was assumed to shear at an angle (——10) to th draw axis where -l<t<l (see Figures 3.5 and A-1.6). The position of the particle was defined on the general spherica surface (pb,0,4>). The parameter t was used to optimise the shear surface by minimizing the shear work. A general pyramidical shear surface was defined at the exit of the deformation zone.

Once a shear surface has been defined, a plane parallel to •exit' or 'entry' planes and passing through the centroid of the particle on the respective shear surfaces can be drawn. Such planes are denoted by (X^, Y^) and (X^, Y£) for the exit and entry shear surfaces respectively. Let the centroid of the triangular elonent at entry be denoted by (X^, Y.^Ki.j) and that of the corresponding triangular element at the exit by $(X_a', Y_a')(i,j)$. By joining the centroids of the corresponding triangular elements, the drawn vector was assumed to define the path followed by the element. Detailed derivations of the flew path parameters are in Appendix A-1, section A-1.2.

Having defined the flew path, the velocity field u(p,9,4>) is established and therefore the strain rates (see Figure A-1.12).

Let li^ be the velocity of an element before shear at the assumed velocity discontinuity surface and u(p,9,4>) the velocity immediately after shear. The component of velocity normal to the shear surface must be of the same magnitude on both sides of the shear surface for continuity of flew (Figure 3.5) i.e.

ll ccstQ = ucosncosf cos(l-t)9

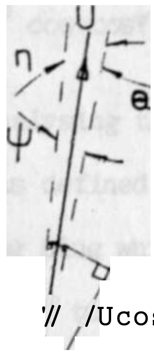

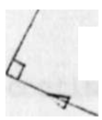

FIGURE 3.5 DETAILED DIAGRAM SHOWING VELOCITY
OF THE PARTICLE IMMEDLATELY AFTER
SHEAR AT THE ENTRY SHEAR SURFACE

or $d = a \dfrac{S2S*}{\cos n \cos f \cos(1-t)\theta}$ (3.1)

For convenience of analysing the final results, an equivalent plug semi-angle a was defined as the semi-angle of the axi-synmetric tube drawing plug which produces the same reduction of area as the polygonal tube drawing plug for the same die length. Detailed derivation of the cross-sectional area (A) of the tube material at any radius p frcm the assumption of an equivalent plug is in Appendix A-1, section A-1.3.

Due to continuity of flow, equation (3.1) becomes

$$uA = OA_D \dfrac{—}{\cos n \cos Y \cos(1-t)6} \qquad (3.2)$$

where A and A^ are obtained from equations (A-1.67) and (A-1.73) on pages (A28) and (A29) respectively.

Therefore, a - t^ costQ ^ p_b C_1 " J $(C_2+p')^2)$

$$\wedge \dfrac{\cos tQ}{\cos r, \cos l \cos(1-t)0} \dfrac{0''^2_b}{p''} \qquad (3.3)$$

v/here

$$p;^2 = P k - c_3 \qquad (3.4)$$

and $$p''^2 = C^P^Cg+p')^2) \qquad (3.5)$$

The velocity a can be resolved into three components, namely u_p, u^ and u^ in the p, 8 and <p directicns. Considering the geometry of Figure A-1.4 on page (A16) and substituting for u from equation (3.3), the velocity ccnponents of the particle thus become:

$$ii_p = u \text{ cosncos\^{}}$$

$$\text{P'7} \quad \frac{\text{costQ}}{\cos(1-t)0} \qquad (3.6)$$

$$U_q = u \text{ cosncosT}$$

$$\text{"b} \; ({}^{P}\text{bl}^{2} \; \text{p}^{n}\text{i} \quad \frac{\cos t6 \tan Y}{\cos(1-t)9} \qquad (3.7)$$

$$u = u \text{ smn}$$

$$\% \quad \frac{\text{costQ tann}}{\cos(1-t)9 \cos y} \qquad (3.8)$$

3.5 STRAIN RATES

i. a

The general expressions for strain rates as functions of velocity components u_p, Uq and in the directions p, 0 and $ respectively, in the general spherical polar co-ordinate system (15) are as follows:-

3u
Ep = (3.9)
3p

u
y p 30 p (3.10)

^ 3u, u Uq

3ue ue i 3UQ
YP0= 30~"0-+P3E- (3_12)

]. 9U9 1 9U. U,
'9* = 559 3T + p 99 " p cot9 (3.13)

' , 1
Y<J>p 3p p psin9 90 (3.14)

Equations (3.9) to (3.14) were applied to the derived velocity expressions (equations (3.6) to (3.8))to yield the strain rates.

The final expressions for the strain rates become:

_ = 2CL "b. CC6t9 [fbW {p-(C2+p»)/Pl_| }p (3.15)
P"2 p os(l-t)e Wp"/ 'p~pbl

where C^, and p' are given in Appendix (A-1.3) by the equations (A-1.68), (A-1.59) and (A-1.70) respectively, while $p"^2_b$ and $p"^2$ are evaluated using equations (3.4) and (3.5) on on page (29).

li /^{p}bl^{2} ocstQ
$^{\pounds}$9 = " p p^{77}/ cos(l−t)9 ($^{1+}$tanY(−t tant9+(l−t)tan(l−t)9

+ ——)) (3.16)
os'f

• ^ (fbf coste . {l + tan* + ₩00tf0QB(^$_{A}$)$_{t}$ (3.17)
P ₩P'7 $_{c}$os(l−t)9 tanQ Z$_{g}$oosf '

where 0_A and Z_S are given by equations (A−1.53) and (A−1.44) on pages (A22) and (A15) respectively.

,A„I2
Ob %) coste {tartf _ l tartf{p−(C$_{9}$+p')
^{Y}P6 " p P l cos(l−t)9 p"^{2} 2

(—£—) }p−t tantQ + (l−t)tan(l−t)9} (3.13)
P−P$_{b}$

bl ccst9tann {<zl_ _ t tant9
^{Y}94> P PI cos(l−t)6cos^{l}F tan9

+ tanQ +(l−t)tan(l−t)6+tan*}

2
= Ui_ /Pu b) cost9tann ("l {p_(c +p,)(_g_)} }
Jb
^{Y}*P p [p"l cos(l−t)9cos4' P"^{2} 2 P−P$_{b}$

3.6 TOTAL POWER REQUIRED FOR DEFORMATION

3.6.1 INTERNAL POWER OF DEFORMATION

The following assumptions were made when deriving the rate of internal work to deform the material in the deforming zone:

(i) The material obeys von Mises yield criterion,

a'j a' . = $2k^2$ (3.23)

where a< . = a. . − . (3.21)

and k is the yield stress of the material in shear.

(ii) The flow obeys the Levy-'lises stress-strain relationship

$._{ij}$ = a'_{ij} dX where dA is a constant (3.22)

of proportionality. *

(iii) The material is rigid perfectly plastic and non work-hardening.

(iv) The inccmpressibility condition is satisfied

i.e. ^ = = 0 (3.23)

The rate of work required to deform an elemental volixne dV is dWj = a_{ij6iJ}dV.

Therefore power to deform material of volume V is

W_I = $\int_V$ $o_{ij} i_{ij}$dV

Multiplying each side of the Levy-Mises expression

by gives

$e_{ij}.e_{ij}$ = dAa'$_{ij}$e$_{iJ}$. (3.24)

Also multiplying the equation by a!$_J$ gives

a!$_{ij}$i.$_{ij}$ = dAa!$_{ij}$a'$_{iJ}$ (3.25)

Therefore, o!$_J$e$_J$ = 2dAk^2 (3.26)

from von Mises equation (3.20).

Equation (3.21) can be rewritten as

a'iy - Ca$_{tj}$ - i a ^ j i y

= a_{ij} i_{ij} (3.27)

and from equations (3.24) and (3.25),

(3.28)

Substituting equations (3.27) and (3.28) into equation

(3.25) gives

By substituting equation (3.29) into the expression for W_I gives

$$W_I = \int_V k \sqrt{2\dot{\epsilon}_{ij}\dot{\epsilon}_{ij}}\, dV \tag{3.30}$$

If k is assumed constant,

$$W_I = k\sqrt{2}\int_V \sqrt{\dot{\epsilon}_{ij}\dot{\epsilon}_{ij}}\, dV \tag{3.31}$$

If the mean yield stress is Y_m, then for the von Mises condition,

$$k = \frac{Y}{\sqrt{3}}$$

Therefore, $W_I = \sqrt{\frac{2}{3}}\, Y_m \int_V \sqrt{\dot{\epsilon}_{ij}\dot{\epsilon}_{ij}}\, dV$ (3.32)

Substituting for the strain rates frcm equations (3.9) to (3.19).

$$\dot{\epsilon}_{ij}\dot{\epsilon}_{ij} = \dot{\epsilon}_1^2 + \dot{\epsilon}_2^2 + \dot{\epsilon}_3^2 + 2(\dot{\epsilon}_{12}^2 + \dot{\epsilon}_{23}^2 + \dot{\epsilon}_{31}^2)$$

Therefore, the expression for the internal power of deformation becomes

$$^{w}i = j_2 \quad '_v \ ^{/\{2(£}p^{+} \quad ^{+} \quad ^{+}4 \ * \quad * \ ^\wedge V^{dv}$$

$$\_ \ \overset{Y}{m} \quad r \quad D \ , \ \overset{or\ 2}{b.} \quad \underline{costs} \quad Ar \ {}_{\cdot v} \qquad (3.34)$$

where

$$^{K} \ = {}^{2} \{ \frac{2C_{,}\varphi}{p^{*}2} \ ^\wedge (p - \overline{(C_2} + P') \quad \frac{Pl}{^\wedge b}) \ )\}^{2}$$

$$+2 \ \{-(1+\tan YC - t\tan te \ +(1-t)\tan(1-t)9 \ + \ \frac{}{\cos Y}))\}^{2}$$

$$+2 \ \{1_{+} \ \tan B \ + \frac{}{\tan(^\wedge - ^\wedge_A)\cos 4'\sin 9}\}^{2}$$

$$+ \{-(\tan f - 2CT\tan¥(p-(C_0+p')(\frac{£}{p-p^\wedge}))\frac{}{p^{"2}} - t\tan t9 + (1-t)\tan(1-t)Q)\}^{2}$$

$$+. \ (.(\tan r^\wedge jJ. \ \frac{}{\tan^\wedge \ \tan Q} \ {}_{ttant9+t}an8 + (1-t)\tan(1-t)9 + \tan*)\})$$

$$'\tan? \qquad '^\wedge{}^\wedge IJ^\wedge{}^\wedge > 2 \ ^\wedge{}^{2} \qquad (3.35)$$

The elemental spherical volume is

$$dV = p^{2}\sin 8dpd9ckj> \qquad (3.36)$$

Therefore,

Y_ A _ ^ u o" 2
W_I », -IS f V " r^{27l"} ^ r^K ^ ^ costs ^ 2 sinedodec^
•3 e ^ J ^ ^ ^
a (3.37)

Y ' , ,2
- IT- J^{27r} (/^p b £,,2 * dp} costesinede^ (3b38)
e <,=0 P=p ^P cos(l-t)0
a

The elemental spherical surface area at entry-

is
2
dA^ = P_b sin6d9cfc> (3.39)

Equation (3.38) becomes:-

* r J s % fb ^2 /^9 2 - F {/P_b 0 ^ do} coste ^ (3.40)
3 ^p b 9=ct e 4>=0 P=P_a oos(l-t)9

Equation (3.4) can be rewritten as

p»» ^ Q
c—) = c_1 - —
0 P_b^2

Substituting for C^ and C_3 from equations (A-1.68) and (A-1.74) on pages (A28) and (A29) respectively and rearranging,

D" 2 A,
(-£) = (3.41)
^p b P,^2

Therefore,

W − f % fb f2n :p costa
1 /3 p^ 9«a •io o 0»2 cos(l−t)9 ""b
b e "a. "

= Y m V V (s) <3−42>

where

f(s) = /³2=a J27T {|Pb _£_ /K do) dA (3.43)

b

f(s) is evaluated numerically by dividing the inlet section into N_o x(M−1)x(N−2) elemental areas which are themselves subdivided into large and small triangles i.e.

f(s) = V ^1 (A dA.} (3.44)
EB/3 M− l=1 J=1 Pa P"2 cos(l−t)6

3.6.2 POWER LOSS IN SHEARING MATERIAL AT INLET AND EXIT SHEAR SURFACES

The internal power Wj derived in the last section is required to overcome the homogeneous deformation and the necessary relative shearing within the material itself as it progresses through the deforming zone. Power is also required to corrpensate for the losses due to the shearing of material on both the inlet and exit shear surfaces.

The rate of work on crossing a shear boundary of elemental area dA_s is given by

$$dW_R = ku^* dA_s \tag{3.45}$$

where

u^* is the velocity discontinuity along the surface,

k is the yield stress of the material in shear equal to $\frac{Y_m}{\sqrt{3}}$ by the von Mises yield criterion.

The velocity discontinuities at the entry and exit shear boundaries are derived in Appendix A-1.4, equations (A-1.78) and (A-1.79) respectively. The rate of work dissipation at the entry shear surface is

= / (3.46)

= / k V SSI? (3.47)

The rate of work dissipation at the exit shear surface is

$$W_{R_a} = \int_a k' u_{ra} \, dA_s \tag{3.48}$$

where

k' = k for a non work-hardening material and

dA'_s is the elemental area on the shear boundary at exit.

$$\text{Therefore,} \quad W^\wedge = \int_a k\, \dot{u}_{ra} \frac{dA}{\ }^\wedge f_{t\,9} \qquad (3.49)$$

Assuming a passage formed by an equivalent conical plug and a conical die,

$$\frac{dA.}{dA_a}^\wedge = \left(\frac{p''_{\ }}{p''_a}\right)^2 \qquad (3.50)$$

$$\text{and} \quad u_{ra} = \left(\frac{pr}{\ }\right)^2 u^\wedge \qquad (3.51)$$

$$\text{Therefore,} \quad W_{Do} - \int_{A_T)} k \left(\frac{-2}{p''_a}\right)^2 \dot{u}. \left(\frac{p_a}{01*_b}\right)^2 \text{ccste}$$

$$= \int_D k u_{rb} S t 9 - \qquad (3.52)$$

The total rate of work of shear at the inlet and exit surfaces of velocity discontinuity is

$$W_R = W_{Ra} + W_{Rb}$$

$$= 2\int_{A_b} k\, \dot{u}_{rb} \frac{dA}{\cos\theta}$$

Y u . dA ,
2 J2 n A / — —1
/3 costQ ^

- ;3 YmVbR(s> (3-53>

where

B(8) - T- / ' cos(1—t)9tan4' i2 • {-sin* •
Afa

cost9 tanf + cost9 tan(1-t)6}2) * (3.54)

frcm equation (A-1.78) on page (32).

R(s) is evaluated numerically by dividing the inlet section into N_sx(M-1)x(N-2) elemental areas which are themselves subdivided into large and small triangles.

Therefore,

N N-2 M-1 ^
R(s) = — lim 2 I ({ccstetann }2 +
A, j=1 cos(1-t)8taM

2 * b
{-sint9+cost9tan4+cost9tan(1-t)9})* —^ (3.55)

Values of -1<t<1 are used to select the shear surface that gives the minimum value of R(s). This if. then the optimum shear surface for the given draw conditions.

3.6.3 FRICTICNAL LOSSES AT THE TOOL-WORKPIECE INTERFACES

Besides the internal paver W^ and the shear power additional power is required to overccme the frictional losses which occur as the tube slides between the die and the plug.

In the case of Coulomb friction, a mean coefficient of friction y is usually assumed for the given relative sliding surfaces. The rate of work loss is given by:-

$$» F = V_{SI} \ W s \wedge s + {}^{f}A_{, S<5} \ W s \wedge s \qquad (3{,}56)$$

where the first term on the right calculates the loss at the die-tube interface and the second term calculates the loss at the plug-tube interface.

The die and plug pressures and the coefficients of friction are unknown. A mean pressure at both interfaces can be assumed and if the distribution of pressure and the mean coefficient of friction axe known, the frictional loss can be calculated. The values are however unknown. To avoid this difficulty, $_r$ can be obtained indirectly by the apparent strain method. The method .allows the calculation of the draw load in the case of Coulcrrb friction without obtaining the distributicn of pressure at the tube-tool interfaces.

3.6.3.1 APPARENT STRAIN METHOD

This is an energy method where the work done 6er unit volume is divided into the plastic work and the surface frictional energy {14}.

Friction produces shear stresses and strains at the interface and these have two major effects on the work done. Energy is dissipated at the interface as a result of the relative motion and when the surface shear stress is significant compared with the yield shear stress, additional internal distortion results within the deformation zone. The two effects increase the work done.

The total work done per unit volume of the material is equated to an area under the equivalent stress-strain curve (see Figure 3.6). The strains i_{dL} and e corresponding to the total work and plastic work per unit volume are known as the apparent and mean.equivalent strains, respectively.

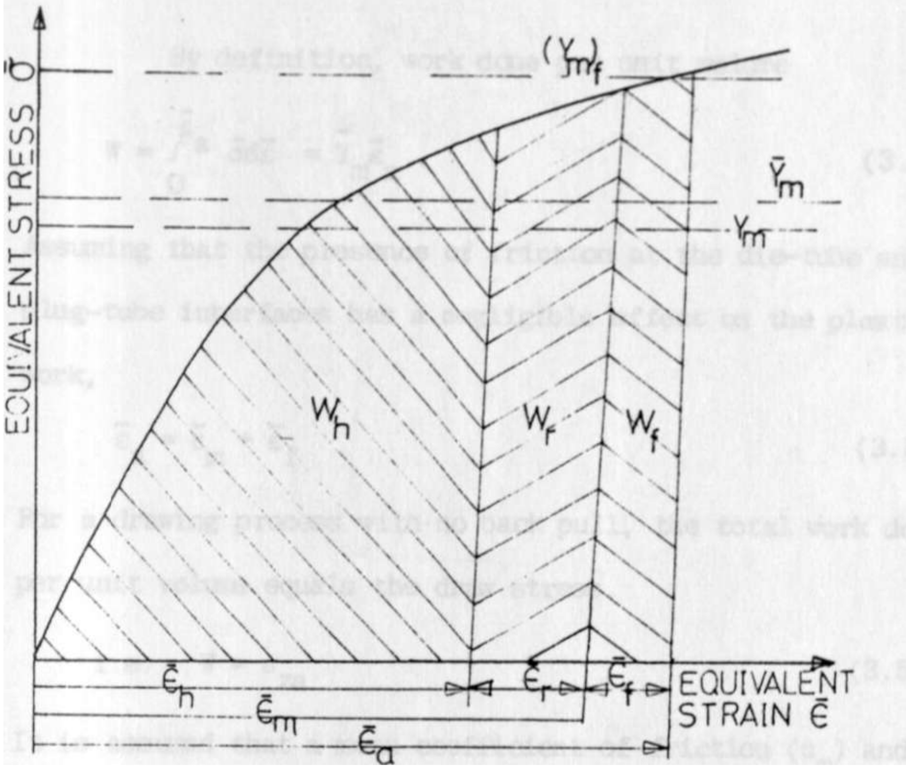

FIGURE 3.6 THE EQUIVALENT STRESS-STRAIN DIAGRAM SHOVING THE TERMS USED IN THE APPARENT STRAIN ANALYSIS

By definition, work dene per unit volime

$$W = \int_0^{\bar{\varepsilon}} \sigma \, d\varepsilon = \bar{Y}_m \varepsilon_a \qquad (3.57)$$

Assuming that the presence of friction at the die-tube and plug-tube interfaces has a negligible effect on the plastic work,

$$e_a = e_m + s_f \qquad \cdot \qquad (3.58)$$

For a drawing process with no back pull, the total work done per unit volume equals the draw stress.

$$\text{i.e.} \quad W = \sigma_{za} \qquad (3.59)$$

It is assured that a mean coefficient of friction (y_m) and a mean pressure (p_m) occur at both the die-tube and the plug-tube interfaces during the drawing process.

Using subscripts s^, c^ and c_9 to denote the straight, conical plug and die surfaces respectively:-

From Figure 3.7 for steady draw, the equilibrium of horizontal forces gives,

$$^a za^A a = {}^P m \quad < {}^E \ll W \gg \gg {}^{+ \, s \, i \, m \,)} \qquad + \qquad (3,33>$$

$$£(U_m cosa_s - si \ll x_s) \; dA_{s1} \cdot I(P_m C06a_c - S i m,) \; dA_{c1}$$

From equations (3.57) and (3.59),

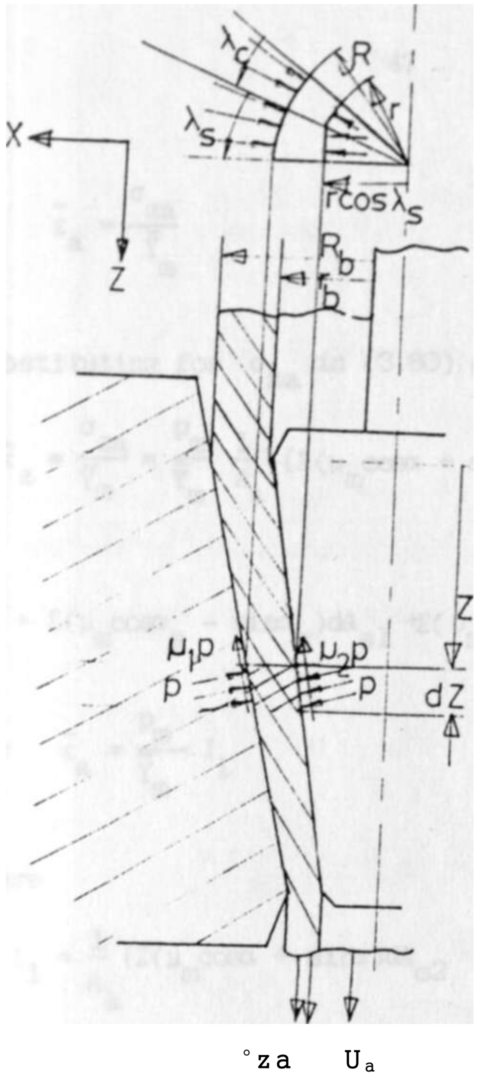

FIGURE 3.7 STRESS AND THE DEFORMATION PATTERN IN THE DRAWING OF POLYGONAL TUBE FROM ROUND THROUGH A CYLINDRICAL DIE

$$e_a = \frac{a_{za}}{TY_m} \qquad (3.61)$$

Substituting for a_{za} in (3.60) gives,

$$\bar{e}_a = \frac{\sigma_{za}}{V_m} = \frac{p_m}{r_m} \frac{1'}{I_a} f \wedge V^{080} + s1nB)^{J \quad v \quad ,A} c2$$

$$+ \wedge(u_m cosa_s - sina_s)dA_{s1} + \pounds(U_m cos>_c - siroJdA\wedge\}$$

$$\text{or} \quad e_a \cdot \frac{P\_}{V_m} I_1 \qquad (3.32)$$

where

$$I_1 = \frac{-}{A_a} \{Z(u_m cosa + sim)dA_{c2} \qquad (3.63)$$

$$+E(M_m cosa_s - sir»_s)dA_{s1} + \pounds(u_m CQsa_c - sinaJdA\wedge\}$$

$$= \text{Apparent strain factor} .$$

Frcm the definition of friction strain work done against friction per unit volume of material

$$W_f = (Y_m)_\wedge \pounds_f \qquad (3.64)$$

The friction work W_f can also be determined by the energy dissipated as the material slides between the die and the plug surfaces as follows:-

Using u_{s1}, u_{Q1} and u_{c2} to represent the respective surface velocities, equation (3.66) gives,

' $^{W}f^{X}$ " V m V s l $^{+}$ V A A l

$+ {}^{U}nPaF\%2^{<iA}c2$ (3-^{0}5)

By expressing the elemental surface velocities in terms of the input velocity u^ gives

V ^{0} ^{1} = dA_{s1} + > dA_{c1}

$+ E(\overset{U_{c2}}{t}\sim)$ d A J (3.66)

%

Substituting for

$^{(}$ V / f $^{V o l}$ = <$*_{8}$i $^{+}$

dA_{c1} + £(^£2) dA_{c2}}

^ "b

or E. $\cdot \frac{P\_}{(Y\_)_{nr_f}}$ I_9 (3.67)

where

•p $^{U}m^{ll}b$ slv ^{u}cl.
2 = T – $^{\{ i : (}$ — > ^ s i $^{+}$ $^{r/}_{£(}$ r – > ^ d
Vol "b

+) d A $_C$ 2 } (3.68)

= Friction strain factor .

Dividing equation (3.62) by (3.67),

i a _ (V h l h

T ' 1 2 B r 2
m

where B = — (3 69}
< V $_f$

Therefore e„ = B — £
f 2 " a

= He (3.70)
dL

I,
where f = B — (3.71)
^{x}2

Substituting equation (3.58) into (3.70) and rearranging,

$e_a = e_m + Ye_a$

$$\varepsilon_a = \frac{e_m}{1-V} \quad (3.72)$$

From equations (3.62) and (3.72),

i
^ _ v a
^{p}m ~ ^{Y}m T 7

= y (3.73)
m I $_L$ (")

Fran equation (3.61),

$$a_{za} » y_m e_a - ?_m \overset{£}{1-i'} \tag{3.74}$$

Therefore, if the value of e_m is known, the draw stress and the mean pressure (equations (3.73) and (3.74))aan be calculated from the geometry of the deforming passage, the velocity distribution, the strain factors and I_2 and the work hardening factor B. e_m can be derived from the total plastic work as shewn below.

3.6.3.2 THE MEAN EQUIVALENT STRAIN

It is assumed that the metal undergoing deformation obeys von Mises yield criterion and Levy-Mises flow rules. The plastic work dene per unit volume can be expressed as

$$W_p = \int_0^{\varepsilon_m} \bar{\sigma} d\bar{\varepsilon} \tag{3.75}$$

where a = /5(a! .a! (3.76)
2 U ^

(3.77)

The mean equivalent strain is defined as the strain which bounds an area under the equivalent stress-strain curve

(Figure 3.6) equal to the total plastic work done per unit volume of the material.

$$i \quad o \quad W_p - f\hat{}_0 \; 5 \, d \, e \, " \qquad (3.78)$$

The plastic work W^ consists of the internal work of deformation (VT) and the redundant work (W) of shearing the material at the assumed surfaces of discontinuity at both the inlet and outlet boundaries.

i.e. $W_p = W_I + W_r$ (3.79)

In terms of pcwer,

$W_P \times Vol = {}^{t}\!AT_{t\,l} + W_{D\,rv}$ (3.3Q)

From equations (3.42) and (3.53),

"i = Y m V V < s)

and $W = \frac{Y}{/3}$ ^ ^ (s)

Equation (3.78) beccmes

<Y m S m> Vol " V b V (s) + W s)

Therefore, = ± ^ H s) * ^ V b R t s)) (3.31)

f(s) and R(s) are evaluated numerically by the use of a computer and hence the value of the mean equivalent strain.

3.6.3.3 WORK HARDENDC FACTOR B

This is the ratio of the mean flow stress over the whole strain range) to the mean flow stress over the cL strain range e_m ^ e . The value will therefore depend on not only the material characteristics but also on the process and the friction.

If the coefficient of friction is anall, the strain range e_m ^ I_a is also small. The mean flow stress over this range can therefore be approximated as,

$$<Y_m)_f = \hat{\ }_a \tag{3.82}$$

By definition,

$$Va = \int_0^{a} f(Od i$$

$$\text{or} \quad Y_m \sim \frac{1}{"a} \int_0^{e_a} f(e)de \tag{3.33}$$

$$\text{Therefore } B = \frac{Y}{< V_f} = \pm- \int_0^{e_a} f(e)de \tag{3.34}$$

$$^5 sr = e_a$$

If the equivalent stress—strain curve of the material follows the pcwer law or

$$f(e) = o = o_Q c^n , \qquad (3.85)$$

where o is the true stress and o_Q is the stress corresponding to unit strain, then equation (3.84) gives

$$B = \frac{}{1+n} \qquad (3.86)$$

3.G.3.4 EVALUATION OF AND

Ij and I_2 given by equations (3.C3) and (3.63) are found by integrating the respective expressions over the relative sliding • surfaces of the deforming tube.

To determine I_2, the product of the elemental respective area and the velocity on the relative sliding surface between the workpiece and the tools must be known. The deforming die is conical but the plug has a corrplex shape. The longitudinal velocity increases towards the plug exit as well as circumferentially. Therefore the flow especially at the intersection of the conical and plane surfaces is very complicated. An approximate method is used to evaluate I_2 when the sliding velocity distribution is estimated for an equivalent conical plug.

Let u –, be the mean sliding velocity at the plug surface; then

$$a_{s1} = \frac{fW \;\; udA}{/._{A_s} \;\; dA_s} \quad (3.87)$$

For a convergent plug and conical die passage and the continuity of flow,

$$u = \sim \quad u_b coso_{te} \quad (3.38)$$

and $dA_g = 2Tr(r_b-(p.-p)cosa \; tana_e)dp$ (3.39)

Therefore,

$$u_{si} = \frac{\overset{f}{P}\% \; (7^{7}) \; cosa_e 27r(r_b"(p_b"p)cosot \; taxia_e)dp}{/_0 2rr(r_D-(p_0-p)cosa \; tana_e)dp} \quad (3.90)$$

$P"_b \; 2$

$$\% \; \hat{} e \frac{2nA}{} f" \quad <^{3,91}>$$

r

For the die-tube interface, the mean sliding velocity u_{g9} is given by:-

$$u_{s2} \quad (u\hat{} + u_a)cosa$$

3.7 LOVER BOUND SOLUTION

The upper bound solution developed in the previous sections is an overestimate of the load required to effect the process. The value overestimates the load. A lower bound solution which neglects the effect of redundant work is thus necessary; the actual load lies within the two limits.

By considering the equilibrium of forces on an elemental volume and applying Tresca's yield criterion, an expression for the draw stress is obtained. A computer prograirme is developed to solve the problem numerically.

3.7.1 DEFORMATION PATTERN OF THE LOWER BOUND SOLLTICN

The four basic tool profiles in the deforming zone are the pyramidical plane surface, the elliptical plane/conical surface, the inverted parabolic plane/conical surface and the triangular plane/conical surface (see Figure 3.2). The lower bound solution is developed for a conical die and the elliptical, plane/conical surface plug. This type of plug allows a gradual deformation in the die-plug deforming passage and the surface equation is readily derived.

The conical surface of the plug is inclined at an angle to the draw axis while the elliptical plane surface is inclined at an angle a_s to the draw axis.

3.7.2 DERIVATION OF THE LOWER BOUND *SOLUTION*

The lower bound solution is derived by considering the equilibrium of forces acting on an element at a distance Z from the selected origin (see Figure 3.8). Figure 3.3 shows a round tube deforming through a conical die on an elliptical plane/conical surface plug to produce a polygonal tube. The following geometrical relations are derived:-

(i) General parameter's for the plug

$$ft_D - \frac{1}{N_s} \qquad (3.92)$$

A^ = Area ratio

$$\frac{\text{Area at entry}}{\text{Area at exit}} \quad \hat{}b \qquad (3\ 93)$$

^{r}b " 2

$$a = \tan^{-1}\left(\frac{i\ \hat{}\ \sim H}{2L}\right) \qquad (A-1.61)$$

$$a_s = \tan^{-1}\left(\frac{\hat{}\ -\ H\ -\ \cos 3}{2L}\right) \qquad (A-1.62)$$

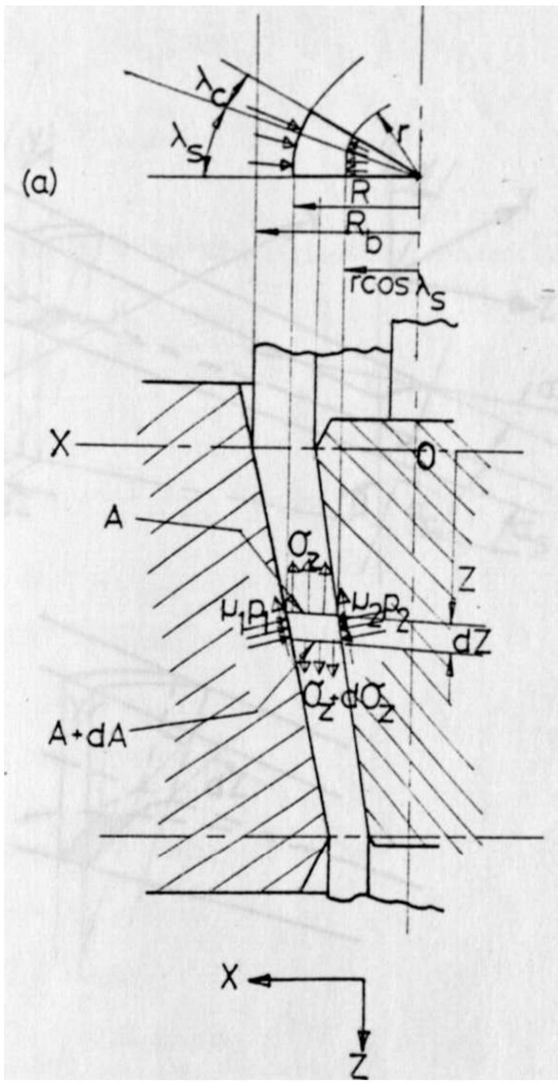

FIGURE 3.8 STRESS AND DEFORMATION PATTERN FOR THE DRAWING OF REGULAR POLYGONAL TUBE FROM ROUND THROUGH A CYLINDRICAL DIE

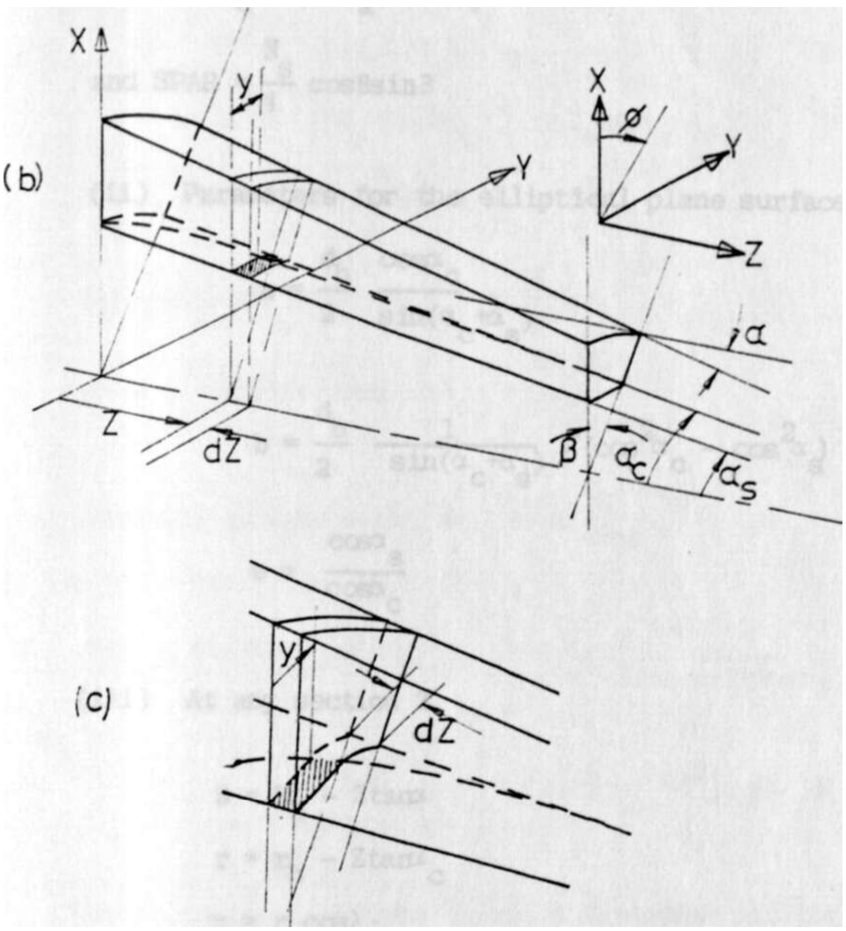

FIGURE 3.8 STRESS AND THE DEFORMATION PATTERN FOR THE DRAWING *OF* REGULAR POLYGONAL TUBE FROM ROUT® THROUGH A CYLINDRICAL DIE

$$\frac{V \quad d \quad e}{2tam_e} \qquad (A-1.eO)$$

where $d_0 = /\{H^2(SPAR)|\}$ (3.94)

and SPAR = $\sum_4^N$ ccsSsinB

(ii) Parameters for the elliptical plane surface

$$a = \frac{\% \quad \cos a_c}{2 \quad \sin(oc_c + ot_s)} \qquad (3.95)$$

$$b = r \quad \cancel{sin(a_c^\wedge)_s} \quad {}^\wedge ccs^{2\wedge} \text{"} \; 006^\wedge \qquad C^{3,96})$$

$$6 = \frac{ccsot}{H \wedge T_c} \qquad (3.97)$$

(iii) At any section Z,

$$R = R^\wedge - Ztam \qquad (3.98)$$

$$r = r_b - Ztam_c \qquad (3.99)$$

$$r_s = r \cos{*}_s \qquad (3.100)$$

$$\frac{{}_b \; /(2aZccsa_s - Z^2)}{\cos a_s}$$

$$\sin As = \sim\sim = r \; \frac{/2aZccsa - Z^2}{cosot_s(r_b - Ztana_c)} \qquad (3.101)$$

$$6 \ll A_c + A_g \qquad (3.102)$$

The cross-sectional area of the tube at any section Z in the deformation zone is given by

$$A = *R^2 3 - (h r j + i r^2 X_c >$$

$$- *RV(Kr_h - Z tam J^2(\cos A_U \sin A_O + A_b)\} \quad (3.103)$$

For a small element dZ at Z,

flat surface area $dA_{si} = y \frac{dZ}{\cos a_s}$ (3.104)

oonical surface area $dA_{c1} = \frac{rX\ dZ}{c}$ (3.105)

tube-die surface area $dA_{c2} = RB_{CQsa}$ (3.106)

$$oA = r\{ (\cos X_s \sin X_s + X_c) \tan a_c + \frac{\sin^2 X_{c}}{\cos a_s \cos X_s}$$

$$\frac{\cdot}{a\ r} - \{ \frac{r(a\cos a - Z)}{(2aZ\cos{}^{\wedge}{}_s - Z)"} rr - r + (2aZc\cos a_s - Z^9")\tan \}\} \quad (3.107)$$

$$-(X_o + X_S)R\tan a$$

Hie forces are resolved in the Z direction and for equilibrium of the element, $\Sigma F_Z = 0$.

$$(a_z + da_z)(A + dA) - c_z dA - P j dA^{\wedge} \sin$$

$$^{+}P_2(dA_{s1} \sin_s + dA_{c1} \sin x_c) - W^{\wedge\wedge}cc\&L$$

$$-M_2 P_2(dA_{s1} \cos a_s + dA_{c1} \cos cc_c) = 0 \quad (3.108)$$

which on rearranging becomes

$$d\sigma_z(A+dA) = - \sigma\text{^}dA + p\text{^}dA\text{^}sirtt$$

$$-p_2(dA_{s1}sinp_{ts+}dA_{c1}si_na_c) + p\text{^}dA\text{^}cosa$$

$$+p_2y_2(dA_{s1}cosa_s+dA_{c1}cosa_c) \qquad (3.109)$$

Equation (3.109) is siirplified by making the following assumptions:-

(i) a mean pressure p_m acts at both the die-tube and plug-tube interfaces,

(ii) a mean coefficient of friction u_m acts at both the die-tube and plug tube interfaces,

(iii) the horizcntal stress a^ and the mean normal pressure P_m are principal stresses

(iv) a mean yield stress Y_m applies.

Applying Tresca's yield criterion,

$$a_Z \sim (\text{"}P_mj = Y_m$$

$$\text{or } o_{*m} = Y_m - a_Z \qquad (3.110)$$

Equation (3.109) after simplifying beccmes

$$d \S_m \} = ds \{-(r^5 dA_{*m}<^1-<T>_m> \text{^}ccsa+si\text{^}dA\text{^}$$

$$+(M_mcosa_s-sinoi_s)dA_{s1}+(y_mcosa_c-sina_c)dA_{c1}\}\} \qquad (3.111)$$

A computer programme is developed to solve equation (3.111) numericallv.

3.8 COMPUTER PROGRAMME

The four sub-programmes consist of:-

(i) the development of the deformation pattern and hence the velocity field,

(ii) the upper bound solution for the polygonal tube drawing ,

(iii) the lower bound solution for the polygonal tube drawing , and

(iv) the upper and lower bound solutions for the corresponding axisymmetric drawing of tube on a conical or cylindrical plug.

In each of the sub-programmes are the following four main components of the flow chart:

(i) the input statement,

(ii) three major Do loops,

(iii) the main programme , and

(iv) print out statements.

The input statement consists mainly of the incoming and outgoing tube dimensions and the stress-strain properties of the material. The three major Do loops generate the number of sides of the bore of drawn section, the die semi-angle and the coefficient of friction.

The main parts of the upper bound solution are:-

(i) conformally mapping triangular elements in the inlet plane to corresponding triangular elements in the exit plane,

(ii) calculation of the flow path parameters for each element,

(iii) optimization of the entry and exit shear surfaces ,

(iv) calculation of the mean equivalent strain,

(v) calculation of strain factors and I_2,

(vi) calculation of the mean draw stress and the die pressure ,

(vii) tabulation of the mean draw stress and the mean die pressure.

The equations for the upper and lower bound solution for axisyrrmetric drawing are reproduced in appendix A-5. The complete programmes are presented in appendix A-3. Sample solutions for the upper and lower bound solution are tabulated in appendix A-4.

Sampled graphical output of the mapped entry and exit tabular sections are shown in Figures 3.9, 3.10 and 3.11 where the points plotted are the centroids of the large triangles at the entry and exit. The flow charts for the

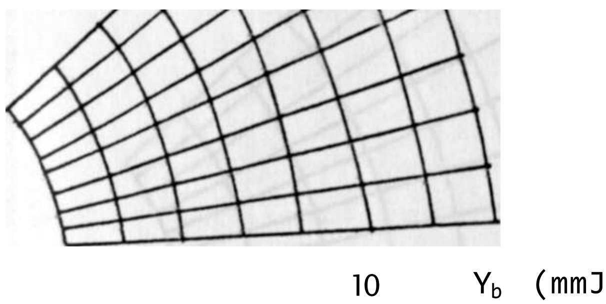

^a) entry plane

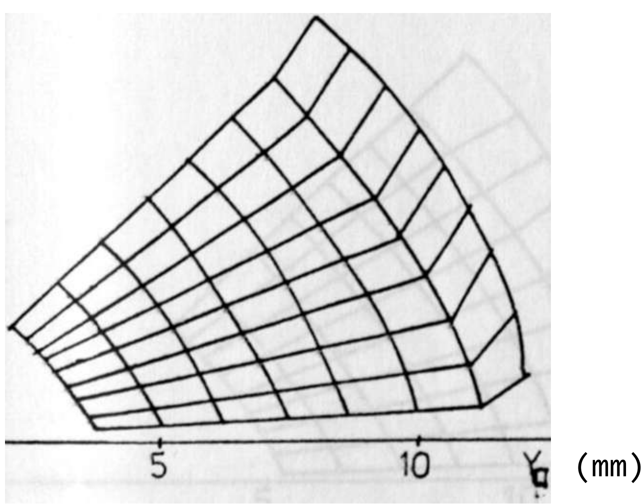

b) exit plane

JRE 3.9 DEFORMATION PATTERN OF THE SYMMETRIC SECTION OF THE SQUARE TUBE FOR THE REDUCTION IN AREA OF 9%

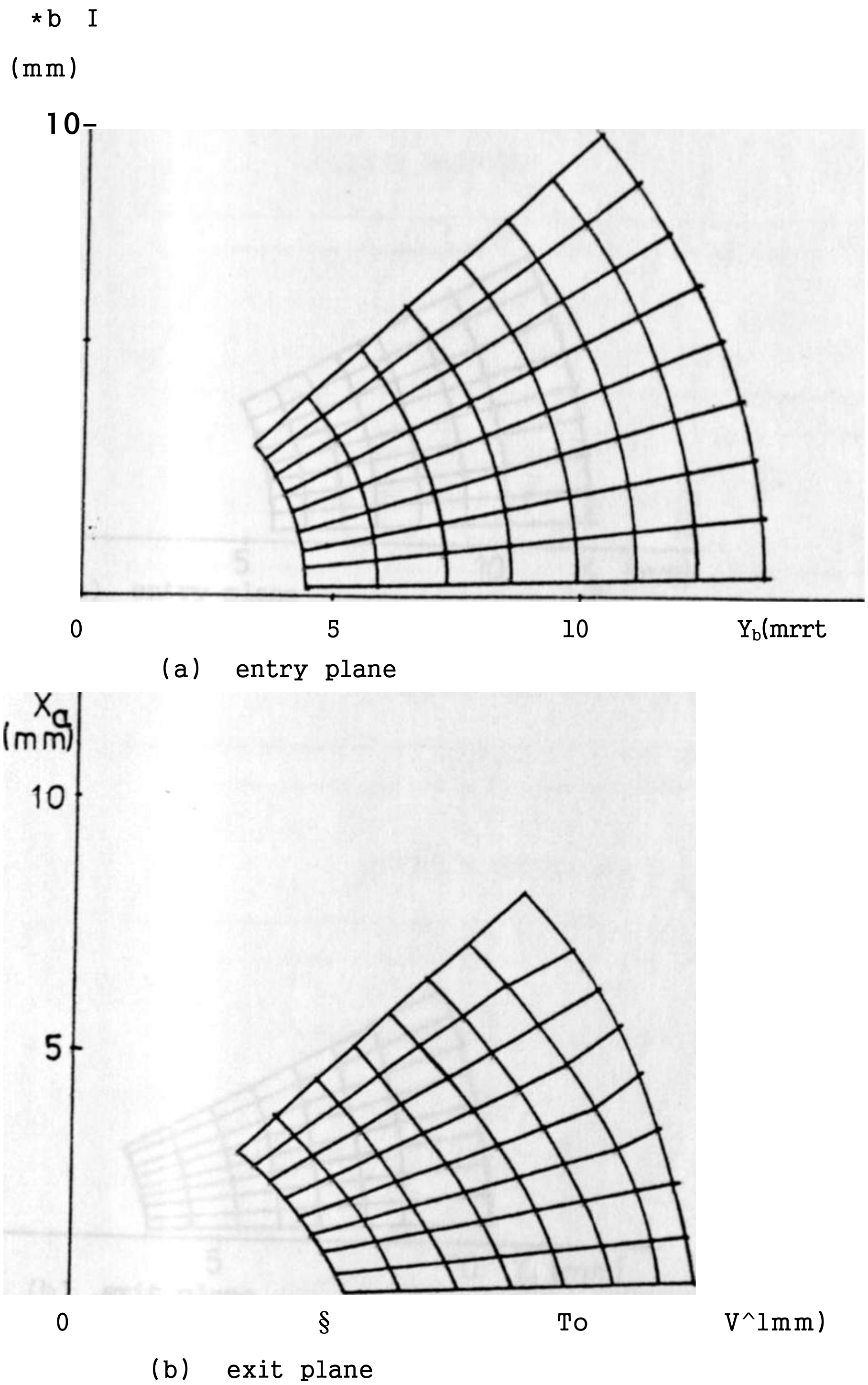

FIGURE 3.10 DEFORMATION PATTERN OF THE SYMMETRIC SECTION OF THE S^ARE TUBE FOR THE REDUCTION IN AREA OF 25%

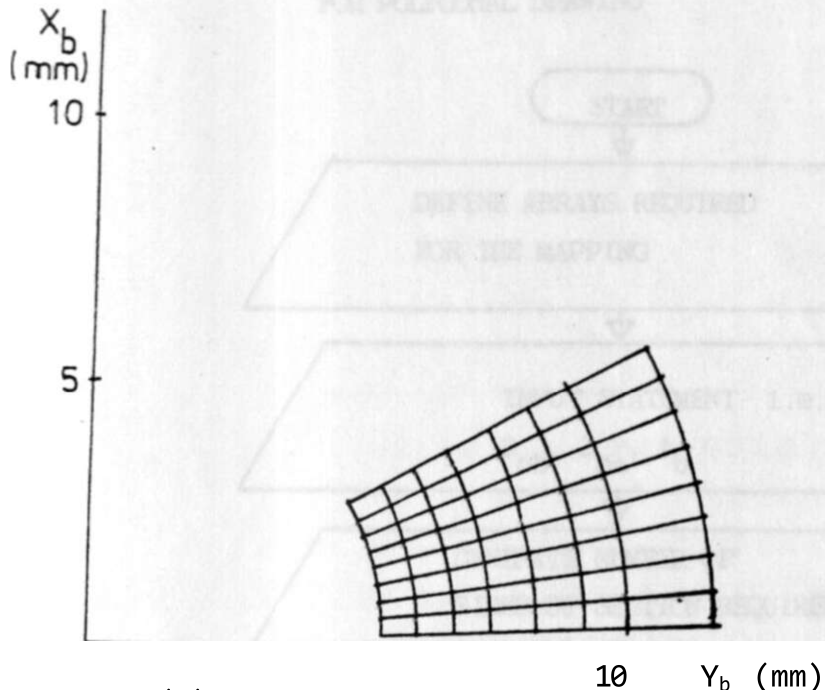

(a) entry plane

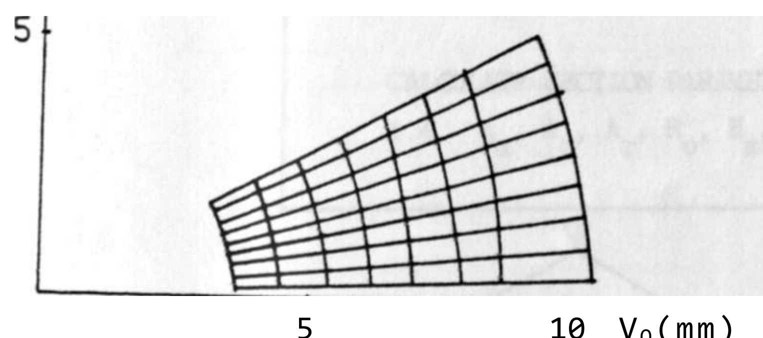

(b) exit plane

FIGURE 3.11 DEFORMATION PATTERN OF THE SYMMETRIC SECTION OF TEE HEXAGCNAL TUBE FOR THE REDUCTION IN AREA OF 15%

FLOW CHART FDR THE UPPER BOUND SOLUTION

FOR POLYGONAL DRAWING

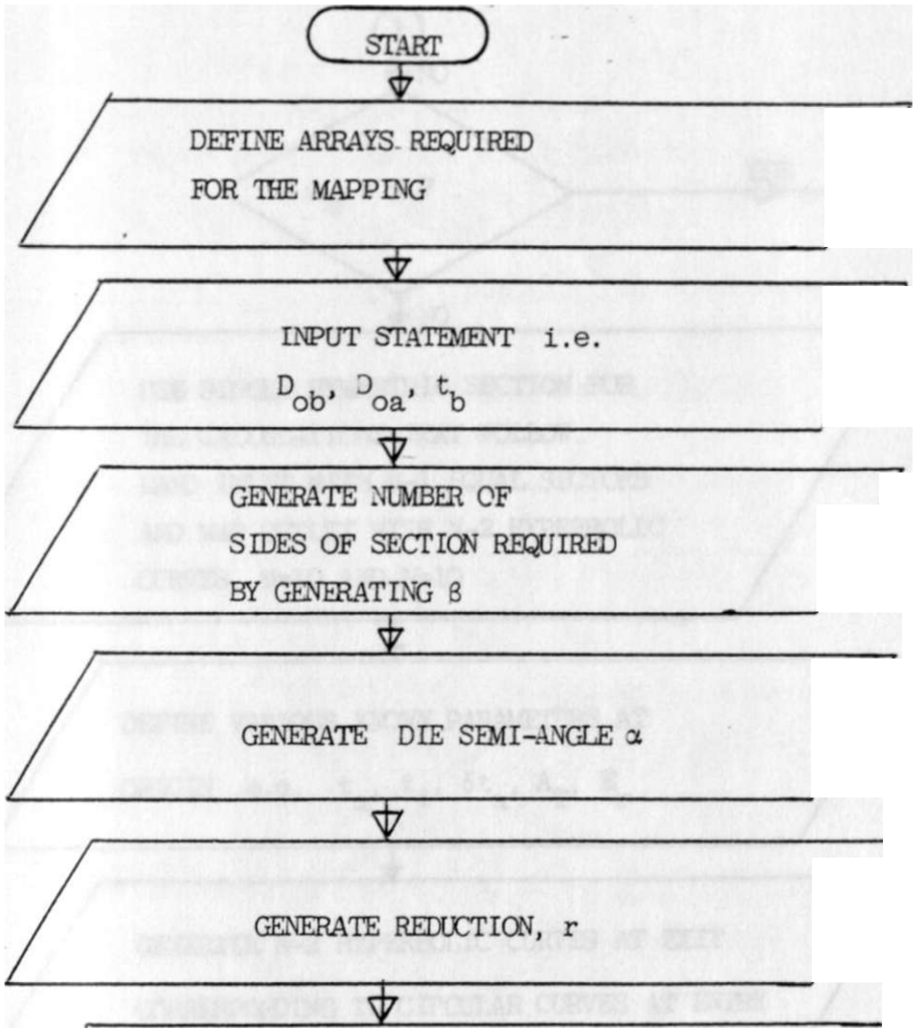

CALCULATE SECTION PARAMETERS

i.e. A_a, A_b, A_r, R_e, H_a,

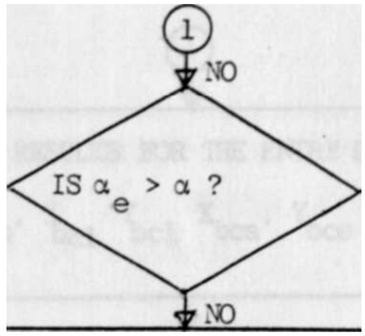

USE SINGLE SYMMETRIC SECTION FOR
THE CALCULATIONS THAT FOLLOW.
BAND INLET WITH M-1 EQUAL SECTORS
AND MAP OUTLET WITH N-2 HYPERBOLIC
CURVES, M=10 AND N=10

DEFINE VARIOUS KNOWN PARAMETERS AT
ORIGIN e.q. $t^{\wedge}$ $l_{\pm}$, $A^{\wedge}$, E_r

GENERATE N-2 HYPERBOLIC CURVES AT EXIT
CORRESPONDING TO CIRCULAR CURVES AT ENTRY

CALCULATE GEOMETRICAL PARAMETERS e.£
l_v x., y_v A E_r, A_s, ^

CALCULATE CO-ORDINATES OF TRIANGLES AT
INLET AND CORRESPONDING CENTROEDS

i

PRINT RESULTS FOR THE ENTRY PLANE i.e.

V V ^ W *bcs' Ybcs ^ Er

TO MAP CORRESPONDING TRIANGLES AT EXIT
PLANE, BEGIN WITH TWO KNOWN
CO-ORDINATES. BEGIN WITH LARGE TRIANGLES

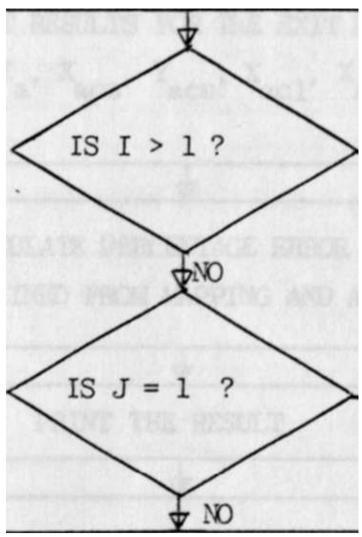

CALCULATE THIRD CO-ORDINATE FROM KNOWN
AREA OF TRIANGLE AND EQUATION OF CURVE
i.e. A CIRCLE

CALCULATE THIRD CO-ORDINATE BY
SUBSTITUTING X AND SOLVING FOR Y

CALCULATE THIRD CO-ORDINATE FROM KNOWN
AREA OF TRIANGLE AND EQUATION OF CURVE
i.e. HYPERBOLA

MAP SMALL TRIANGLES AT EXIT BY BEGINNING WITH TWO KNCWN CO-ORDINATES, AREA AND EQUATION OF

0 — CURVE i.e. HYPERBOLA

CALCULATE THE CENTROIDS OF THE LARGE AND SMALL TRIANGLES AT EXIT

PRINT RESULTS FOR TIE EXIT PLANE i.e.

X_a, Y_a, X_{acs}, Y_{acs} i X_{acl} i X_{acl}

CALCULATE PERCENTAGE ERROR IN AREA OBTAINED FROM MAPPING AND ACTUAL VALUE A

PRINT THE RESULT

CALCULATE RADIAL DISTANCE OF PARTICLES R_{a}> R^

DEFLECTICN ANGLES n» <P AND LENGTH OF FLOW PATH Z FOR ALL (i,j)

OPTIMIZE THE SHEAR SURFACES i.e.

MINIMIZE R(s) FOR 0<t<+1

CALCULATE INTERNAL POWER OF DEFORMATION FACTOR f(s) FOR OPTIMAL VALUE OF t

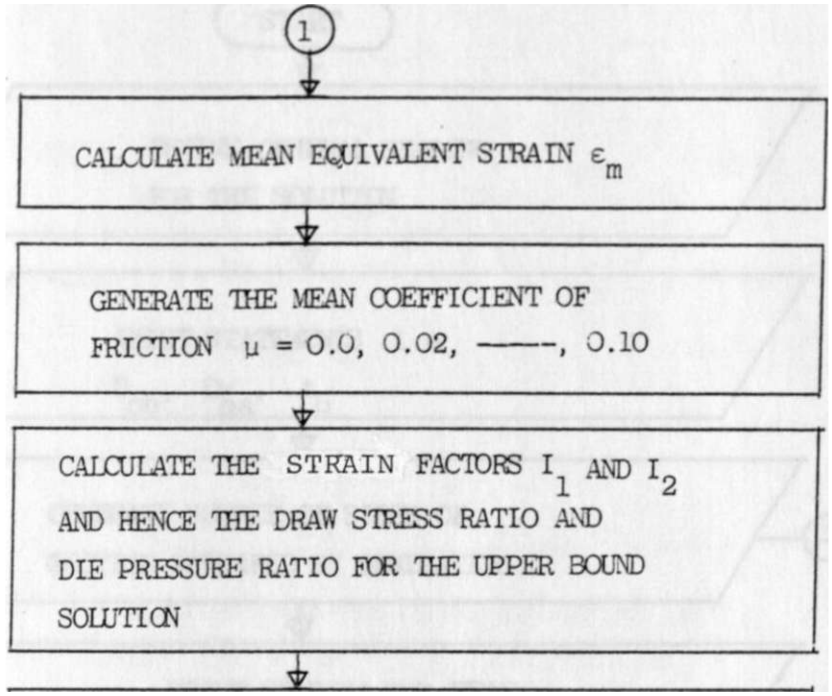

TABULATE THE RESULTS

FLOW CHART FOR THE LOWER BOUND SOLUTION FOR
POLYGONAL DRAWING

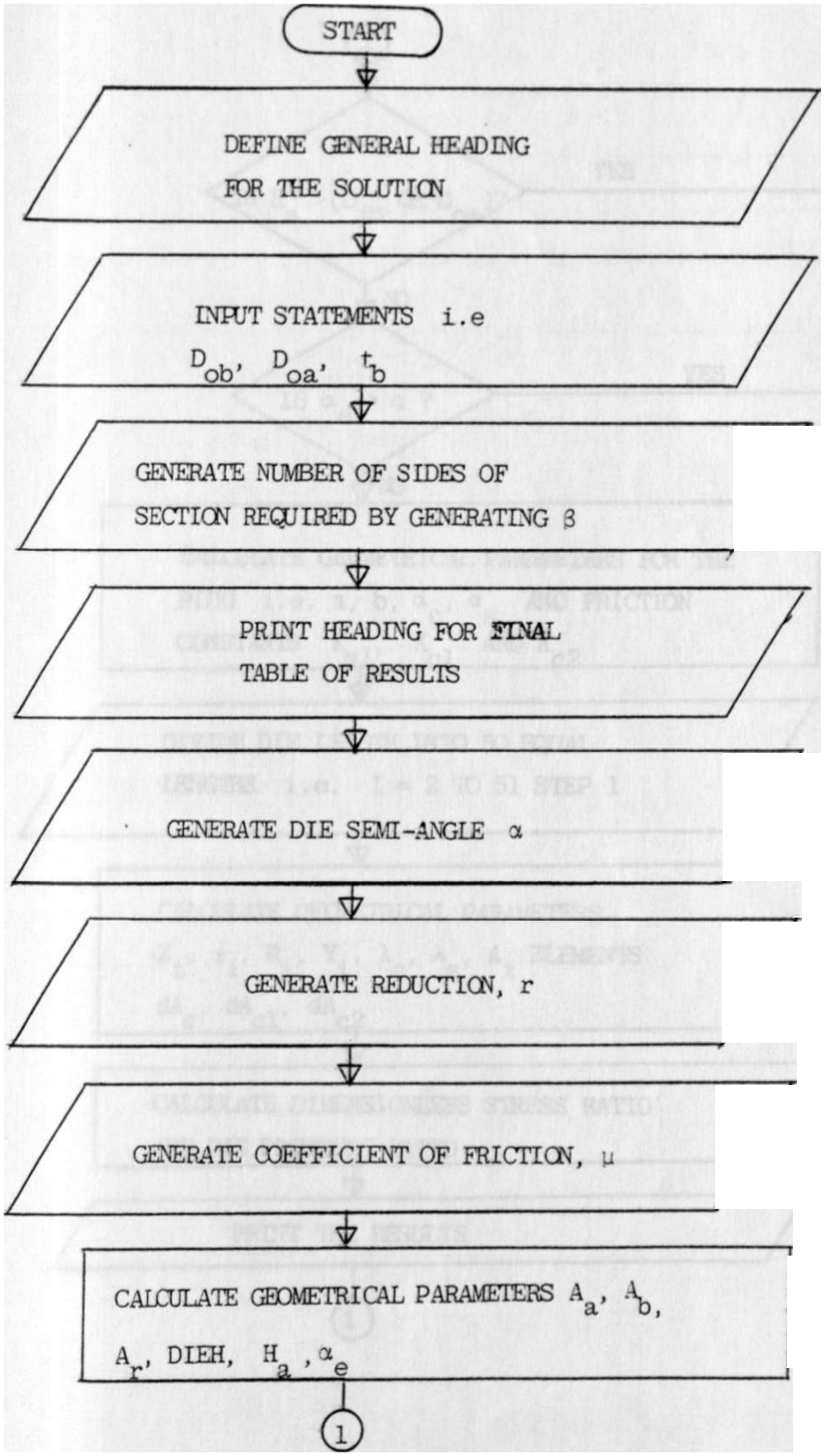

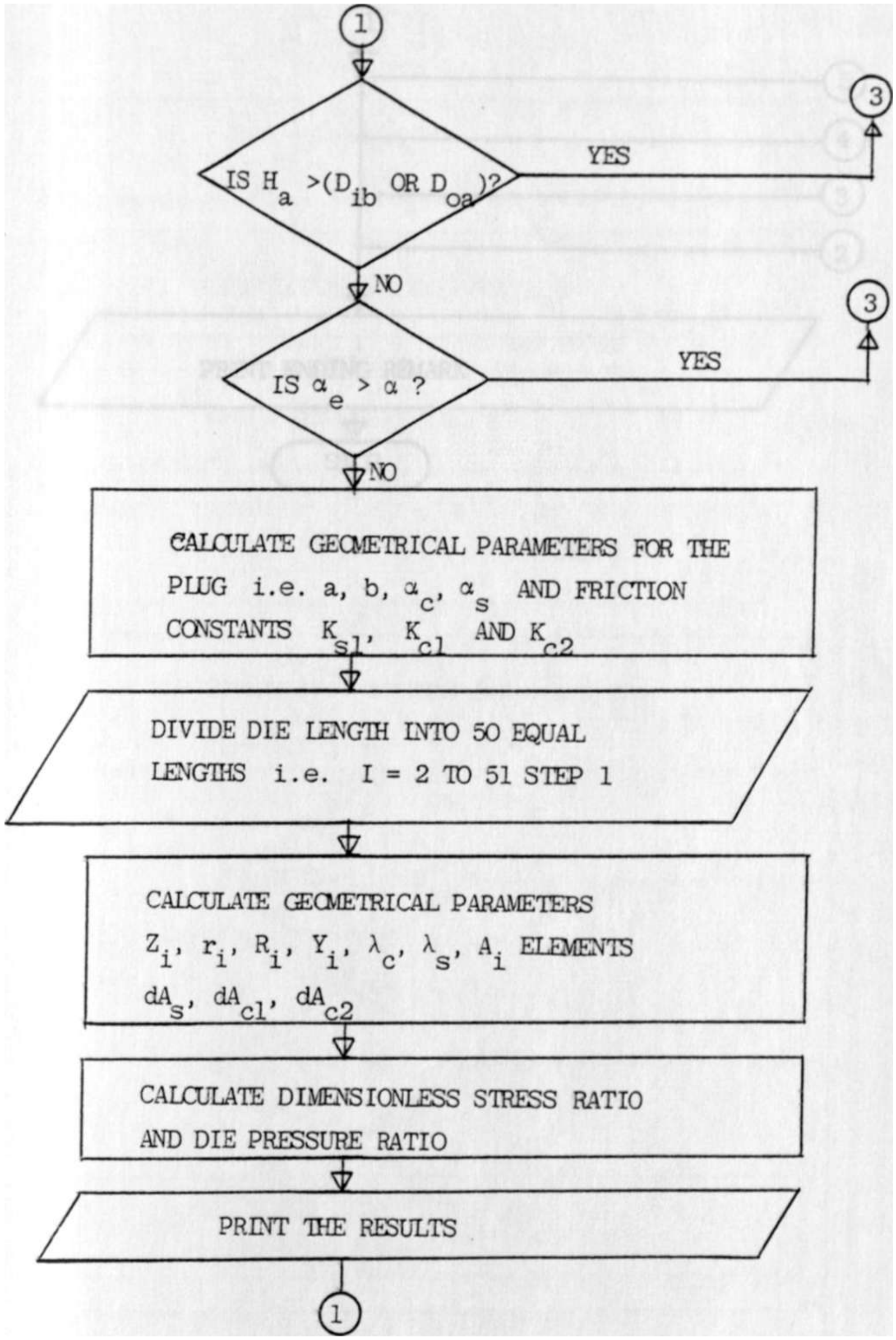
1
IS H_a >(D_{ib} OR D_{oa})?
YES
3
NO
IS α_e > α ?
YES
3
NO
CALCULATE GEOMETRICAL PARAMETERS FOR THE PLUG i.e. a, b, α_c, α_s AND FRICTION CONSTANTS K_{s1}, K_{c1} AND K_{c2}
DIVIDE DIE LENGTH INTO 50 EQUAL LENGTHS i.e. I = 2 TO 51 STEP 1
CALCULATE GEOMETRICAL PARAMETERS Z_i, r_i, R_i, Y_i, λ_c, λ_s, A_i ELEMENTS dA_s, dA_{c1}, dA_{c2}
CALCULATE DIMENSIONLESS STRESS RATIO AND DIE PRESSURE RATIO
PRINT THE RESULTS
1

i

G

PRINT ENDING REMARK

FLON CHART FOR THE UPPER BOUND SOLUTION FOR AXISYMMETRIC DRAWING

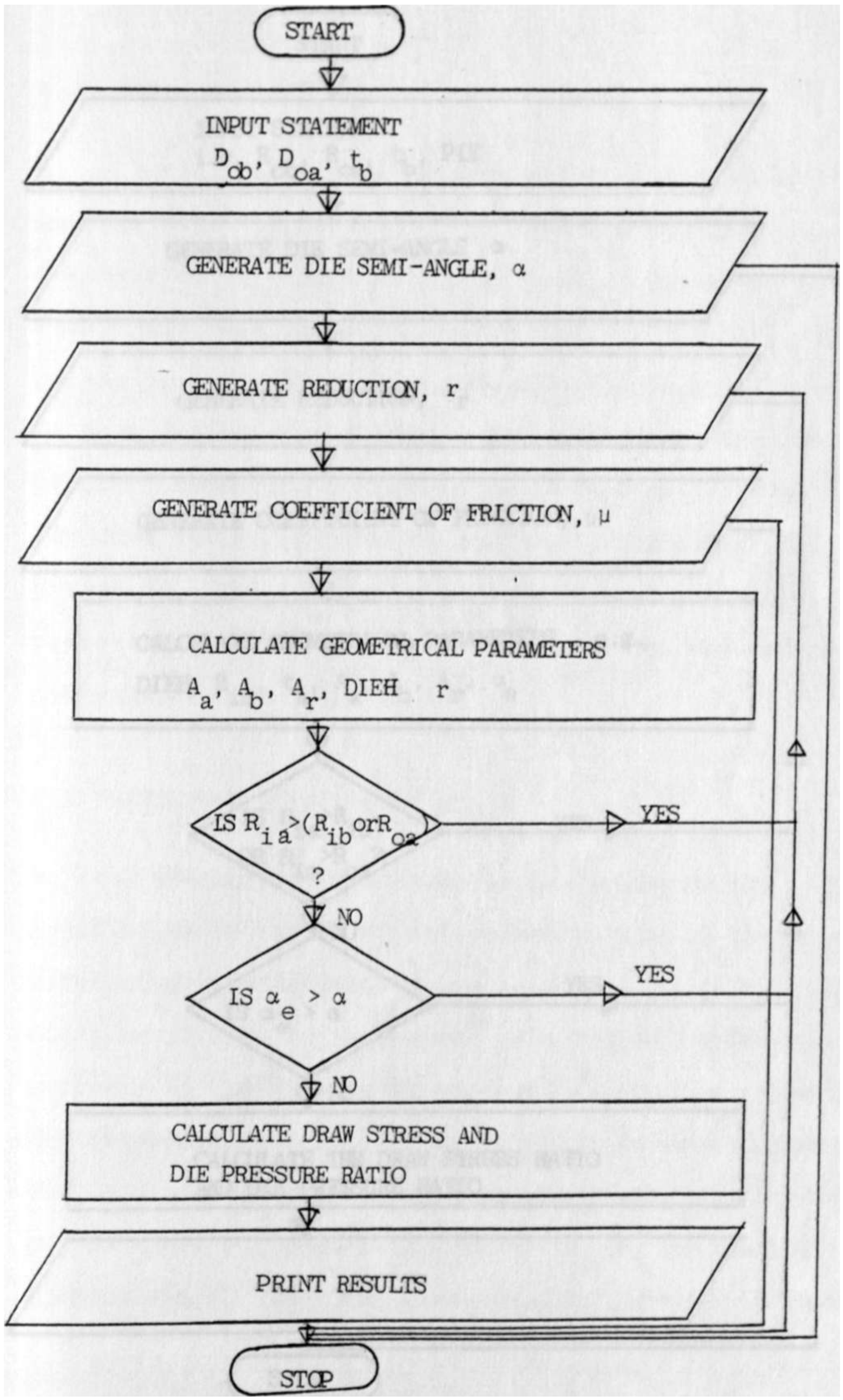

FLOW CHART FOR THE LOWER BOUND SOLUTION FOR AXISYMMETRIC DRAWING

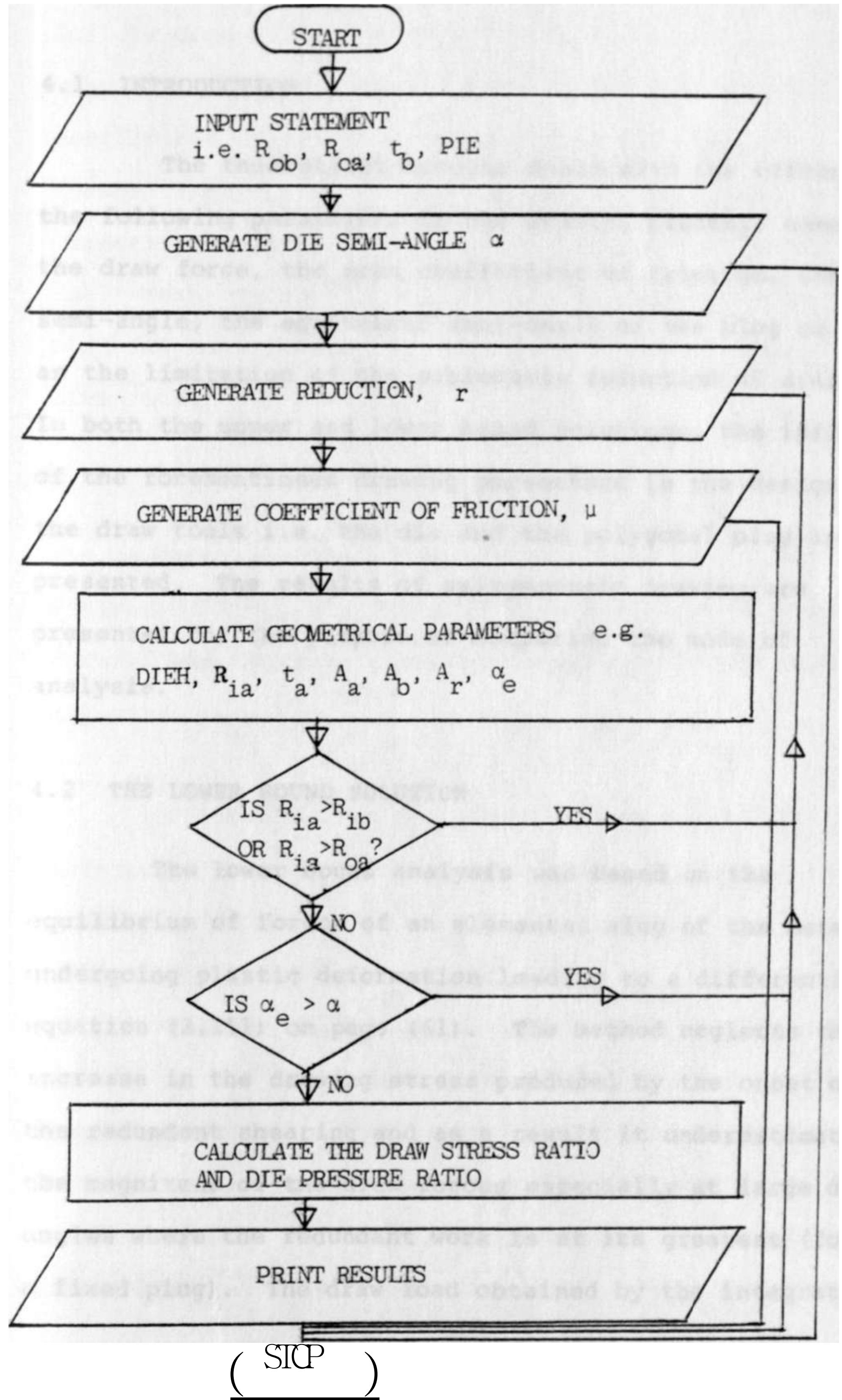

4 RESULTS AND DISCUSSION

4.1 INTRODUCTION

The theoretical account deals with the effect of the following parameters on the drawing process; namely, the draw force, the mean coefficient of friction, the die semi-angle, the equivalent semi-angle of the plug as well as the limitation of the achievable reduction of area. In both the upper and lower bound solutions, the influence of the forementioned drawing parameters in the design of the draw tools i.e. the die and the polygonal plug are presented. The results of axisymmetric drawing are presented for the purpose of comparing the mode of analysis.

4.2 THE LOWER BOUND SOLUTION

The lower bound analysis was based on the equilibrium of forces of an elemental slug of the material undergoing plastic deformation leading to a differential equation (3.111) on page (61). The method neglects the increase in the drawing stress produced by the onset of the redundant shearing and as a result it underestimates the magnitude of the draw forces especially at large die angles where the redundant work is at its greatest (for a fixed plug). The draw load obtained by the integration of the basic differential equation (3.111) can be shown, for the case of N_g = ® to comprise approximately of a constant term and a second term which incorporates the mean coefficient of friction and the die semi-angle (7). The former term represents the homogeneous component which is virtually a constant for a given reduction of area. The later term represents the frictional component and decreases with die semi-angle (i.e. shorter contact lengths), for a given input-output tubing.

Although the lower bound analysis oversimplifies the mechanics of the process by ignoring the effect of the pattern of flow, the analysis involved is usually straight-forward and forms an important conjugate in the upper bound analysis.

Figures 4.1 to 4.5 show the effect of different parameters on the draw force for the axisymmetric tube drawing.

Figures (4.3) and (4.4) show that for a particular reduction, the total draw stress decreases as the die semi-angle increases. The explanation for this is that increasir the die angle implies decreasing the die length and hence surface area of tool-workpiece contact. This results in lower friction work. The homogenous work remains constant

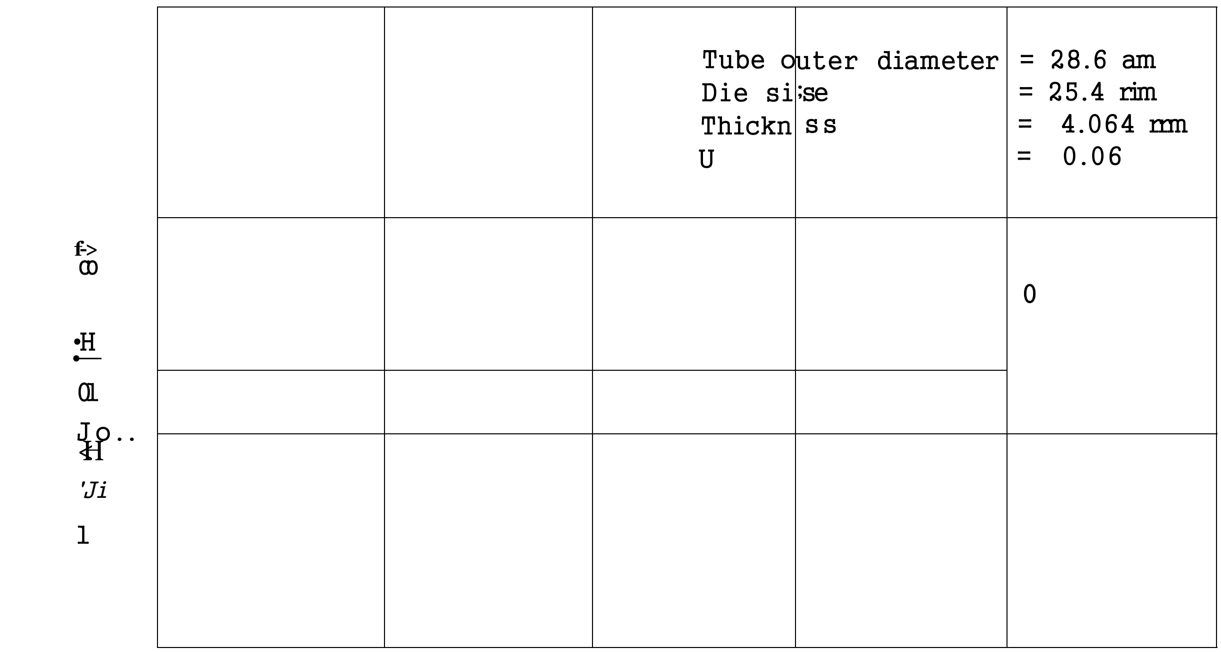

FIGURE 4.1 VARIATION CF THE MEAN DRAW STRESS WITH THE DIE SEMI-ANGLE AND THE EQUIVALENT PLUG SEMI-ANGLE FOR THE LOWER BOUND SOLUTION FOR AXISYWMETKIC DRAWING

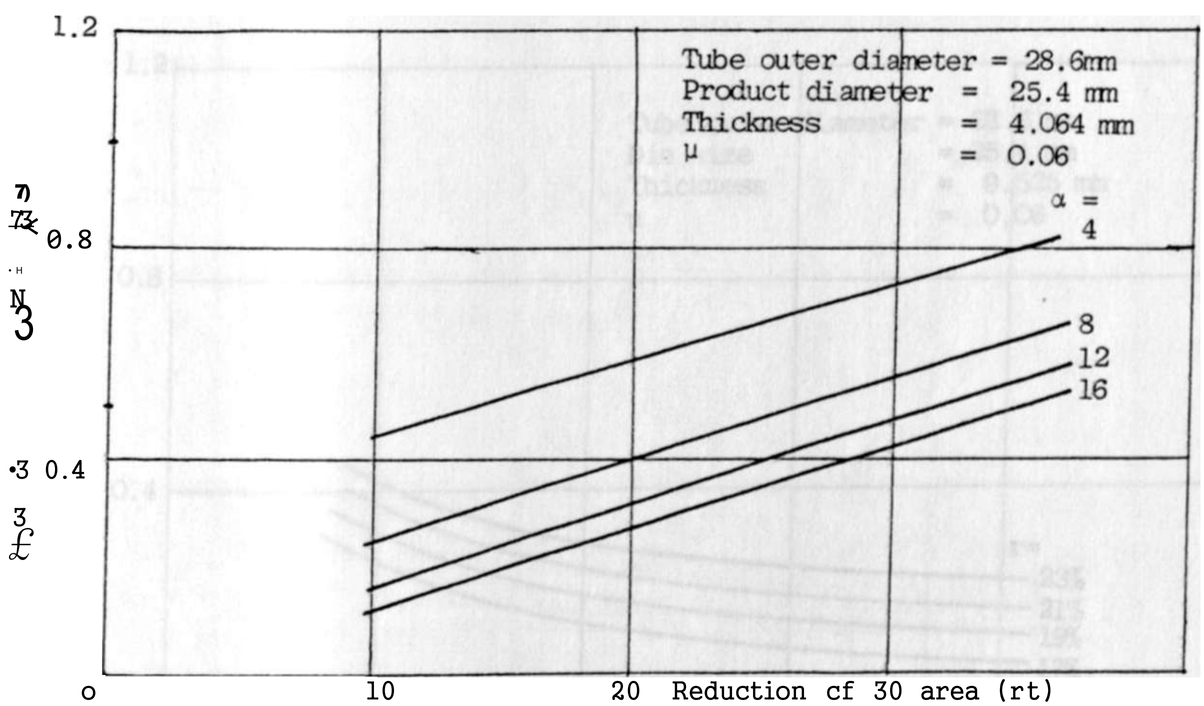

FIGURE 4.2 VARIATION OF THE MEAN DRAW STRESS WITH THE REDUCTION OF AREA AND THE DIE SEMI-ANGLE FOR THE L3VER BOUND SOLUTION FOR AXISYfcMETRIC DRAWING

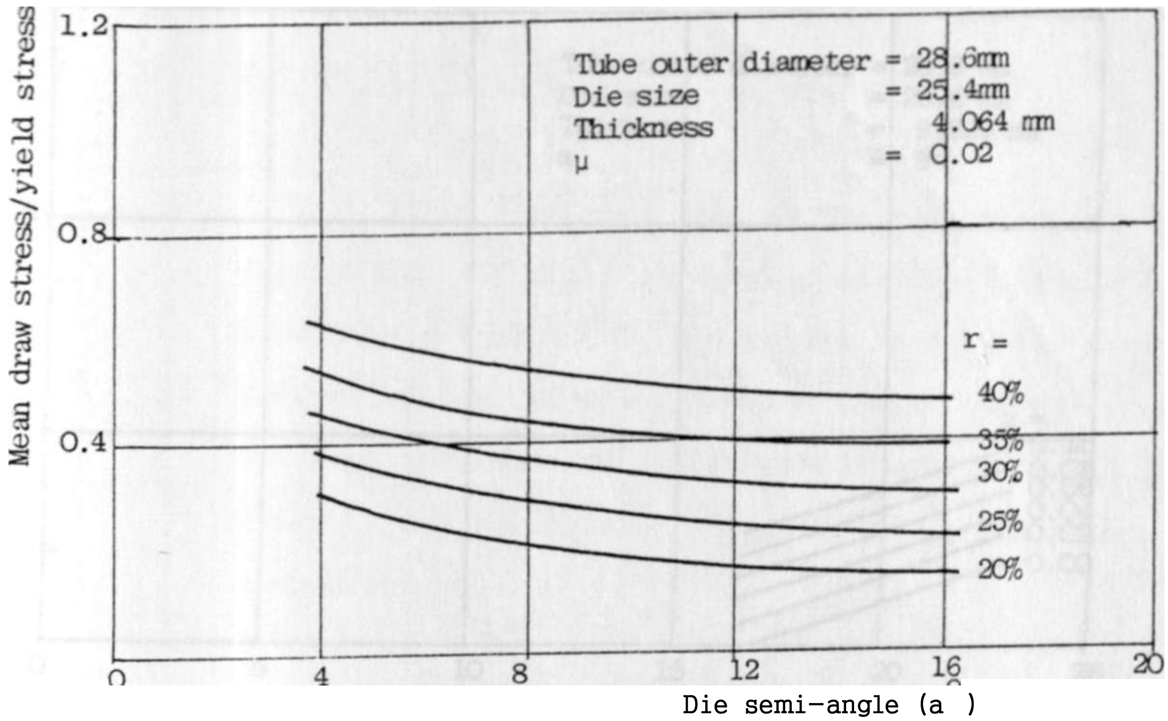

FIGURE 4.3 VARIATION OF THE MEAN DRAW **STRESS** WITH DIE SEMI-ANGLE AND REDUCTION OF AREA FOR THE LCWER BOUND SOLUTION FOR AXISYMETRIC DRAWING

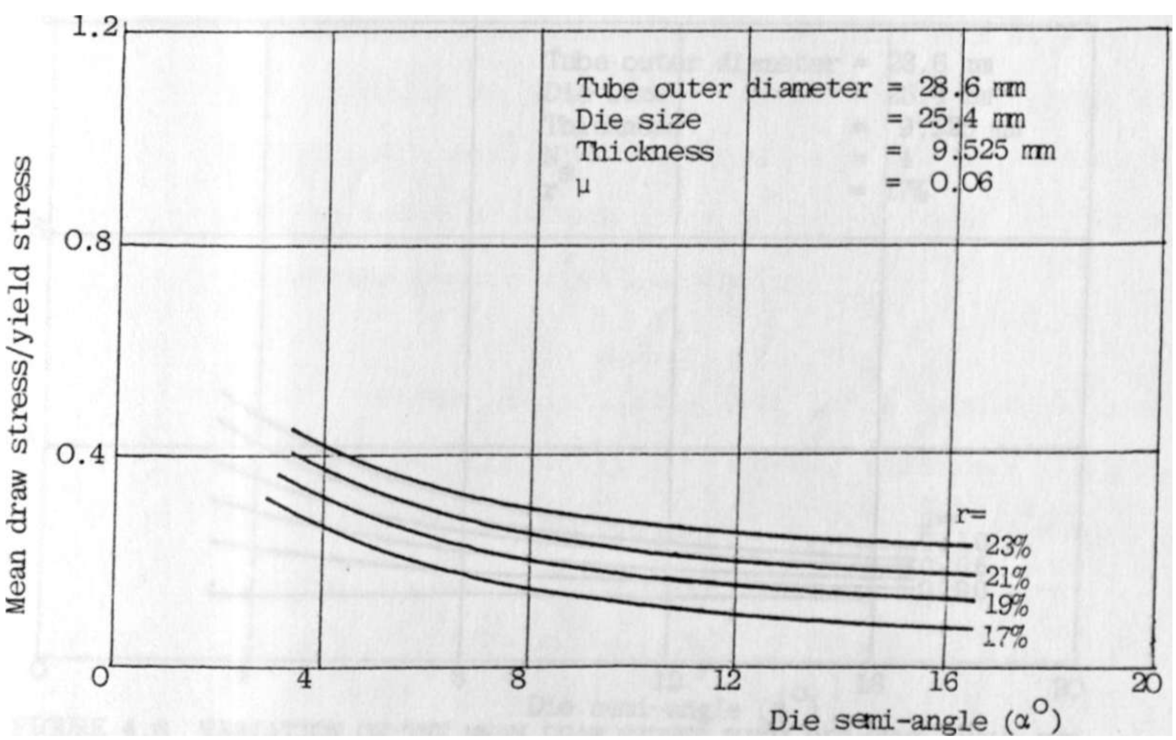

FIGURE 4.4 VARIATION OF THE MEAN DRAW STRESS -WITH THE DIE SEMI-ANGLE AND REDUCTION OF AREA FOR THE LOWER BOUND SOLUTION FOR AXISYMMETRIC DRAWING

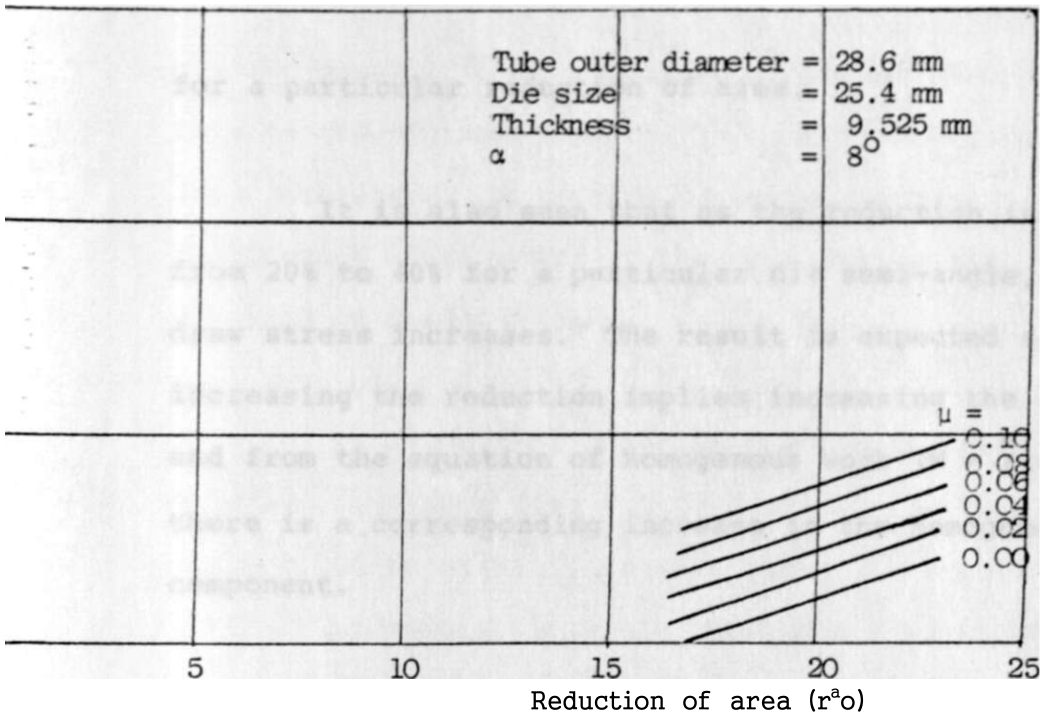

XJRE 4.5 VARIATION OF THE MEAN DRAW STRESS WITH REDUCTION OF AREA AND COEFFICIENT OF FRICTION FOR THE LCWER BOUND SOLUTION FOR AXISYMMETRIC DRAWING

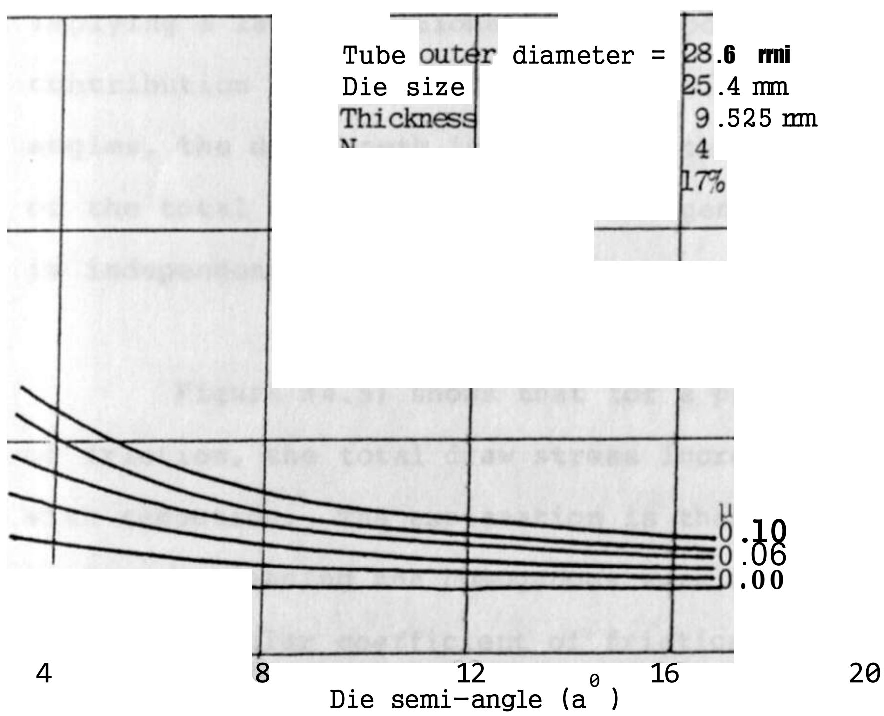

fRE 4.6 VARIATION OF THE MEAN DRAW STRESS WITH DIE SEMI-ANGLE AND COEFFICIENT OF FRICTION FOR THE LOWER BOUND SOLUTION FOR

for a particular reduction of **area.**

It is also seen that as the reduction increases from 20% to 40% for a particular die semi-angle, the tot draw stress increases. The result is expected since increasing the reduction implies increasing the area rat and from the equation of homogenous work (W • Yfcn there is a corresponding increase in the homogenous work component.

Another feature that is observed from the graphs that when the die semi-angle is small (about 4°), the cu are very steep but when the die semi-angle is large (abc 20°), the curves are almost horizontal. The explanation that at very low die semi-angles, the die length is larg implying a large frictional work component as the main contribution to the total draw stress. For large die se angles, the die length is small and the main contributio of the total draw stress is the homogenous component whi is independent of the die angle.

Figure (4.5) shows that for a particular coeffic of friction, the total draw stress increases almost line with reduction. The explanation is that increasing redu implies increasing the homogenous work component. Furth for a particular coefficient of friction, e.g. u « 0, th.

curve crosses the abscissa at a reduction of about 16.5%. This is the minimum possible reduction for the given set o] draw parameters. A smaller reduction implies a smaller an ratio which would occur if the plug semi-angle is less thar 0° which is inadmissible.

It is further observed that as the coefficient of friction increases from 0.0 to 0.1 for a particular reducti the total draw stress increases since the frictional work i directly proportional to the coefficient of friction.

In the case of polygonal drawing, figures (4.6) and (4.7) show that for any coefficient of friction not equal t zero, the total draw stress decreases as the die semi-angle increases. This result is expected since as the die semi-angle increases the frictional work component decreases whi the homogenous work component remains constant for constant reduction of area. When u = 0, the frictional work component is zero and the graph is a straight horizontal line representing the homogenous work component.

Figure (4.8) shows that for any particular die, the total draw stress increases with reduction since the homogenous work component increases with reduction.

Figures (4.9), (4.10) and (4.11) show the variation of the total draw stress with the number of sides of drawn

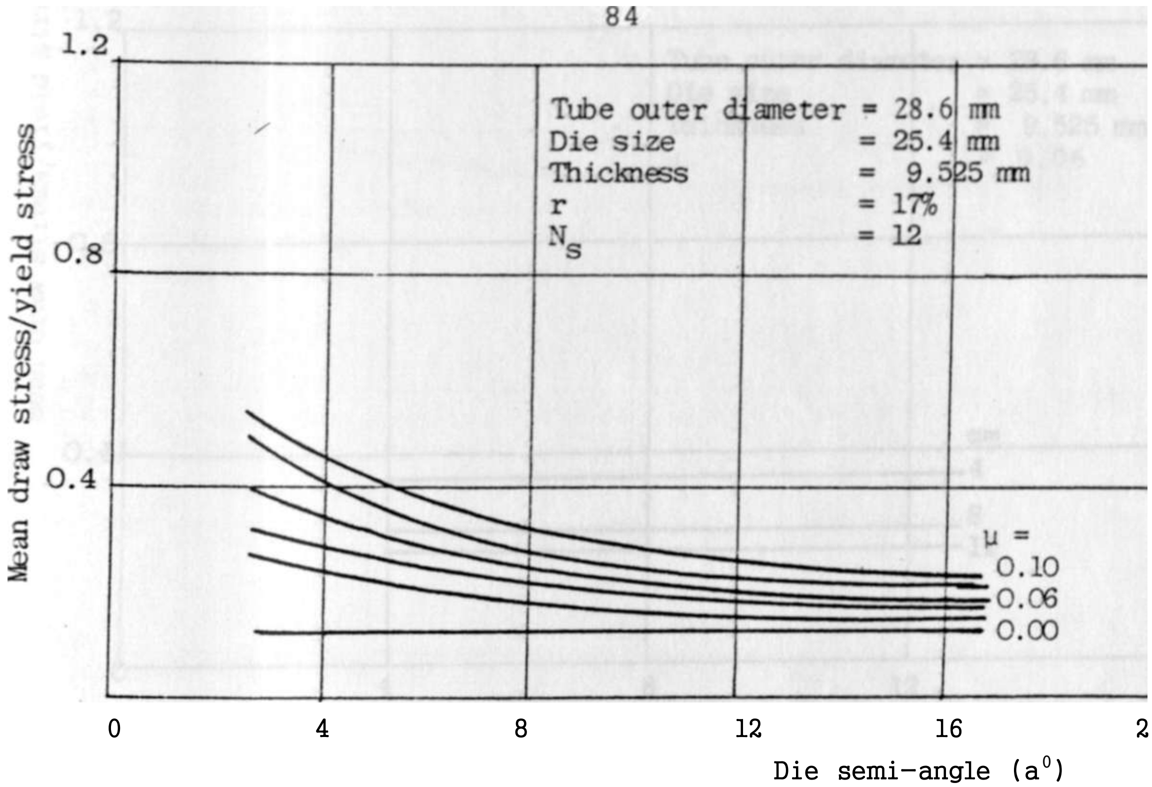

FIGURE 4.7 VARIATION OF THE MEAN DRAW STRESS WITH THE DIE SEMI-ANGLE AND COEFFICIENT OF FRICTION FOR THE LOWER BOUND SOLUTION FOR POLYGONAL TUBE DRAWING

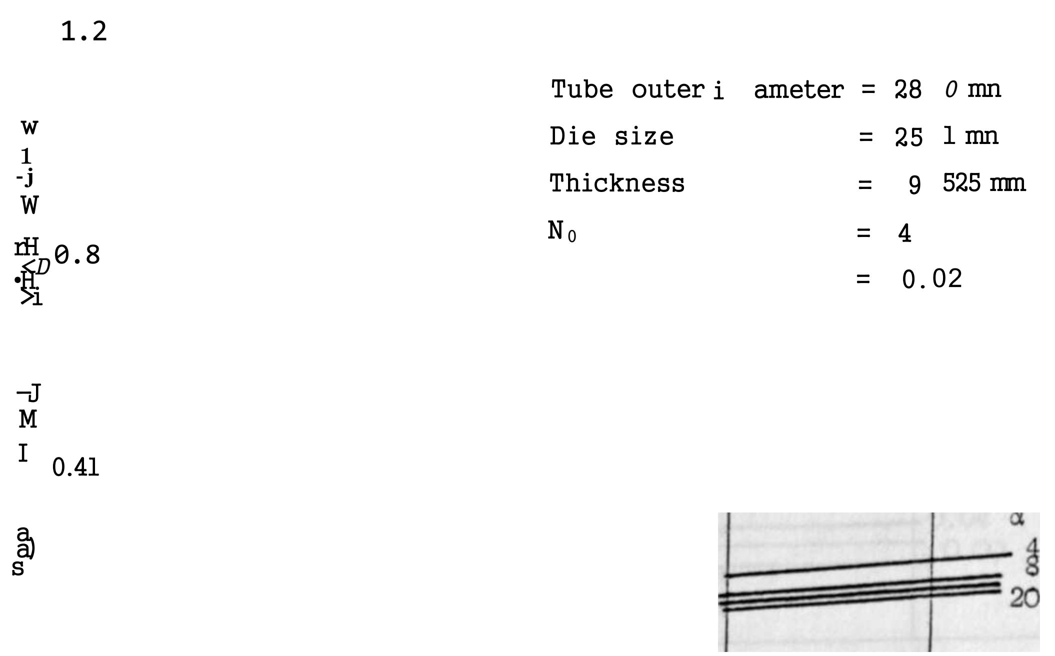

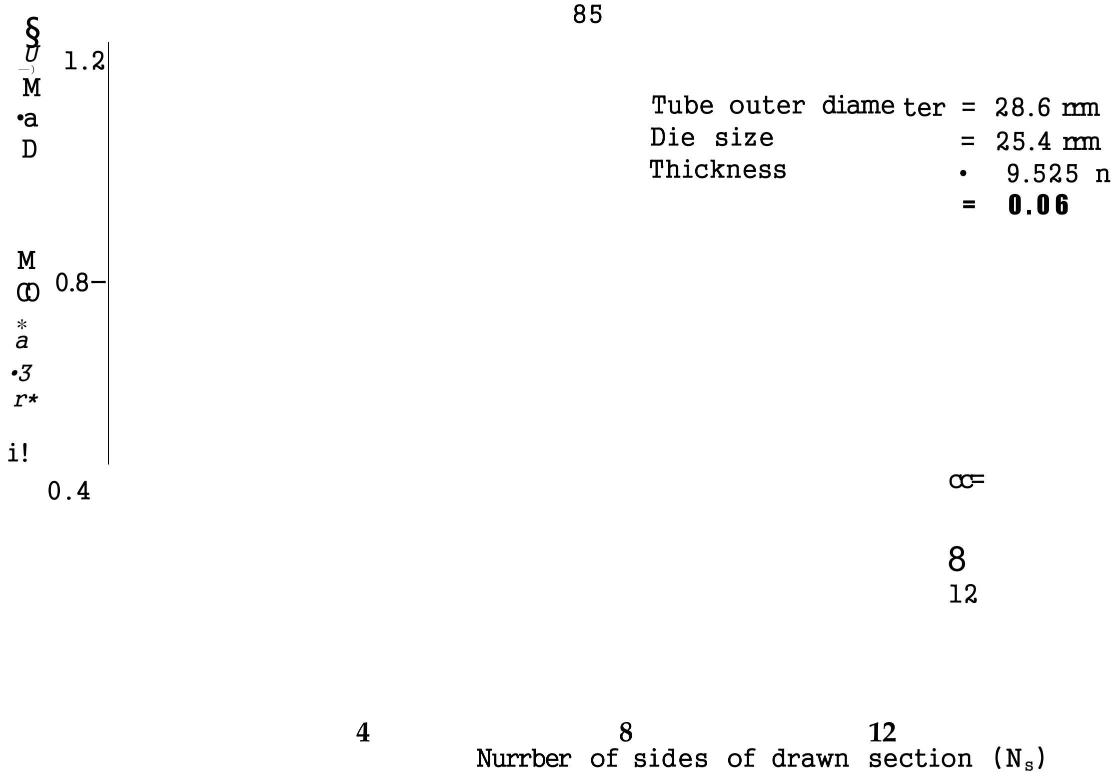

FIGURE 4.9 VARIATION OF TEE MEAN DRAW STRESS WITH NTM3ER OF SIDES POLYGONAL TUBE AND DIE SEMI-ANGLE FOR THE LOWER BOUND SOLUTION" *FOR* POLYGONAL TUBE DRAWING

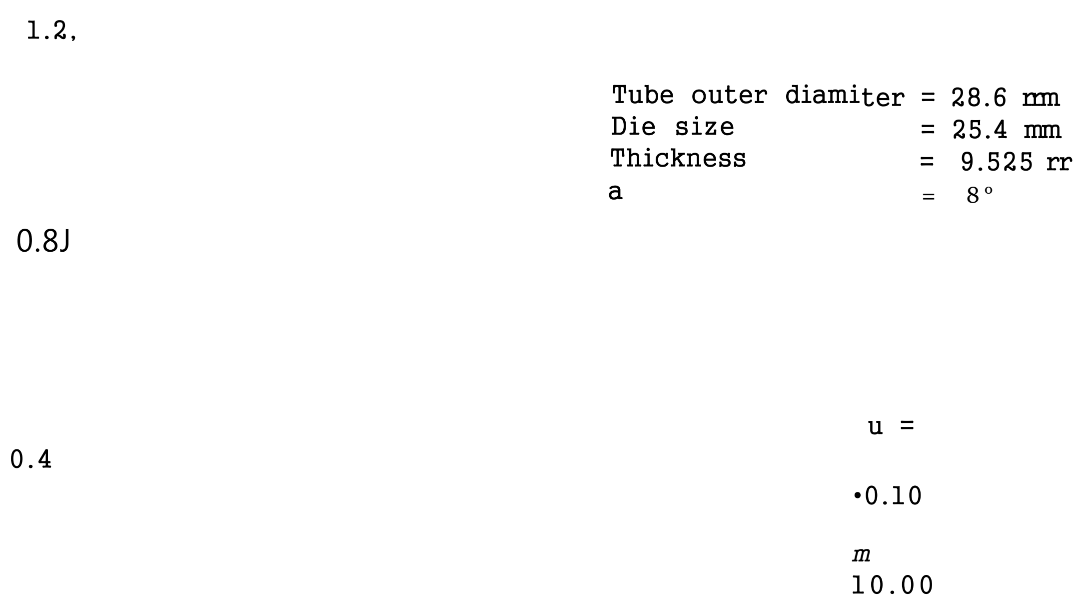

Tube outer diameter 28.6 mm
Die size 25.4 mm
Thickness 9.525 mm
0.06

0.25

0.243

0.24

0 8 12

Number of sides of drawn section (N_s)

FIGURE 4.11 VARIATION OF THE MEAN DRAW STRESS WITH NUMBER OF SIDES OF POLYGONAL PLUG FOR THE LOWER BOUND SOLUTION FOR POLYGONAL TUBE DRAWING

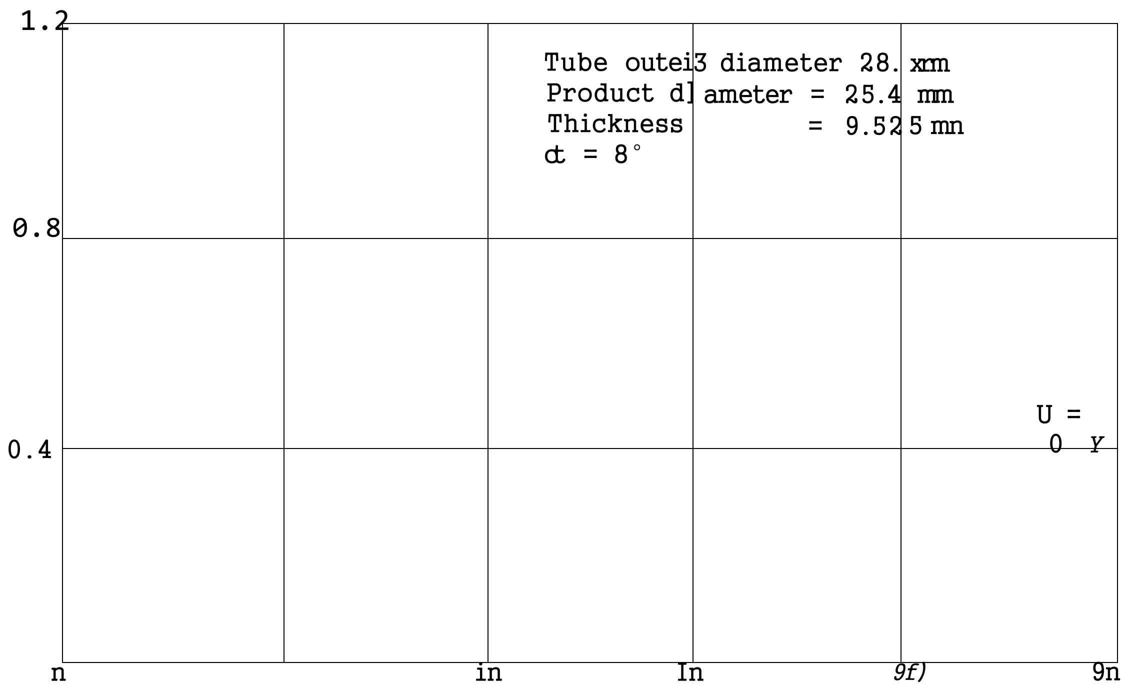

section for a given tube using the concept of close {
drawing. For a given input tube and drawing die, and
constant coefficient of friction, the draw stress dec
slightly with the number of sides. Although the surfc
increases with consequential increase in the frictior
component, there is a decrease in the homogeneous wor
component because of the decrease in reduction of are

4.3 THE UPPER BOUND SOLUTION

The upper bound solution was obtained from a
velocity field that minimizes the energy to effect th
deformation and incorporates an apparent strain metho<
include Coulomb friction. The velocity pattern was
developed by conformal mapping of triangular elements
entry plane to the positions at the exit plane. The
solution therefore accounts for the mode of deformatic

Figure (4.12) shows that for a given die semj
angle and coefficient of friction, the total draw stre
increases with the reduction of area for the case of o
symmetric drawing. Figures (4.13) and (4.14) show the
variation of the total draw stress with the die semi-a
for axisymmetric drawing.

Figure (4.16) shows the variation of the draw
ratio against the die semi-angle in the upper bound so
for drawing a square tube directly from round. At ver
die angles the draw stress ratio tends to infinity. T

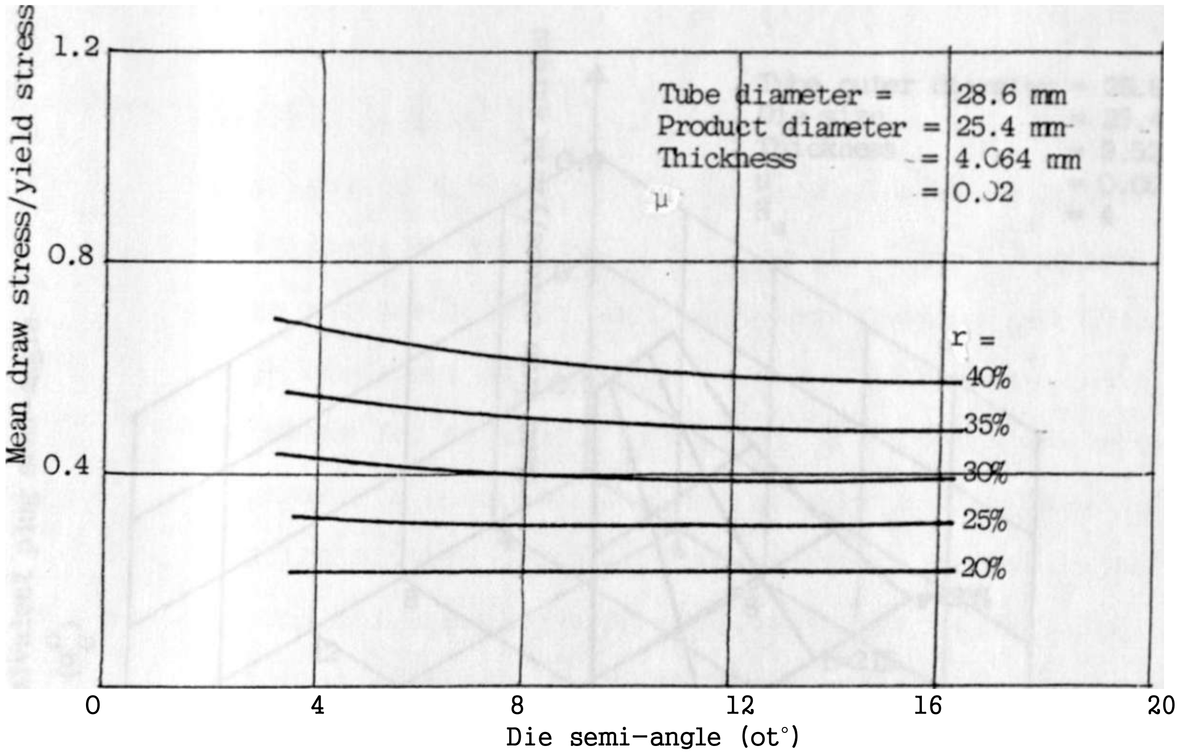

FIGURE 4.13 VARIATION CF THE MEAN DRAW STRESS WITH DIE SEMI-ANGLE AND REDUCTION OF AREA FOR THE UPPER BOUND SOLUTION FOR AXISYMMETRIC DRAWING

1.2t

Tube diarreter = 28.6 17171
Product c iameter = 25.4 mm
Thickness = 9. ?25 mm
= 0.)6

μ •M M o.a

–a rt 0)

I •M ϖ 0.4 ci

23%
21%

J

m

0 4 "§ 12 ~ 1 6 20

Die semi-angle (a)

FIGURE 4.14 VARIATION OF THE MEAN DRAW STRESS WITH DIE SEMI-BANGLE AND REDUCTION OF AREA IN THE UPPER BOUND SOLUTION FOR AXISYMMETRIC DRAWING

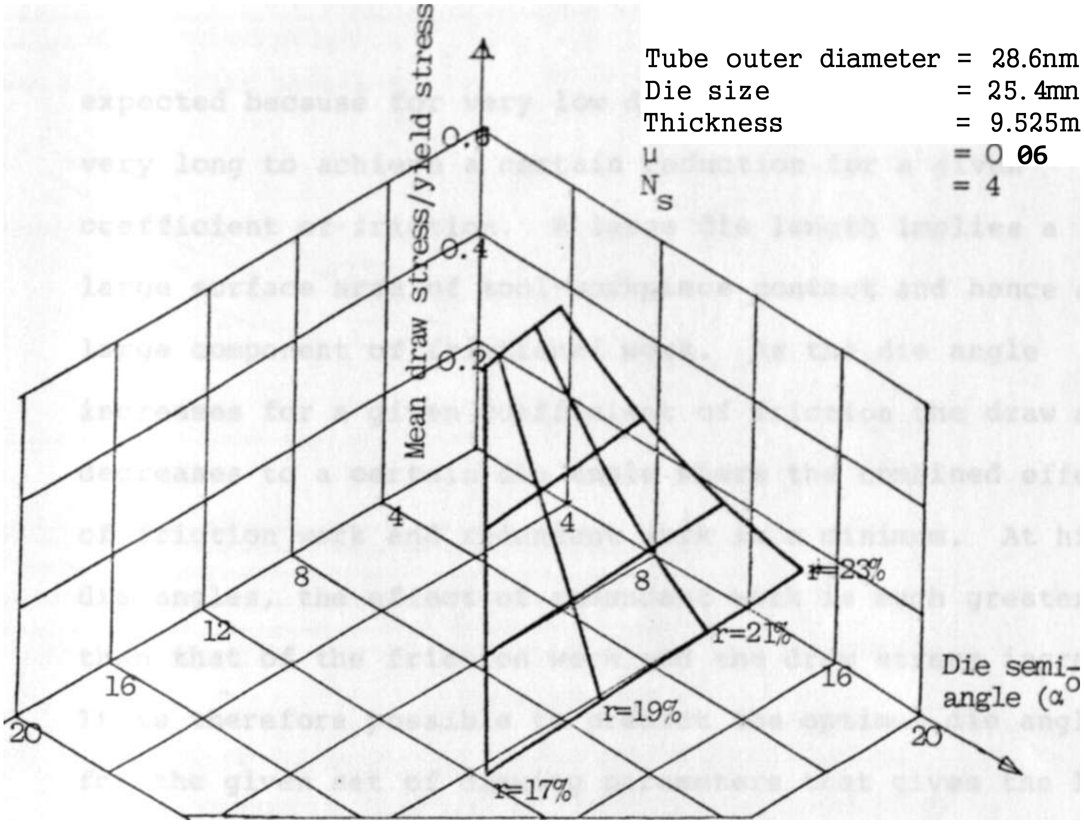

4.15 THREE DIMENSIONAL PLOT OF THE VARIATION. OF THE MEAN DRAW STRESS WITH THE DIE SEMI-ANGLE AND THE EQUIVALENT PLUG SEMI-ANGLE FOR THE LOVER BOUND SOLUTION FOR POLYGONAL TUBE DRAWING

Tube outer diameter	31.75 mm
Die size	25.4 rim
Thidkness	9.525 mm
r	35.9%
N	4

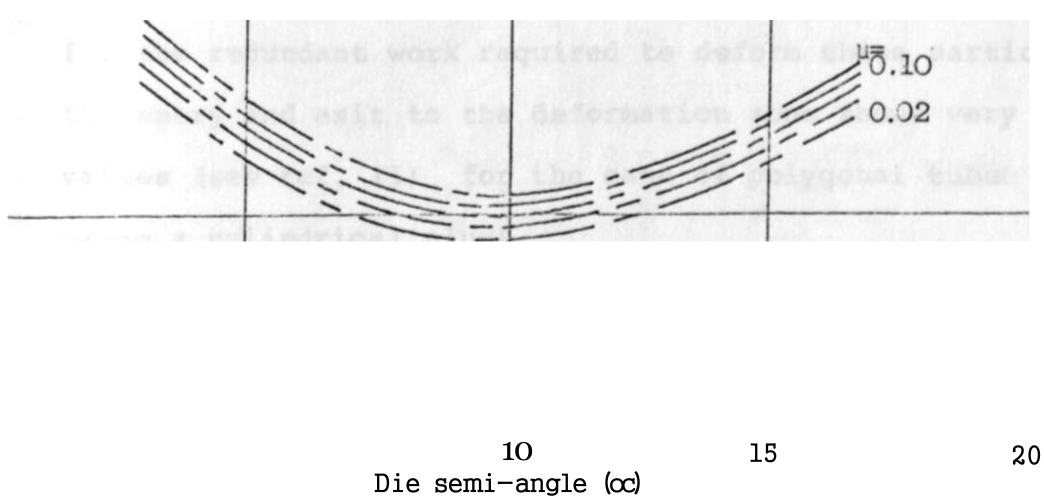

[GURE 4.16 VARIATION OF THE MEAN DRAW STRESS WITH DIE SEMI-ANGLE AND COEFFICIENT OF FRICTION FOR THE UPPER BOUND SOLUTION FOR POLYGONAL TUBE DRAWING expected because for very low die angles, the die must be very long to achieve a certain reduction for a given coefficient of friction. A large die length implies a large surface area of tool-workpiece contact and hence a large component of frictional work. As the die angle increases for a given coefficient of friction the draw stre decreases to a certain die angle where the combined effect of friction work and redundant work is a minimum. At highe die angles, the effect of redundant work is much greater than that of the friction work and the draw stress increase It is therefore possible to predict the optimum die angle for the given set of drawing parameters that gives the leas work of deformation.

Figures (4.17) and (4.18) show a comparison of the upper and lower bound solution for drawing a square tube. In the case of square drawing, the particles of the tube undergo severe distortion as they pass through the deformat passage. Therefore, the upper bound analysis which account for the redundant work required to deform these particles a the entry and exit to the deformation zone shows very high values (see ref. (5) for the case of polygonal tube drawi using a cylindrical plug).

Figures (4.19) and (4.20) shows the values of the upper and lower bound solution for the hexagon and octagon

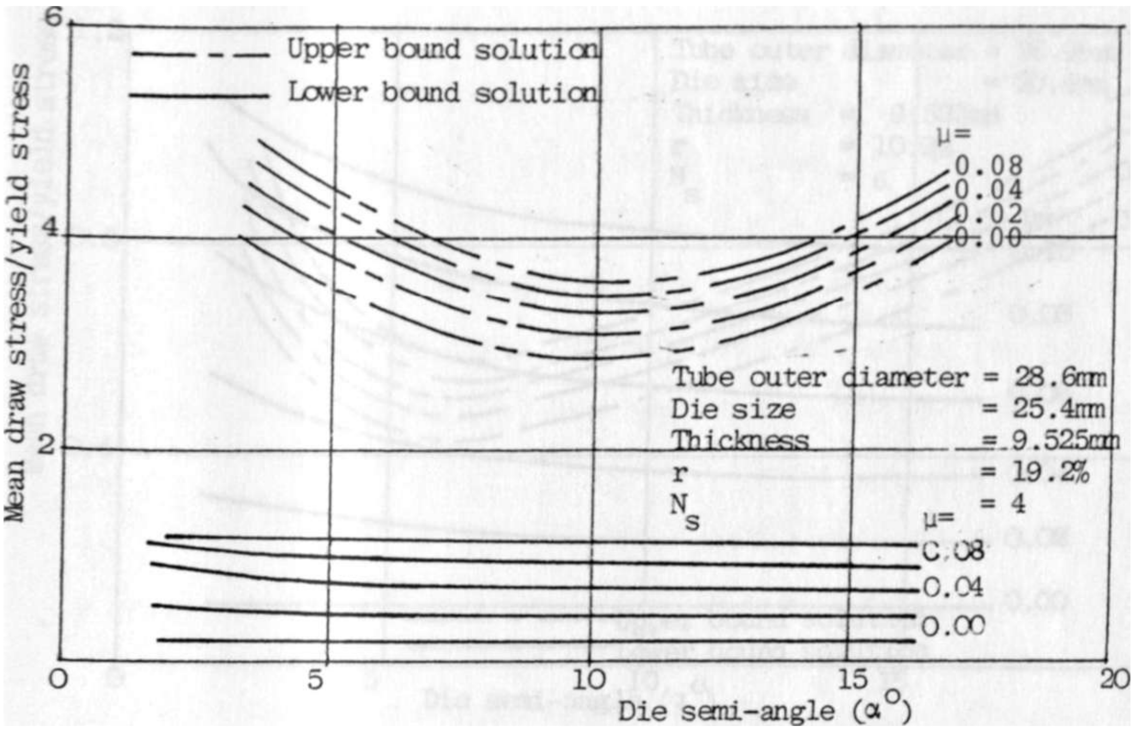

FIGURE 4.17 VARIATION OF THE MEAN DRAW STRESS WITH THE DIE SEMI-ANGLE AND COEFFICIENT OF FRICTION FOR THE UPPER AND LOVER BOUND SOLUTIONS FOR POLYGONAL TUBE DRAWING

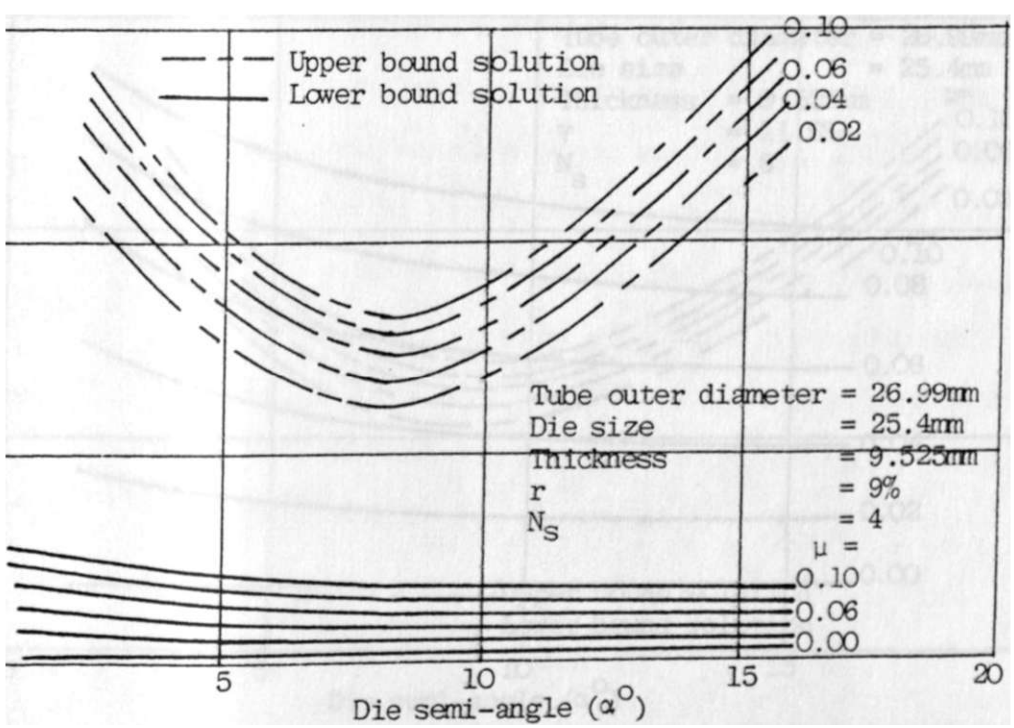

FIGURE 4.18 VARIATION OF THE MEAN DRAW STRESS WITH THE DIE SEMI-ANGLE AMD COEFFICIENT OF FRICTION FOR THE UPPER AND LOWER BOUND SOLUTIONS FOR POLYGONAL TUBE DRAWING

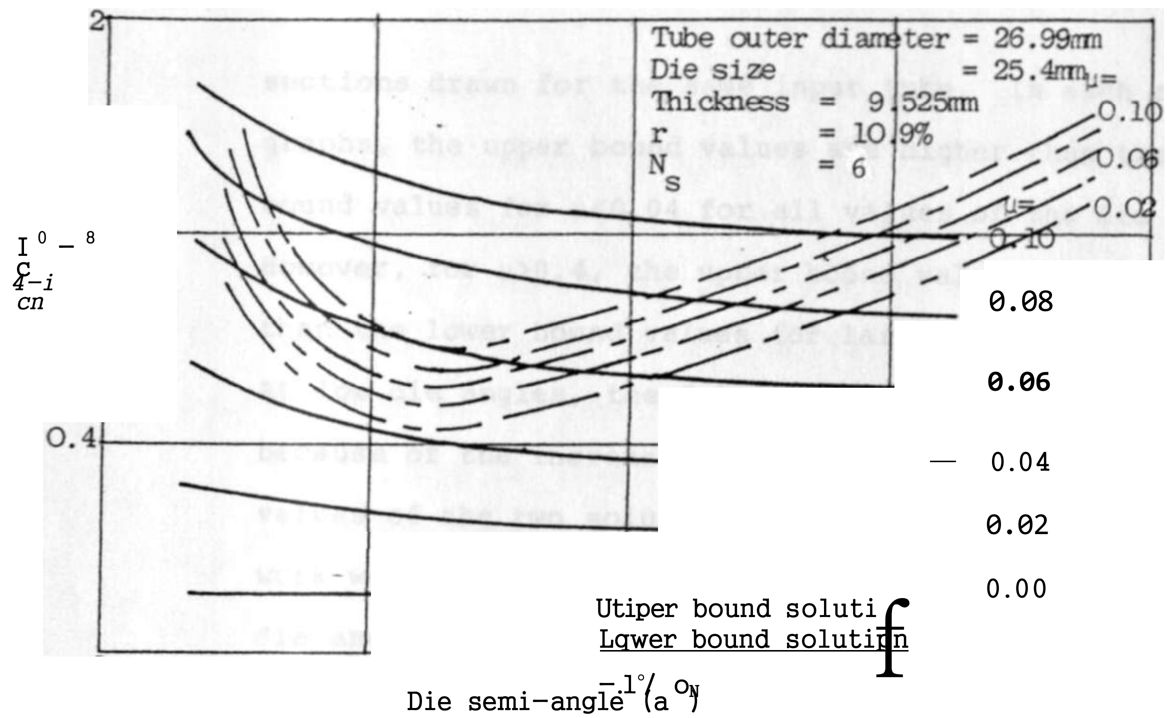

FIGURE 4.19 VARIATICN OF THE MEAN DRAW STRESS WITH THE DIE SEMI-ANGLE AND COEFFICIENT OF FRICTION FOR THE UPPER AND LOWER BOUND SOLUTIONS FOR POLYGONAL TUBE DRAWING

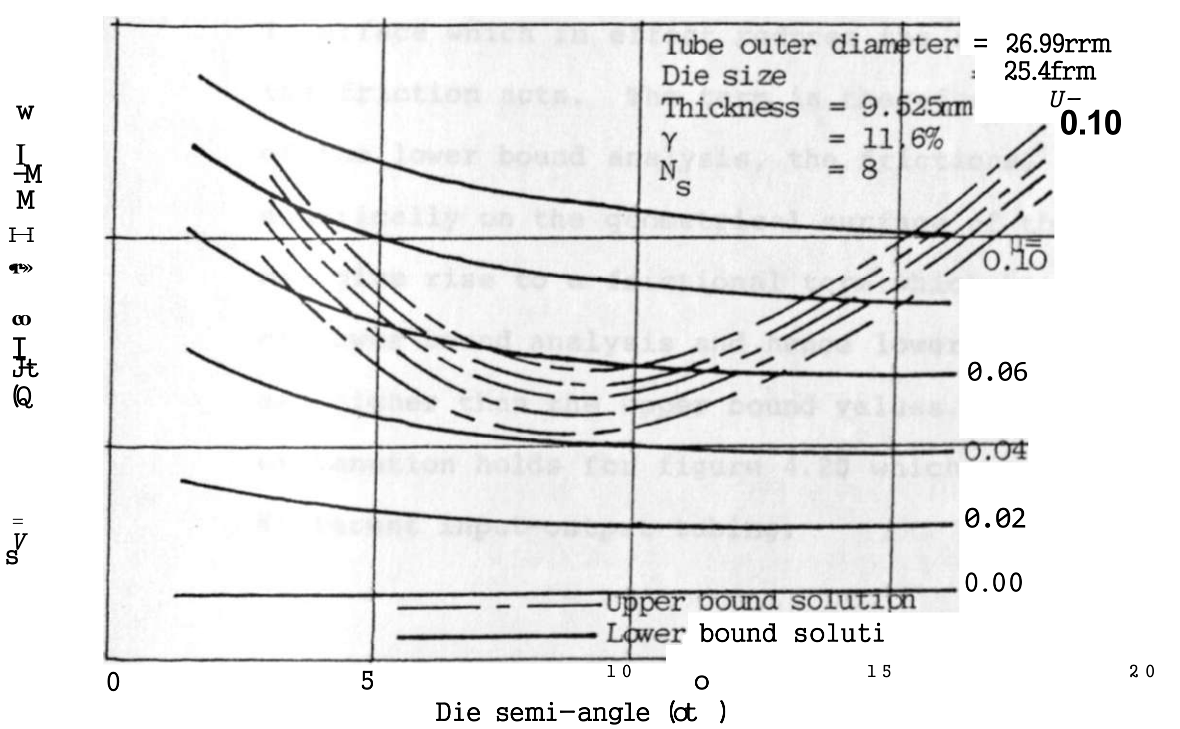

FIGURE 4.20 VARIATICN OF THE MEAN DRAW STOESS WITH THE DIE SEMI-ANGLE AM) COEFFICIENT OF FRICTION FOR THE UPPER AND LOVER BCUND SOLUTIONS FOR POLYGONAL TUBE DRAWING

sections drawn for the same input tube. In each of the graphs, the upper bound values are higher than the lower bound values for $y<0.04$ for all values of the die angle a. However, for $p>0.4$, the upper bound values are only higher than the lower bound values for large and low die angles. At low die angles, the friction contribution is higher because of the increased contact surface area and hence the values of the two solutions almost agree since the redundant work would be low for low reductions. In the case of large die angles, the redundant work predominates and the upper bound solution takes it into account.

At the intermediate die angles, the effects of friction and redundant work on the draw load are comparable. The upper bound analysis assumes an equivalent plug-tube interface which in effect reduces the surface area on which the friction acts. The term is therefore lower. In the case of the lower bound analysis, the frictional term is evaluated numerically on the geometrical surface of the plug. This may give rise to a frictional term which is lower than that of lower bound analysis and hence lower bound values which are higher than the upper bound values. The foregoing explanation holds for figure 4.20 which is drawn for a different input-output tubing.

Figure 4.21 shows the variation of the draw stress against the number of sides of the drawn section from the same input tube. The lower bound curve shows that as the number of sides of drawn section increases the draw stress increases slightly due to the increase in reduction of area. However, in the case of the upper bound values which are higher than the lower bound values, the load decreases with increased number of sides though the homogeneous work increases. This is due to the reduced distortion the element undergo with increased number of sides.

The variation of the draw stress with the semi-angle (a) of the conical die and the plug shape described by the equivalent plug semi-angle (a_e) is shown in Figures (4.15) and (4.23). The graphs enable the capacity of the draw bench to be estimated to produce a given input-output tubing, the selection of the optimum draw tools and lubricant which give the least work of deformation.

Tube outer diameter 26.99
Die size 25.4
Thickness 9.525
0.Q4
10*
r for N =4,6 9.0,10.9
and 8 and 11.64

Upper bound solut
Lcwer bound solut

0 8

Nunber of sides of drawn section (N_3)

FIGURE 4.21 VARIATION OF THE MEAN DRAW STRESS WITH NUMBER OF SIDES OF DRAWN SECTION FOR THE UPPER AND LOWER BOUND SOLUTIONS FOR POLYGONAL TUBE DRAWING

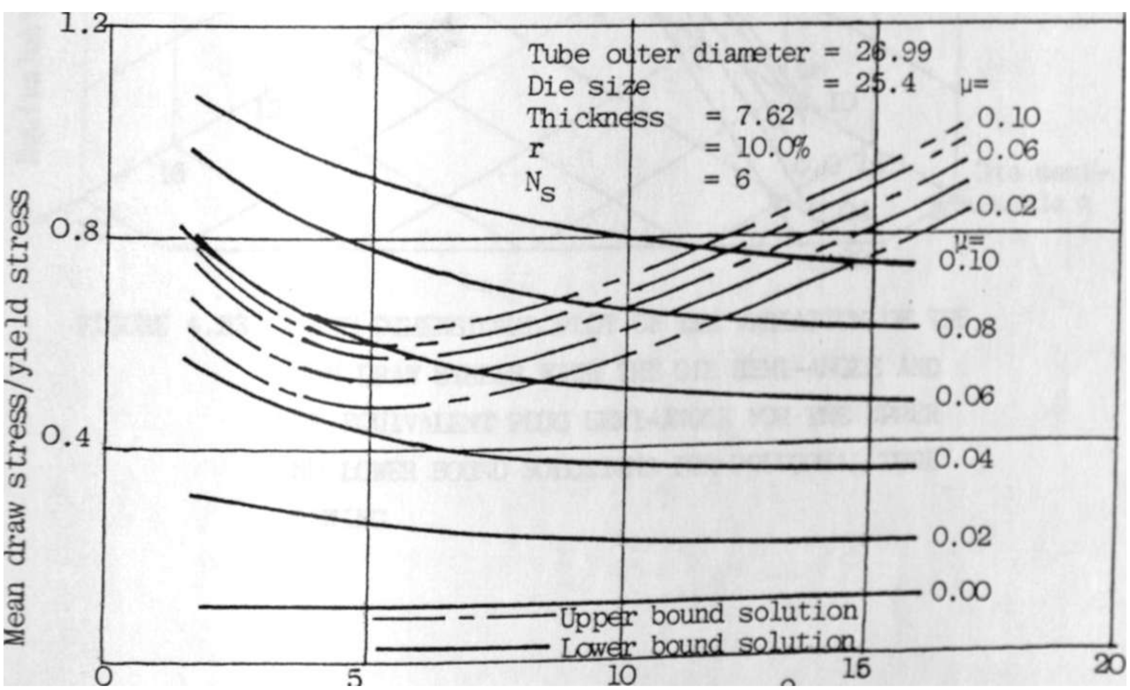

Die semi-angle (a)

FIGURE 4.22 VARIATION OF THE MEAN DRAW STRESS WITH DIE ^ ^ ^ AND COEFFICIENT OF FRICTION FOR THE UPPER AND LOWER BCUMD SOLUTIONS FOR POLYGONAL TUBE DRAWING

Tube outer diametei*=31.75fnn
Die size =25.4rrm
Thickness =9.525mn
r =36%
N_s =4

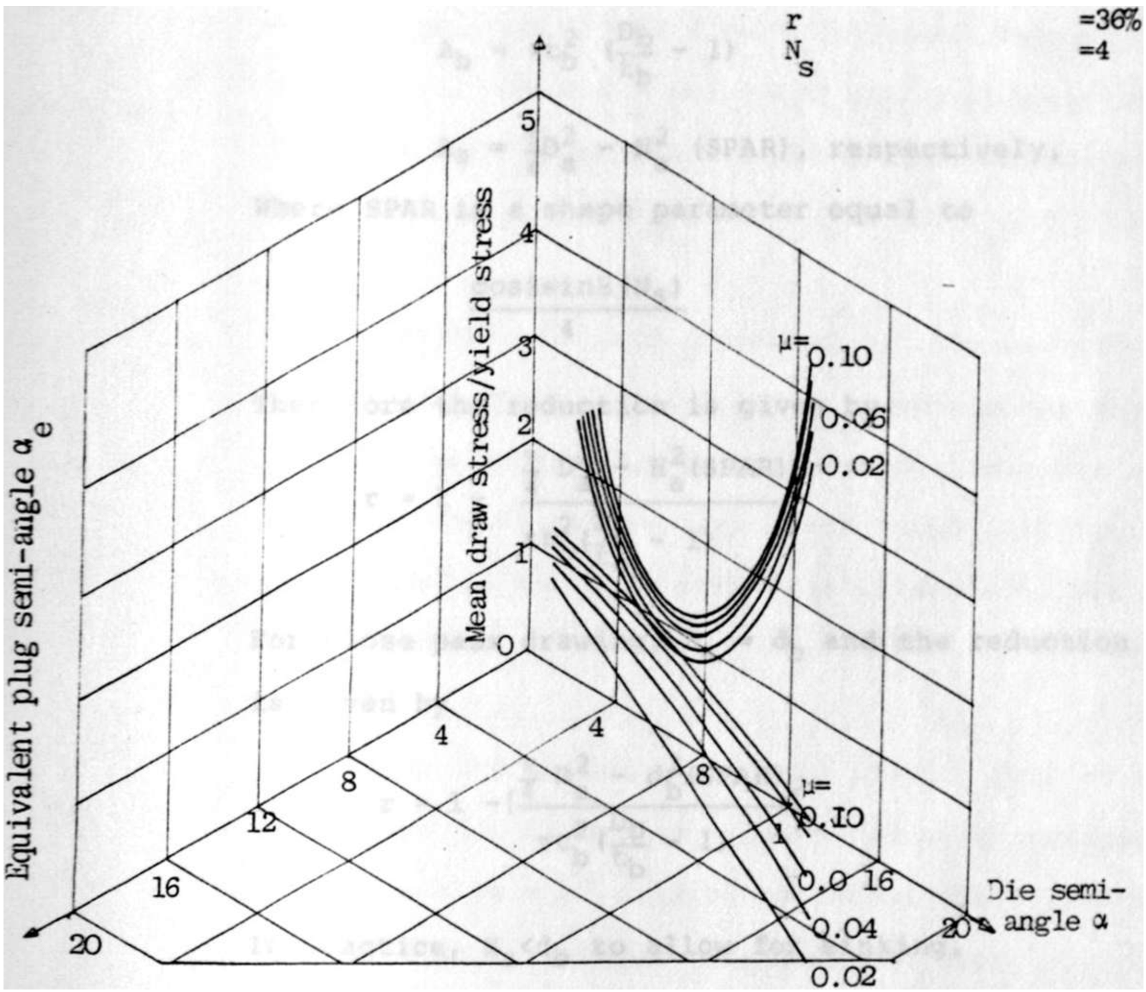

FIGURE 4.23 THREE DIMENSIONAL PLOT OF THE VARIATION* OF THE MEAN DRAW STRESS WITH THE DIE SEMI-ANGLE AND THE EQUIVALENT PLUG SEMI-ANGLE FOR THE UPPER AND LOWER BOUND SOLUTIONS FOR POLYGONAL TUBE DRAWING

5.4 LIMITATION OF ACHIEVABLE REDUCTION OF AREA

The expressions for the cross-sectional area of the tube material at entry and exit are:-

$$A_b = \hat{} b \quad " \tag{5.1}$$

$$A_a = \frac{-}{4} D_a^2 - H_a^2 \text{ (SPAR), respectively,} \tag{5.2}$$

Where SPAR is a shape parameter equal to

cos|3sin8 (N_s)

Therefore the reduction is given by:

$$r = 1 - \frac{I D^2 - H^2(SPAR)}{i - -} \tag{5.4}$$

For close pass drawing, $H_a = d_b$ and the reduction of area is given by

$$r = 1 \quad \frac{I D^2 - d_b^2 (SPAR)}{* t_b^2 a > t_b - 1)} \} \tag{5.5}$$

In practice, $H_a < d_b$ to allow for sinking.

i

The maximum reduction of area possible occurs when

$H_a = d_b = D_a$ and $t_b = D_b - D_a$ and is given by:

$$r = 1 - \frac{\hat{} 4D_a^2 (\pi/4 - SPAR) x}{M D* - D2)}$$

5 CONCLUSIONS

An extensive investigation of the mechanics of drawing polygonal tube from round stock through a cylindrical die and a polygonal plug has been accomplished theoretically to enable the following conclusions to be drawn.

1. In general for any given set of draw parameters, the derived upper bound solution predicts a higher value of draw stress due to the account taken for redundant work whilst the simpler lower bound solution under-estimates the draw stress as it neglects the redundant effect.

2. Unlike the axisymmetric tube drawing problem, the shape of the die deforming passage forms an integral part of the analysis of drawing polygonal tube directly from round stock through a cylindrical die.

3. The predicted loads in the drawing of a square section proved to be the severest of all polygonal sections implying that it may be very difficult to draw the section (Figures 4.16, 4.17 and 4.18). This is because the material suffers the greatest lateral displacement as the bore of the workpiece transforms

from round to square with the external surface remaining circular for a particular reduction of area.

4. The upper bound solution predicts the optimum die semi-angle a and the corresponding plug semi-angle a_e. The predicted values form a useful guide in the design of draw tools that would dissipate the least amount of energy.

5. The developed theory and accompanying computer program form a useful guide when producing draw schedules and in the design of draw tools for any given set of draw parameters.

6 SUGGESTIONS FOR FURTHER WORK

On the basis of the present study of mechanics of drawing regular polygonal tube directly from round stock through a cylindrical die and a polygonal plug, further work is suggested as follows:-

1. Experimental investigation of the process:

   Because of the unavailability of a draw bench, the experimentation was not part of the project study. It it suggested that experimental investigations be carried out using dies and plugs designed according to the proposed theory. The study would provide the actual data for the drawing process and hence the verification of the theoretical solutions. It is expected that the actual draw loads would lie between the upper and lower bound values.

2. Irregular polygonal tube drawing:

   The derived theoretical solution was limited to regular polygonal sections. The solution could be extended to include irregular polygonal sections.

Other plug profiles:

The theoretical solutions were confined to the drawing on plug made of elliptical plane/conical surfaces. The study could be extended to other profiles such as those shown in Figure 3.2.

Equivalent plug semi-angle cc^:

In the present study, the theory was developed for a conical die with a semi-angle a and a plug with an equivalent semi-angle . The results however were obtained for close pass drawing where H^ = d^. It is suggested that adjustments be made for the case where H <<± by taking account of the prior sinking.

REFERENCES

Wistreich, J.G. Investigation of the mechanics of wire drawing, Proc. Instn. Mech. Engrs., 1955, Vol. 169, pp 654-665

Juneja, B.L. & PraJkash, R An analysis for drawing and extrusion of polygonal sections, Int. J. Mach. Tool. Des. Res., 1975, Vol. 15, pp 1-18

Basily, B.B. & Sansone, D.H. Some theoretical considerations for the direct drawing of section rod from round bar, Int. J. Mech. Sci., 1976, Vol. 18, pp 201-208

Kariyawasam, V.P. & Sansome, D.H. An experimental study of the direct drawing of round tube to any regular polygonal section pp 1-14

wa Muriuki, M The mechanics of drawing polygonal tube frcm round on a cylindrical plug. PhD thesis (1980) University of .Aston in Birmingham

Rove, G.W. An introduction to the principles of metal working, Edvard Arnold (publishers) Ltd., 1965.

Blazynski, T.Z. Metal forming, tool profiles and flow, The Maanillan Press Ltd., 1976

Swift, H.W. Stresses and strains in tube drawing, SER. 7, No. 308, 1949, Vol. 40, pp 882-903

Chung, S.Y. Theory of hollow sinking of thin walled tubes, Metallurgia, 1951 pp 215-218

Moore, G.G. & Wallace, J.F. Theories and experiments on tube sinking through conical dies, Proc. Instn. Mech. Engrs., 1967-68, Vol. 182, pp 19-27

Blazynski, T.Z. & Cole, I.M. An investigation of sinking and mandrel drawing processes, Proc. Instn. Mech. Engrs., 1963-64, Vol. 178.

Avitzur, B. Metal forming: Processes and analysis, Mcgraw-Hill book carpany, 1968

13. Juneja, B.L. & Prakash, R. A general solution to axi-symnetric contained plastic flow processes, Proc. Indo Brit. Conf. Engg. Prod., 1976, pp C93-C107

14. Thonpson, P.J. & Sansome, D.H. Apparent strain method for analysis of steady-state metal-working operations, Metals Technology, November 1976 pp 497-5C2

15. Ford, H. & Alexander, J.il. Advanced mechanics of materials Ellis Horwood Ltd., 1977.

16. Prager, W. & Hodge, P.G. Theory of perfectly plastic solids, Chapman & Hall, London, 1951.

17. Sachs, J. & Baldwin, W.M. Stress analysis of tube sinking, Trans. A.S.M.E. 68, 1946 pp 655-662.

APPENDIX

A-L UPPER BOUND SOLUTION

A-L.L DETAILED DEFORMATION PATTERN

The general equation of a hyperbola with respect to the x_i, y_i axis (Figure 3.3 on page 22) is

$$\frac{x_i^2}{a_i^2} - \frac{y_i^2}{b_i^2} = 1 \qquad \text{(A-1.1)}$$

The equation with respect to the X_a, Y_a axis becomes

$$\frac{(X_a \sin\delta + Y_a \cos\delta - l_i)^2}{a_i^2} - \frac{(X_a \cos\delta - Y_a \sin\delta)^2}{b_i^2} = 1 \qquad \text{(A-1.2)}$$

The orientation of the X_a, Y_a axis is selected such that $\delta = 0 (=0)$.

The equation of the line inclined at 2δ to the Y_a axis is

$$y_1 = -x_1 \tan\phi + l_1 \tan\phi \qquad \text{(A-1.3)}$$

and its intersection with the hyperbola i (equation A-1.1) is

$$\frac{x_i^2}{a_i^2} - \frac{(l_1 \tan\phi - x_1 \tan\phi)^2}{b_i^2} = 1$$

which yields

2

1 $(b_i^2 - a_i^2 \tan^2 \phi)$ (A-1.4)

Equation (A-1.1) can be re-written in the form

$x_i^2 = \ldots \frac{a_i^2}{\ldots}$

$\ldots = y_i^2 \ldots \frac{a_i^2}{b_i^2 x_i}$

Therefore, $y_i = \pm$ ... is the equation of the asynptotes

of the hyperbola i.

Also from Figure A-1.1, the slope of the asynptotes with

respect to the x_i, y_i axis is $\tan(\pi/2 - \phi)$.

The foregoing analysis yields

$b_i = \ldots \tan\phi$ (A-1.5)

Referring to equation (A-1.4) let $(v,w) = (x_i, y_i)$ the point

of intersection; then

$$v = x_i = \frac{-Z \ldots \tan^4\phi \pm \sqrt{U^2 \tan \ldots (1-\tan^4\phi\ \ldots \tan^4\phi)}}{1-\tan\phi}$$ (A-1.6)

and $w = y = \tan\phi(-v + iL)$ (A-1.7)

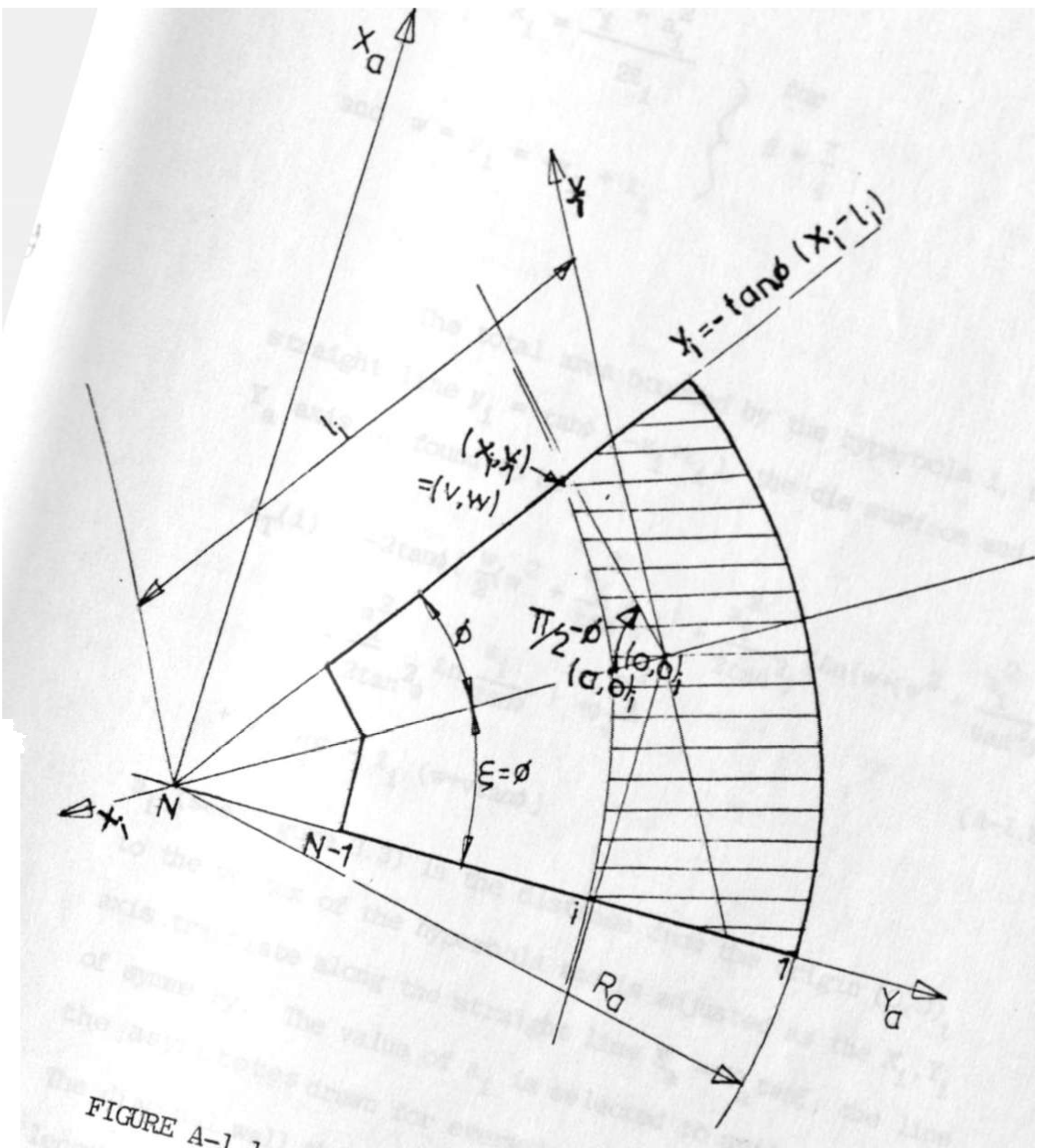

FIGURE A-1.1 AREA BOUNDED BY THE HYPERBOLA i AND THE DIE SURFACE or $v = x_1 = \frac{I_i + a_i^2}{2Z_1}$ for

$8 = —$

and $w = y_i = -x_1 + I_1$

Hie total area bounded by the hyperbola i, the straight line y^ = *tanp O-x^H^),* the die surface and the Y_a axis is found to be

$$A_T(i) = -2\tan\$ \{ \frac{}{2} + \frac{a^2}{\tan 9} + \frac{a^2}{2\tan \$} \mathrm{Un}\{w+(w^2 + \frac{a^2}{\tan \$})*\})$$

a² a· D²

" ian²/" ^ } ^

$$+ v^2 \tan np - JL \; (w+v\tan 0)$$

a (see Figure 3.3) is the distance frcm the origin (0,0^ to the vertex of the hyperbola and is adjusted as the X^,Y^ axis translate along the straight line $X_a = Y_a \tan$:, the line of symmetry. The value of a_i is selected to suit the corners o the asymptotes drawn for every l_{jL} e.g. $a_L = 1 - $ ^ .
The diagonal wall thickness is divided into N-2 elemental lengths. Let the elemental lengths be At_2, $At_{3>}$ At_4

At_{3-1} such that $\sum_{i=2}^{N-1} At_i = t_a$

Then A. « ~ − £ At , (2<i<N−1)
$\quad\quad_1 \quad _2 \quad D \quad\quad n=2 \quad 1$

Let $At_2 = At_3 = \_\_\_\_\_\_ At_{N-1} = At$

Then $At = \dfrac{D_a \_\_\_\_ H_a}{N-2}$ —

$$i_{\pm} = \frac{D_r}{\sim 2} - (i-1)At \qquad \text{(A-1.9)}$$

Assuming a constant reduction in area, the inner radius u (i) (Figure A-1.2) of the cross-sectional area at the entry plane corresponding to the area A^,(i) can be deteirnined.

Let A_r = Area ratio

$$= \frac{\text{Area at entry}}{\text{Area at exit}}$$

$$\frac{fb}{A_a} \qquad \text{(A-1. 10)}$$

Then, −J § − mi² (!)(§)−

which simplifies to

$$u_r(i) = \{ \frac{D_b}{T} \sim r\, Y^{i} \} > \quad * \qquad \text{(A-1.II)}$$

The area banded by the radii $u_r(i+1)$ and $u_r(i)$ (Figure A-1.2) is divided into M-1 equal sectors each subtending an angle $d\phi_j$ where j refers to the element between the radial lines j and j+1. Let the inclination of the radial line j to the axis be ϕ_j then $d\phi_j = \phi_{j+1} - \phi_j$.

Let + $d\phi_2$ + + $d\phi$ = $\Sigma d\phi$ = 2π

and $d\phi_1 = d\phi_2 =$ $d\phi$ = $d\rho$,

then $d\rho = \frac{}{M-1}$ (A-1.12)

From Figure (A-1.2), J J-1 + J-1

= + $d\phi_2$ + + ^j-1

= (j-1)<#

$= (j-1) \frac{}{M-1}$ (A-1.13)

The elemental area enclosed by the radial lines and circular bands, say ABCD is divided into two triangles; a large triangle ADB and a small triangle DBC. Let the angle subtended at the centre $_j$ = dy and the radial increment AD = δR, where u (i) = R.

The approximate area of the large triangle ADB is

AL - &R6R5Y (A-1.14)

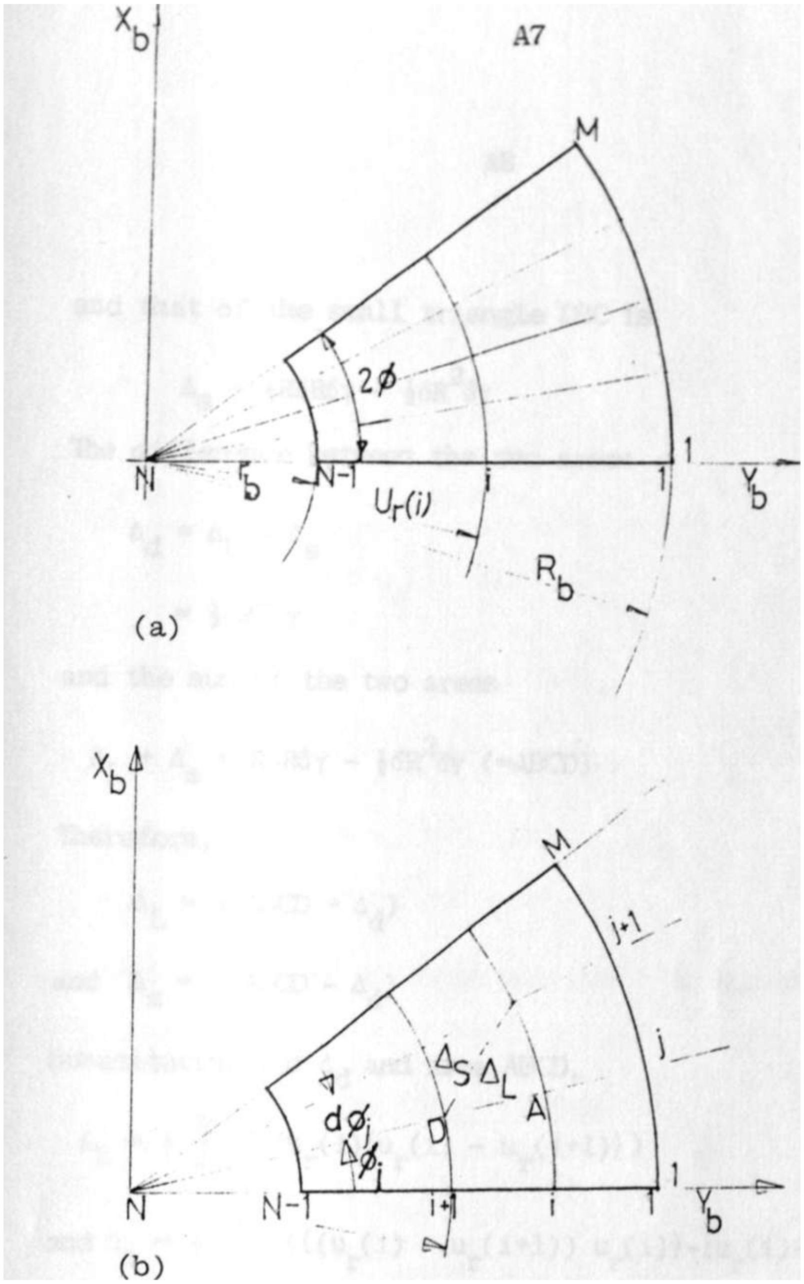

FIGURE A-1.2 (a) DIVIDING THE ENTRY PLANE INTO (N-2) BANDS X(M-1) SECTORS

(b) EACH ELEMENTAL AREA IS FURTHER SUBDIVIDED INTO A LARGE AND SMALL TRIANGLE and that of the small triangle DBC is

$$A_s = £RcR5y - *6R^2 6y \qquad (A-1.15)$$

The difference between the two areas

$$A_d = A_L - A_s$$

$$= *6R^2 6y \qquad (A-1.16)$$

and the sum of the two areas

$$A_l + A_s = R6R6y - i<5R^2 5y \ (=ABCD) \qquad (A-1.17)$$

Therefore,

$$A_l = KABCD + A_d) \qquad (A-1.18)$$

and $A_s = *(ABCD - A_d)$ (A-1.19)

Substituting for A^ and area ABCD,

$$A_l = J \quad (u_r(i)\{u_r(i) - u_r<i+1)\}) \qquad (A-1.20)$$

and $A_s = i\ f\hat{}\ (\{(u_r(i) - u_r(i+1» u_r(i)\}-\{u_r(i)-u_r(i+1)\}^2)$

(A-1.21)

Equations (A-1.20) and (A-1.21) are the expressions for the elemental areas of the large and small triangles.

The co-ordinates of the vertices A, B, C and D are obtained as follows;

At A, $\quad$ j) = u (i) sin<J>$_J$ $\quad$ (A-1.22)

$Y_b(i,j) = u_r(i)$ cos0^

At B, y i , j + 1) = $u_r(i)$ siat>$_{.+1}$ $\quad$ (A-1.23)

$Y_b(i,j+1) = u_r(i)$ cos0$_{j+1}$

At C, y i + 1 j + 1) = u.U+1) sir*J)$_{j+1}$ $\quad$ (A-1.24)

Y_b(i+1$_f$j+1) = u_r(i+1) ccs$$_{j+1}$

At D, $X_b(i+1,j) = u_r(i+1)$ sin? . $\quad$ (A-1.25)

$Y_b(i+1,j) = u_r(i+1)$ *cast.*

The centroids of the large and small triangles are located as follows:-

The centroid of the large triangle ABD

x^cLCi, j) = cy i, j) + -yi+i, j) + y i. j+i))/3 $\quad$ CA-I.26)

$Y_bCL(i,j) = (Y_b(i,j) + Y_b(i+1,j) + Y_b(i,j+1))/3$

and the centroid of the small triangle DCB,

^ C S d J) = (y i + 1 j) + yi+1, j+1) * yi, j+1)) / 3 $\quad$ (A-1.27)

$Y_bCS(i,j)$ = cyi+1, j) + $Y_b(i+1,j+1) + Y_b(i,j+1))/3$

Assuming the same constant reduction A^, each triangle at the entry plane is transformed into a corresponding triangle at the exit plane where r

and $A_s = $ ^ (A-1.28)

r

Considering the Y_a axis and its intersection with the hyperbola i and i+1, the vertices © and (2) (or $(X_a, Y_a)_{1,j}$ and $(X_a, Y_a)_{j+1}$ j where J=1) of the large triangle are known.

is known and the third vertex must lie on hyperbola i.

To determine the third vertex, consider the triangle A' B' D' (Figure A-1.3a). Let the co-ordinates of the triangle be A'(X_1,Y_1), B'(X_2,Y_2) and D'(X_3,Y_3). Applying the trapezium rule,

$$A_L = \tfrac{1}{2}\{X_1(Y_3 - Y_2) + X_2(Y_1 - Y_3) + X_3(Y_2 - Y_1)\} \qquad (A-1.29)$$

Vertex (I) lies on the intersection of the outer curve (a circle) and the Y_a axis (Figure A-1.3b).

Therefore, $X_a\ (=X_1) = 0$

and $Y_a(=Y_1) = \pm \frac{D}{2}$ (A-1.30)

where the appropriate value of Y_1 is the positive value.

Vertex © lies on the intersection of the hyperbola i and the Y_a axis,

i.e. $X_a(=X_2) = 0$ (A-1.31a)

$Y_a(=Y_2)$ is obtained frcm equations (A-1.2) and (A-1.3) as

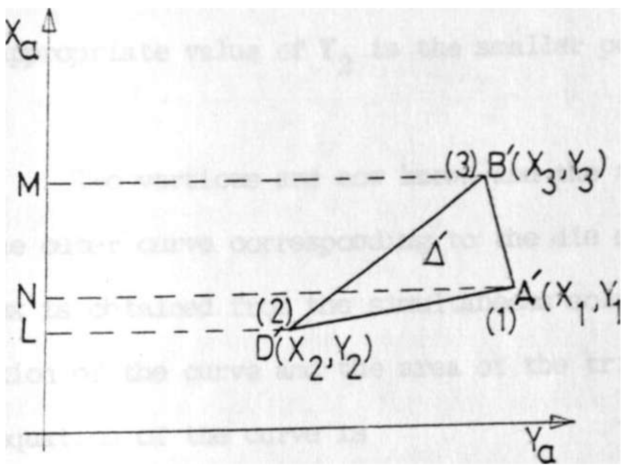

(a)

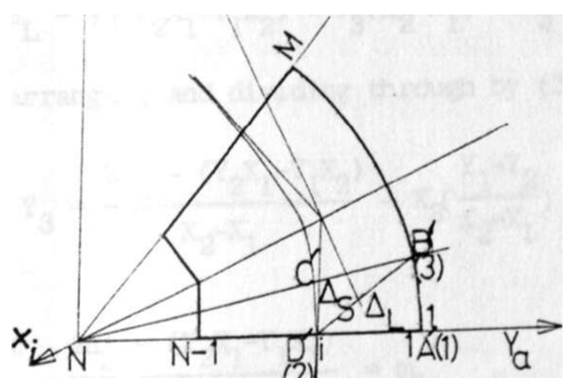

(b)

FIGURE A-1.3 (a) APPLICATION OF TRAPEZIUM RULE

(b) DETAILED LOCATION CF *TAJBD* VERTEX

$$v_{ig} = \frac{}{\cos\pounds(1-\tan^4\pounds)} \qquad \text{(A-1.31b)}$$

The appropriate value of Y_9 is the smaller positive value.

TWo vertices are new known and the third vertex lies on the outer curve corresponding to the die surface. The vertex is obtained fran the simultaneous solution of the equation of the curve and the area of the triangle.

The equation of the curve is

$$X_3^2 + Y_3^2 - \hat{} \, {}^D a^2 \qquad \text{(A-1.32)}$$

and equation (A-1.29) is re-written in the form

$$^A L = * \ll W \, Y_1 X_2) + Y_3(X_2 " X_1) + W V > \qquad \text{(A-1.33)}$$

rearranging and dividing through by (Xg-X^) gives

$$Y_3 \quad " \frac{(W \, Y_1 X_2)}{X_2 " X_1} \quad Y_1 - Y_2$$

$$\text{Let} \quad \frac{2A\pounds - (Y\hat{} - Y\hat{})}{V \, X_1} \qquad \text{(A-1.34)}$$

$$\text{and} \quad \frac{V \, Y_2}{V \, X_1} = K\neg, \qquad \text{(A-1.35)}$$

$$\text{Then} \quad Y_3 = \quad \sim \qquad \text{(A-1.36)}$$

Substituting for Y_3 in equation (A−1.32), expanding and rearranging yields

$$X_3 = \frac{W \wedge W^2 - (1\wedge X m\wedge - C\wedge)^2)\}}{1+K_1^2} \qquad \text{(A−1.37)}$$

The appropriate value of Xg is the larger positive value.

Having determined vertex (3) (X^.Y^) of the large triangle, vertex (2) (X_2, Y_2) of the large triangle becomes vertex @ of ^ 3nall triangle and vertex (D $(X_3 > Y_3)$ of the large triangle becomes vertex ***(2)*** of the small triangle.

Two vertices of the small triangle are known and the third one lies on the hyperbola i, i.e.

$$\frac{(X_3 \sin\pounds + Y_3 \cos\pounds - I_\pm)^2}{a_i^2} \quad \frac{(X\wedge ccsC - Y_3 \sin\pounds)^2}{b_1^2} = 1 \qquad \text{(A−1.38)}$$

and $Y_3 = (m\wedge - K\wedge X\wedge)$ (A−1.39)

where $m' = \frac{2A' - (YJC,-Y_{2\,1\,1}}{X_2 - X_1}$ (A−1.40)

Equations (A−1.39), (A−1.38) and (A−1.5) are solved simultaneously to yield X^ as

4 c3 + *3c2 + c1 " 4*3 −V2 " d1 " ai " 0

which on factorizing gives

$$3 \; " \; \frac{-(C_2-d_2)\pm/\{(C_2-d_2)^2-4(C_3\wedge_2)(C_1-d_1-af)\}}{2(C_3-d_3)}$$

where

$C\wedge = \sin^9 C - \wedge\sin\wedge + k^2\wedge ccs^{2-} *$

$C_9 = rn\wedge\sin 2\wedge - 2£_i\sin\wedge - a7i\wedge k_1\cos^2{}^w C^+ 2k_1 il_i\cos C$

$C_1 = m\wedge^2 ccs^2 C - 2m\wedge il_i\cos C\wedge i$

$d_3 = \tan^2 0(\cos^2 C + kjSii\wedge + k^2 j\sin^2 £)$

$d_2 = \tan^2 \$(-HnJ\sin 2£ - 2m\wedge k\wedge \sin^2 S)$

$d_i = m_i - 9 \; ^2 £$

The appropriate value of X^ is the smaller positive value,

The centroids of the triangles at the exit plane can now be obtained.

For the large triangle,

$X_a CL(i,j) = (X_a(i,j) + X_a(i,j+1) \cdot X_a Ci+1.j)>/3$ (A−1.42)

$Y a(i,j) = \{Y (i.j) * Y (i,j+1) * Y (i+1,j)\}/3$

For the small triangle,

$$X_aCS(i,j) = (X_a(i+1,j) + X_a(i+1,j+1) + X_a(i,j+1))/3 \quad \text{(A-1.}$$

$$Y_aCS(i,j) = (Y_a(i+1,j) + Y_a(i+1,j+1) + Y_a(i,j+1))/3$$

A-1.2 DERIVATION OF THE FLOW PATH PARAMETERS

$\delta_b(i,j)$ is the horizontal distance a particle travels after shearing at the assumed discontinuity boundary, measured relative to the entry plane (see Figures A-1.4 and A-1.5). $\delta_a(i,j)$ is the horizontal distance the particle travels after shear at the assumed discontinuity boundary, measured relative to the exit plane.

Therefore the total distance covered by the particle in the deforming zone is

$$Z_s(i,j) = L + \delta_b(i,j) - \delta_a(i,j) \quad \text{(Figures A-1.6 and A-1.7)} \qquad \text{(A-1.44)}$$

The length of the flow path Z_t for each element and the relative angular diflections η and ψ as the element flews through the deformation zone are determined from geometry as follows;

$$\sin\theta(i,j) = \frac{R_u(i,j)}{\quad} \quad \text{or} \quad \theta(i,j) = \sin^{-1}\left(\frac{R}{\quad}\right) \qquad \text{(A-1.45)}$$

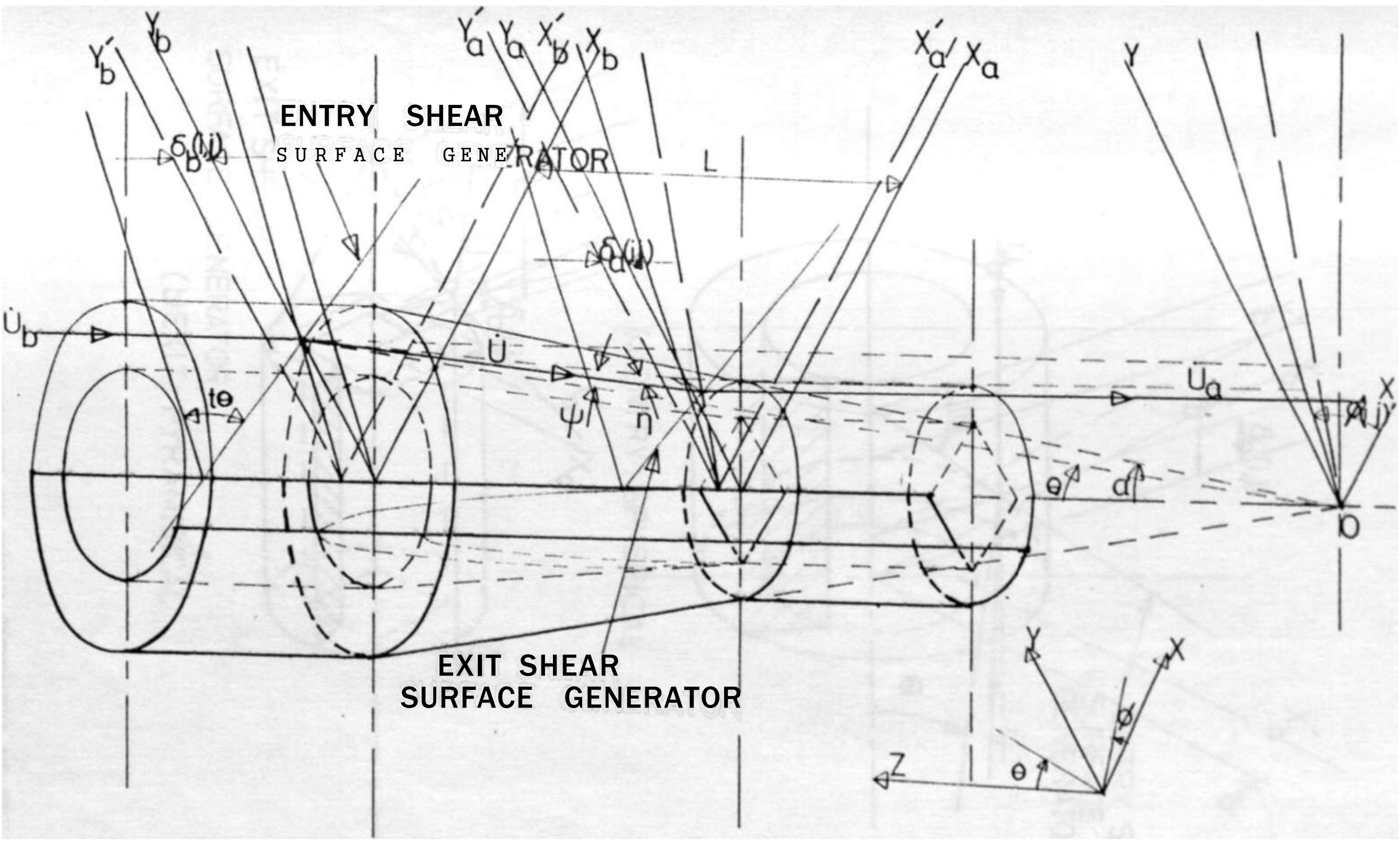

M
O

FIGURE A-1.4 FLOY PAW OF AN E I M A R Y PARTICLE FOR TllLi DRAWING OF POL/
TUBE DIRECTLY IBOM ROUND

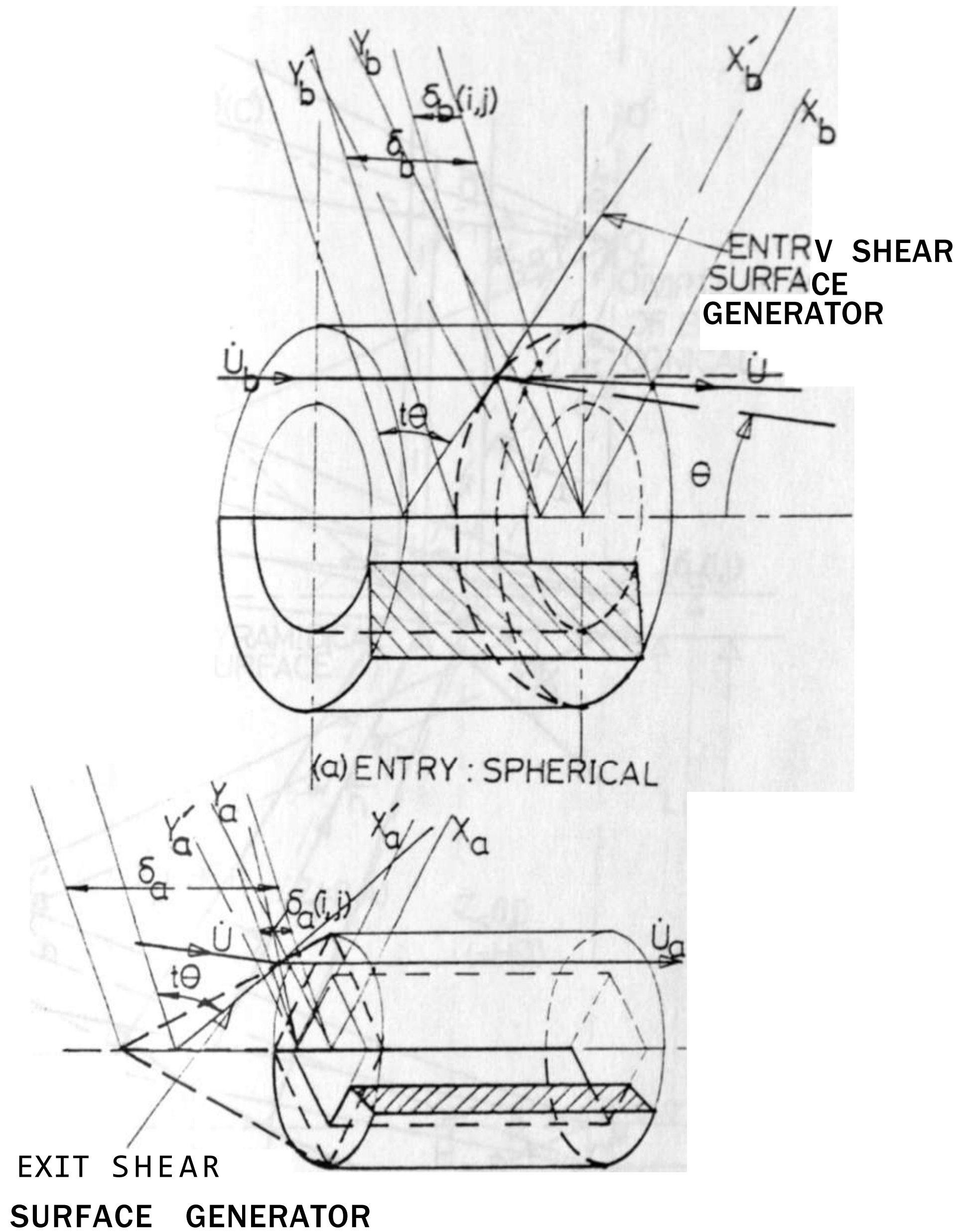

FIGURE A-1.5 GENERAL PCSITICN OF SHEAR SURFACES AT THE ENTRY
AND EXIT ID THE DEFORMATION ZONE

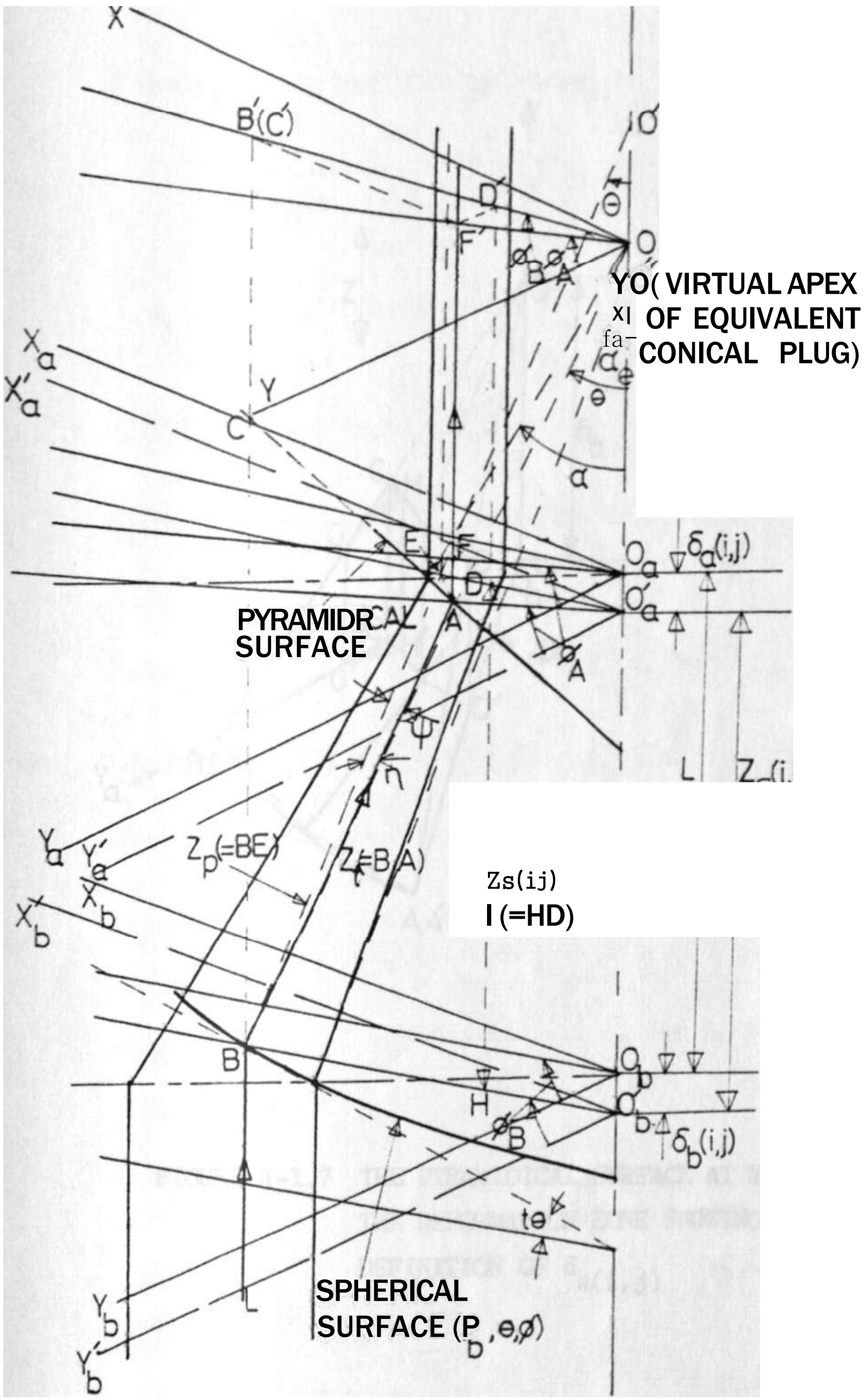

FIGURE A-1.6 DIAGRAM TO ILLUSTRATE THE APPROXIMATE FLOW PATH OF AN ELEMENT IN THE DEFORMATION ZONE

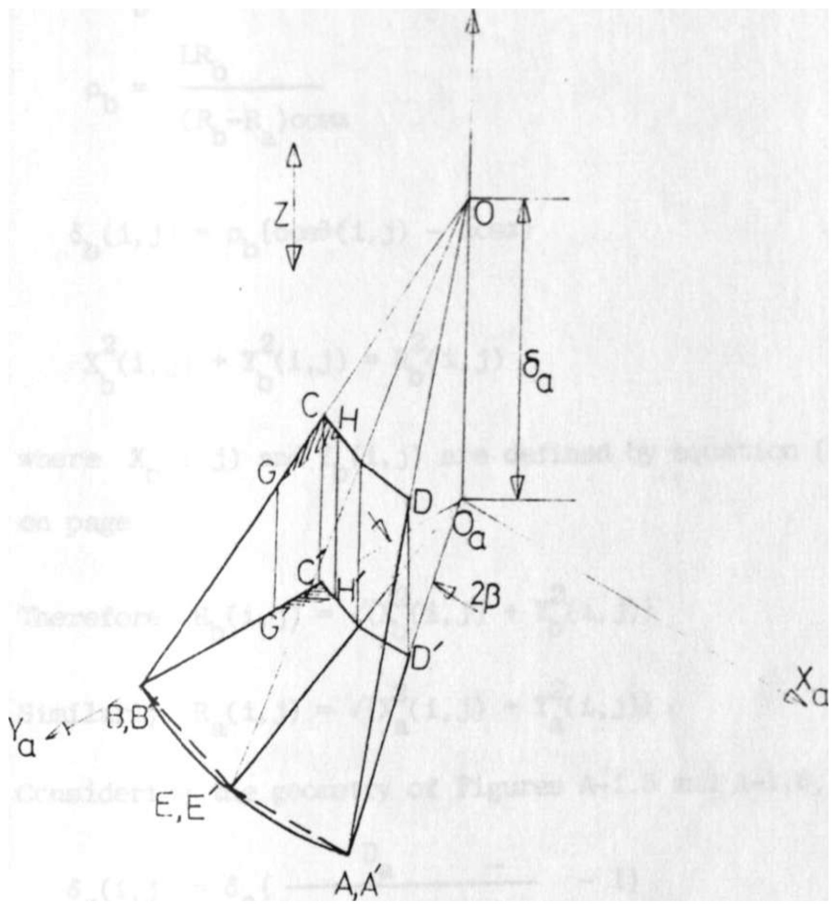

FIGURE A-1.7 THE PYRAMIDICAL SURFACE AT THE EXIT TO THE DEFORMATION ZONE SHOWING THE DEFINITION OF $\delta_{a}(i,j)$

where $p^\wedge$ is derived frcm gecmetry as

$$P_b = \frac{La}{—^2 \; (\wedge o o w} \tag{A-1.46}$$

$$<\$_b(i,j) = P_b\{cos9(i,j) - ccsa\} \tag{A-1.47}$$

$$X j i j) + Y^2(i,j) = R^\wedge(i,j)$$

where $X^\wedge i,j)$ and $Y^\wedge d.j)$ are defined by equation (A-1.22) on page

Therefore $R_b(i,j) = AX^\wedge U.j) + Y^2(i,j)\}$ (A-1.48)

Similarly $R_a(i,j) = /\{xf_a(i,j) + Yf_a(iJ)\}$ (A-1.49)

Considering the geometry of Figures A-1.5 and A-1.6,

$$\delta_a(i|j) = \delta_a\{\frac{—}{2R_a(i,j)Cos4)_A(i,j)} - 1\} \tag{A-1.50}$$

where

$$\bullet_A U.J) - \begin{cases} \tan^{-1}\{\frac{X(i,j)}{Y_A(i,j)}\} & \text{for} * <6 \\ 2\theta-\tan^{-1}\{\frac{X_a(iJ)}{Y_a(iJ)}\}, & \text{for } \phi_A > 0 \end{cases} \tag{A-1.51}$$

Considering Figure A-1.3a,

$$Z_t(iJ) = (C y iJ) - X_a(i,j)\}^Z + \{Y_b(i,j) - Y_a(i,j)\}^\wedge(i,j)) \tag{A-1.52}$$

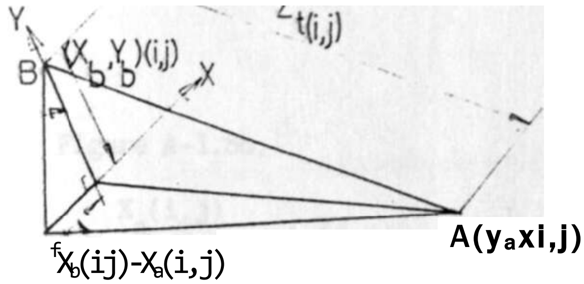

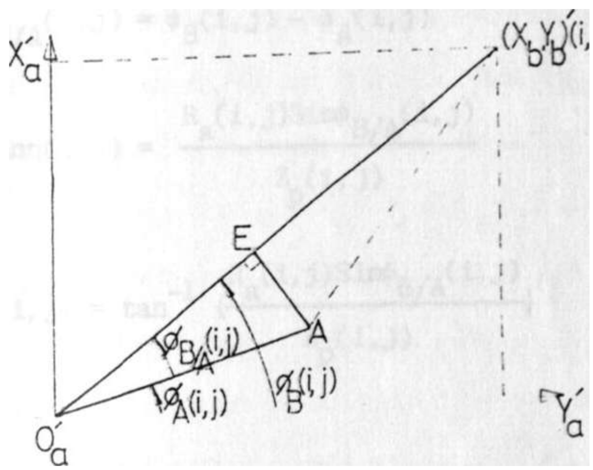

FIGURE A-1.8 (a) DETAILED DERIVATION OF Z^ti, j)

(b) PLANE THROUGH THE ELEMENT (i, j) WHERE IT CEASES TO DEFORM

Considering Figure A-1.8b,

X (i,j) -1 / V i , J W /A-1 53)

a

$$^{X}{}_{b}(i.J) \qquad -1 \quad {}_{r}\frac{X_b(i,J}{}W \qquad (A-1.54)$$

^ B ^ " j) = Y ^ I j I or * B (1,J) = tan Yj|(iJ)

$$\tan n(i,j) = \frac{R_a(i,j)Sin4>_{B/A}(i>j)}{Z_p(i.j)}$$

$$\text{or} \quad n(i.j) = \tan \left\{ \frac{R_a(i.j)Sln»_{B/A}(i.j)}{Z\ (i.j)} \right. \qquad (A-1.56)$$

where

$$z_D(ij) = (CB_b(i.j)-a_k(i.J)<»B/A^{(1,J)\}} + Z^2_s{}^{(i,j))} \quad J \qquad (A"1,57)$$

$$\tan G = \frac{R_b(i,J)-R\hat{}iiJ)Cosl>_{B/A}(i»J)}{Z_s}$$

$$\text{or} \quad 0 = \tan \left\{ \frac{B_h(1,3)-1t.(i.J)0«*B/A^{(1,J)}{}_1}{\hat{}} \right. \qquad (A-1.58)$$

(A-1.59)

j) = |ec±.J> " ®(i.J>l

A-1.3 EQUIVALENT PLUG SE?II-ANGLE AND CROSS-SECTICNAL AREA OF TUBE MATERIAL

In the drawing of polygonal tube from round through cylindrical die on a polygonal plug, a circular section at entry transforms into a polygonal section at the exit in a single pass. The die-plug passage consists of conical and plane surfaces of different inclinations to the tube axis to allow for gradual deformation (Figure A-1.9). The conventional plug conical semi-angle is not applicable since the plug angle changes from a minimum at the diagonals to a maximum at the mid-section of the plug. It is therefore necessary to define an equivalent plug semi-angle 'a^ to facilitate comparison between plugs used for drawing tubes with the same number of sides and with different number of sides.

From the equivalent axisynmstric drawing, Figure A-1.10,

$$\tan a_e = \frac{d. - d}{\wedge} \quad \text{or} \quad L = \frac{d. - d}{2\tan a_e} \qquad \text{(A-1.00)}$$

The inclinations of the conical and plane surfaces of the polygonal tube drawing plug become;

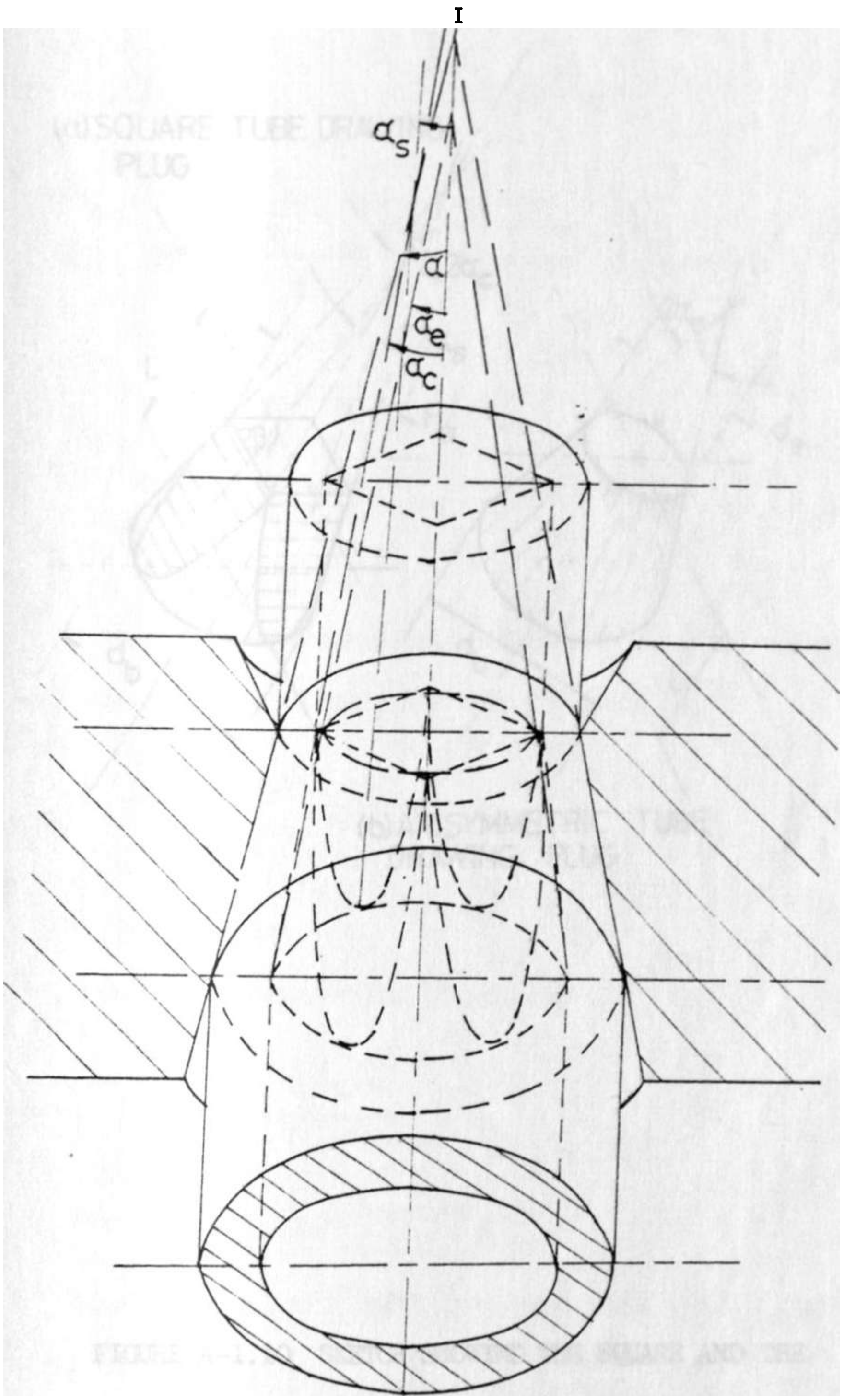

FIGURE A-1.9 SKETCH SHOWING THE DRAWING OF REGULAR POLYGONAL TUBE FRCM ROUND THRGjGH A CYLINDRICAL DIE

(A)SQUARE TUBF. DRAWING ,
PLUG

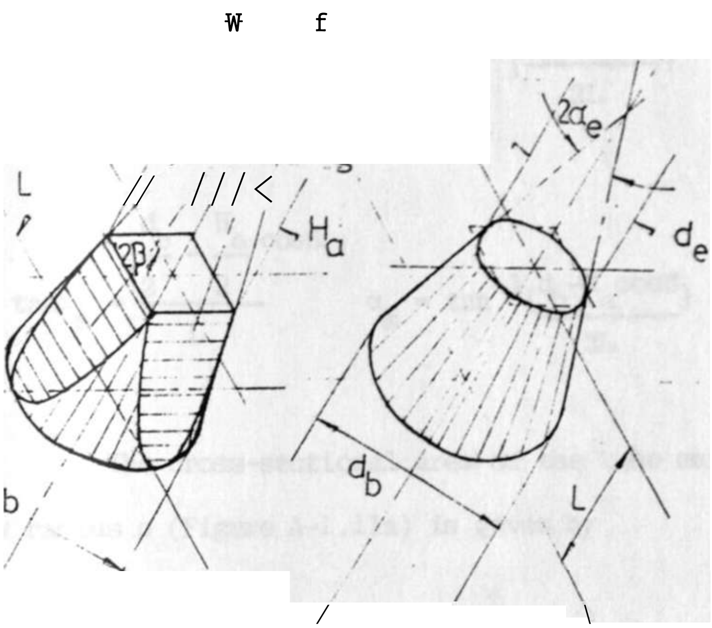

(b)AXISVMMETRIC TUBE
DRAWING PLUG

FIGURE A-1.IO SKETCH SHOWING THE SQUARE AND THE CORRESPONDING AXISYMMFTRIC TUBE DRAWING PLUG

$$\tan* = \frac{\frac{"b}{2} - \frac{H}{?}}{L} \quad \text{or } a_c = \tan^{1}\{\frac{\hat{}h \sim \hat{}}{2L}\} \qquad \text{(A-1.S1)}$$

$$\tan pc_s = \frac{\frac{\hat{}b}{2} - \frac{^{H}a}{2} co60}{\frac{T}{L}} \quad ot_s = \tan^{-1}\{\frac{c_rL - H_o\ a \cos8,}{2L}\} \qquad \text{(A-1.62)}$$

The cross-sectional area of the tube material at any radius p (Figure A-1.11a) is given by

$$A_p = 7r(R^2 - r^2) \qquad \text{(A-1.63)}$$

where

$$R = psinct \qquad \text{(A-1.64)}$$

and r Is obtained from the expression

$$\tan a_e = \frac{r. - r}{(p_b - p)ccsa}$$

as

$$r = \quad - (p_b - p)cosatana_e \qquad \text{(A-1.65)}$$

Substituting for r and R into equation (A-1.63) and factorizing,

$$A_p = Tr3in^2 3(p^2 - \{\sim\frac{j*r}{sine} + (p - P_K)_d cotatam\ \}^2) \qquad \text{(A-1.66)}$$

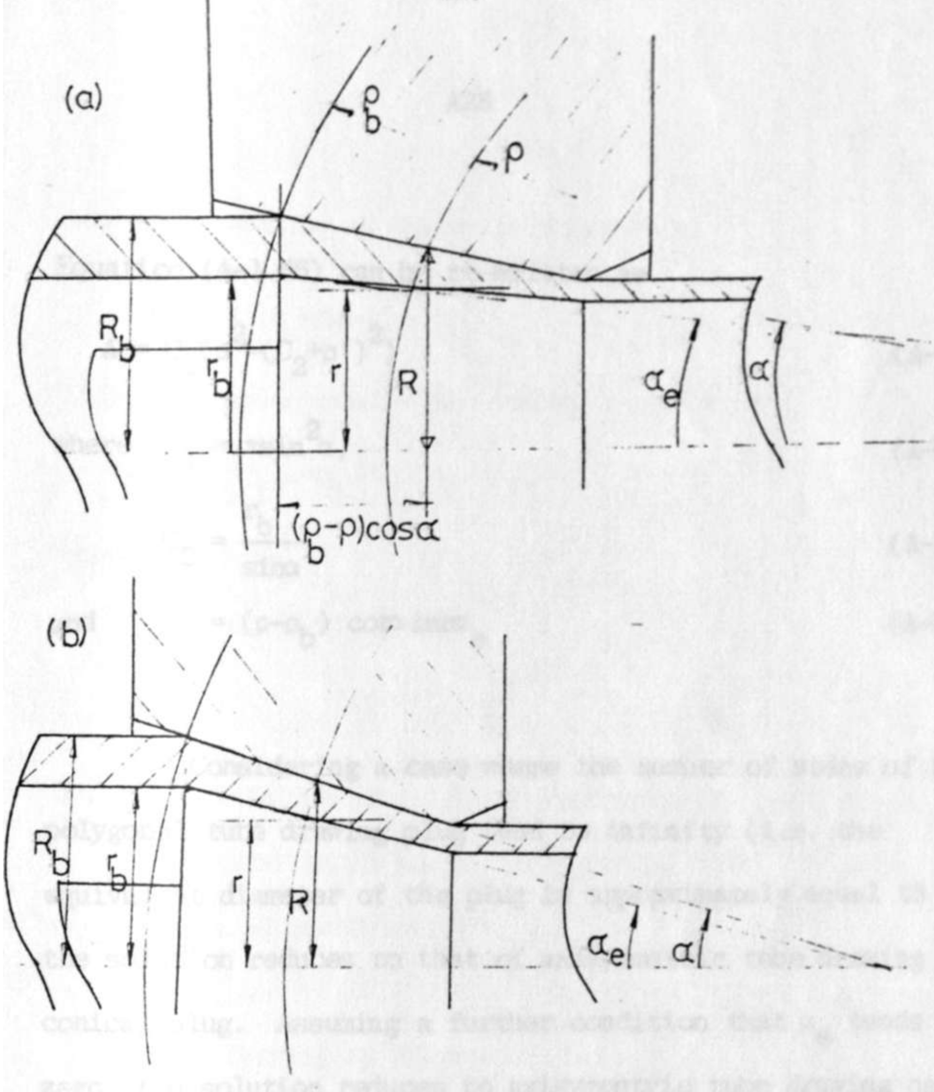

FIGURE A-1.11 (a) DETAILED DIAGRAM SHOWING THE CROSS-SECTIONAL AREA OF THE TUBE MATERIAL AT ANY RADIUS p

(b) SPECIAL CASE OF POLYGONAL TUBE DRAWING WHERE THE DIE AND EQUIVALENT PLUG SURFACES CONVERGE TO ONE VIRTUAL APEX

Equation (A-1.66) can be re-written as

A = C^P^Cg+p')²) (A-1.67)

where $C_1 = \pi \sin^2\alpha$, (A-1.68)

(A-1.69)

sina

and p' = (p-p,) comanw$_e$ (A-1.70)

Considering a case where the nurrtoer of sides of the polygonal tube drawing plug tend to infinity (i.e. the equivalent diameter of the plug is approximately equal to H_a), the solution reduces to that of axisyrrmetric tube drawing on a conical plug. Assuming a further condition that tends to zero, the solution reduces to axisymnetric tube drawing on a cylindrical plug. Equation (A-1.66) becomes

area = Tr(psina)^2 - A_p (A-1.71)

Considering the case when the plug radius tends to zero, then A_p = 0 and the solution reduces to axisyrrmetric wire (or bar) drawing. Equation (A-1.66) becomes

area = Tr(psina)^2 (A-1.72)

When p = p. (equation A-1.66), the cross-sectional area of the tube material at entry is obtained as

$$W = \mathrm{Tr}\{(p_b \mathrm{siflc} 0^{2} - r£\}^{0}$$

This expression can be re-written in the form

$$, \quad \bar{\sim}\ {}^{p}b^{C}1^{2r} \ "^{r}\ 3 \qquad \text{(A-1.73)}$$

where $C_3 = \mathrm{Trr}^2_{a}$ (A-1.74)

and C, is equation (A-1.38).

A-1.4 DERIVATION OF VELOCITY DISCONTINUITY SUFFERED BY AN ELEMENT ENTERING THE DEFORMATION ZONE (Figures A-1.12 and A-1.13)

Referring to Figure A-1.13a,

$$\hat{}rsl = -\%\mathrm{sint}9\hat{}\cos(e-t9)+u_p\sin(6-t9) \qquad \text{(A-1.75)}$$

Referring to Figure A-1.13b,

$u_\$$ is the corponent of velocity nonral to the p-8 plane and

$$u_{rb} = , .2-2 \ * \ rsl \qquad \text{(A-1.76)}$$

$$= \{u\hat{}C-i\hat{}\mathrm{sintS}+U_g\mathrm{COsCe}-\mathrm{tfi})ni_p\sin(9-t9))>^{2,i}$$

The resultant velocity (of the tangential carponents) on bo* sides of the shear surface gives the velocity discontinuity.

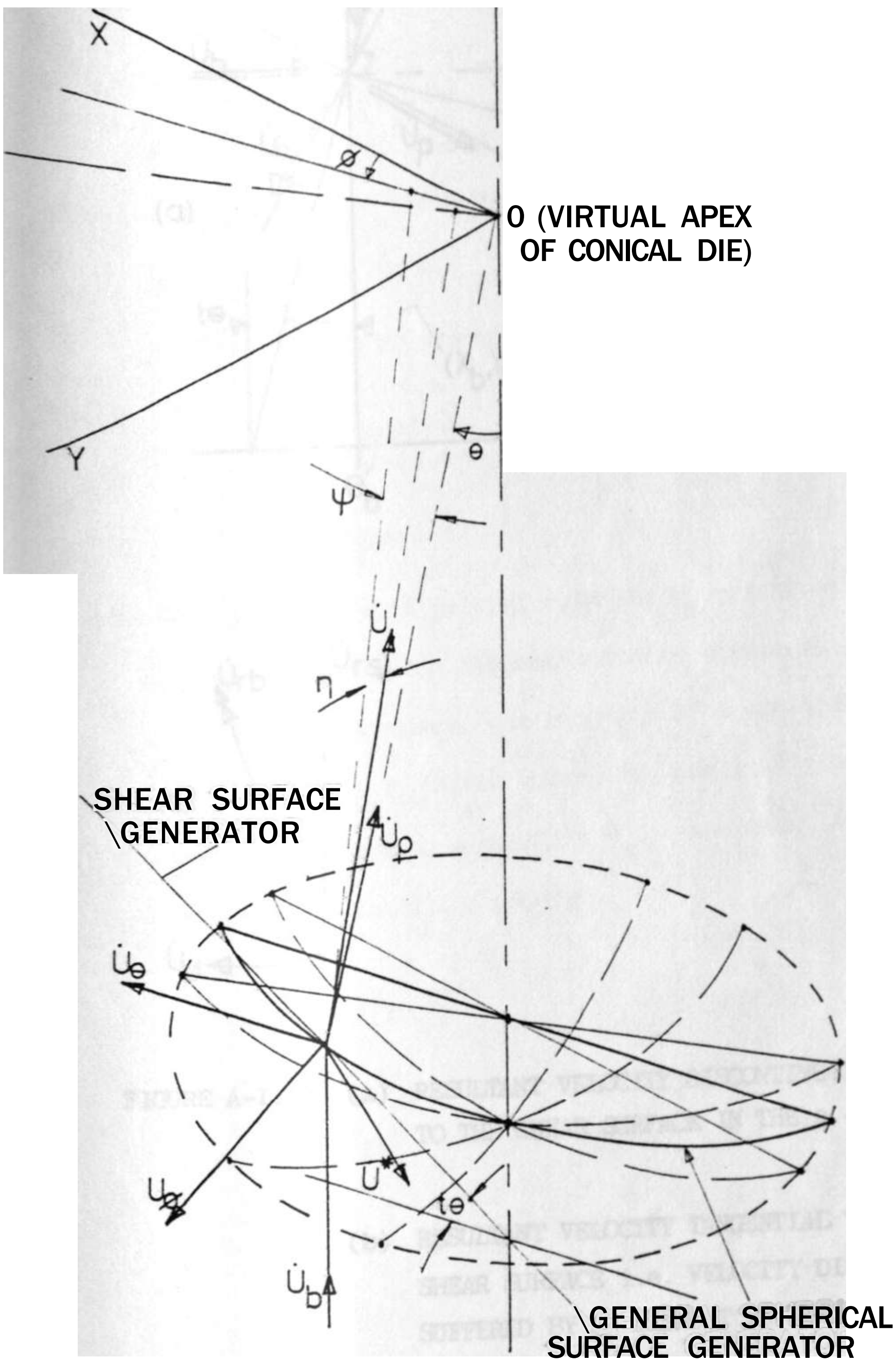
X
Y
ø
O (VIRTUAL APEX
OF CONICAL DIE)
θ
ψ
U
η
SHEAR SURFACE
GENERATOR
Uρ
Uθ
U
tθ
Uø
Ub
GENERAL SPHERICAL
SURFACE GENERATOR

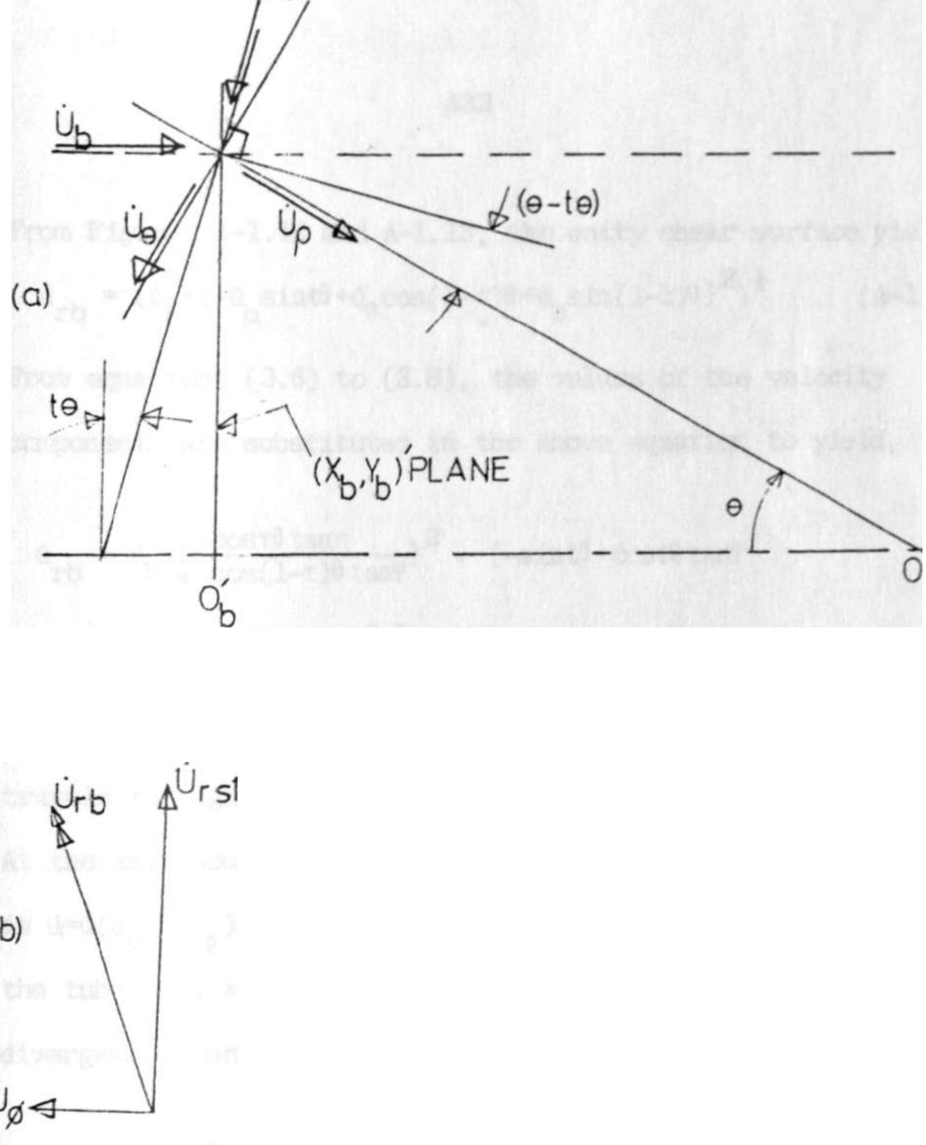

FIGURE A-1.13 (a) RESULTANT VELOCITY DISCONTINUITY TANGENTIAL TO THE SHEAR SURFACE IN THE p - & PLANE

(b) RESULTANT VELOCITY TANGENTIAL TO THE SHEAR SURFACE i.e. VELOCITY DISCONTINUITY SUFFERED BY AN ELEMENT ON ENTERING THE DEFORMATION ZCNE

From Figures A-1.12 and A-1.13, the entry shear surface yields

$$u_{rb} = Cu^2+\{-u_b\sin t9+u_9\cos(1-t)9^{\wedge}_p\sin(1-t)e\}^2)^i \qquad (A-1.77)$$

From equations C3.6) to (3.8), the values of the velocity components are substituted in the above equation to yield,

$$a_{rb} = a_o ((\frac{\cancel{ccstetann}}{\cos(1-t)9\tanf})^2 +$$

$$+ ccst9\tan(1-t)6\}^2)^i \qquad (A-1.78)$$

Any particle with initial velocity u^ before deformation, travels through the deformation zone with a velocity LI=U(U_2,Uq). At the exit boundary, the velocity of a particle just before shear is u=d(u_p,UQ^). After shear, the particle travels parallel to the tube axis with a velocity il_a. Assuming an equivalent divergent deformation passage,

$$u_{ra} = u_{rb} C(\frac{p»}{p''_a})^2 \qquad (A-1.79)$$

where p''^2_b is equation (3.4) and P''^2_a is obtained from equation C3.5).

2 LOWER BOUND SOLUTION

2.1 LOWER BOUND NUMERICAL INTERORATION

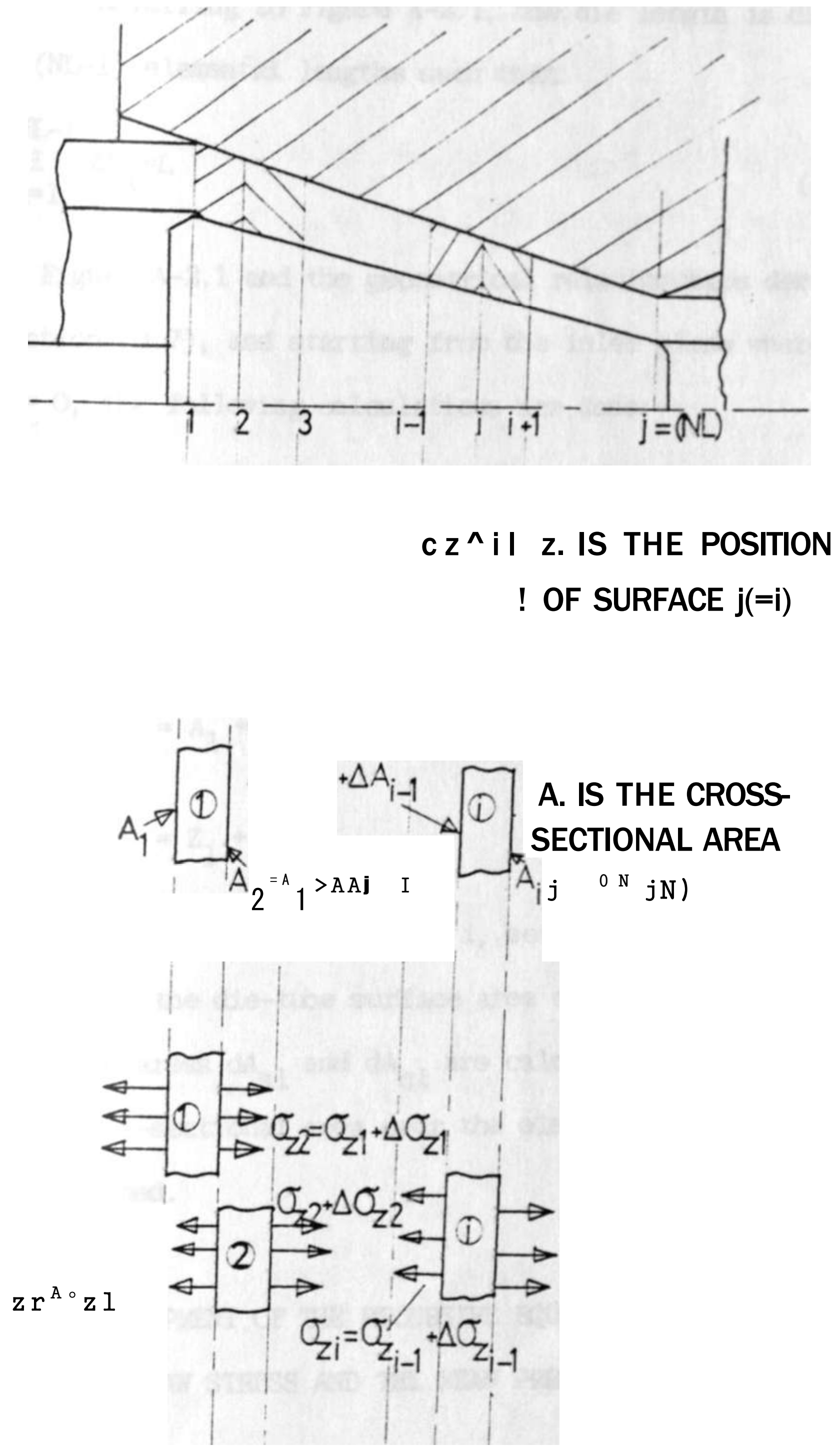

FIGURE A-2.I ROUND TUBE DRAWN THROUCE A CYLINDRICAL DIE ON A POLYGONAL PLUG DIVIDED INTO ELEMENTS FOR THE LOWER BOUND SOLUTION

A-2.1.1 GEOMETRICAL DERIVATIONS

Referring to Figure A-2.1, the die length *is* divided into (NL-1) elemental lengths such that

$$\sum_{i=1}^{NL-1} \Delta Z_i = L \qquad \text{(A-2.1)}$$

Using Figure A-2.1 and the geometrical relationships derived in section (3.7), and starting frcm the inlet plane where = 0, the following calculations are done:-

(a) At any section Z_i, calculate R(i), r(i), and A_i. From Figure A-2.1, the following relationship is developed:-

$$A_i = A_1 + \sum_{j=2}^{i} \Delta A_{j-1} \qquad \text{(A-2.2)}$$

and $$Z_i = Z_1 + \sum_{j=2}^{i} \Delta Z_j \qquad \text{(A-2.3)}$$

(b) Considering the tube element i, between the surfaces i and i+1, the die-tube surface area dA_{ci} and the plug-tube surface areas dA_{si} and dA_{el} are calculated. The change in cross-sectional area over the element i, ΔA_i is also determined.

A-2.1.2 DEVELOPMENT OF THE RECURSIVE EQUATIONS TO EVALUATE THE DRAW STRESS AND THE MEAN PRESSURE

Starting frcm the inlet plane surface i = 1, and assuming no backpull (σ =0), the stress on the surface i=2 can be determined from the equilibrium equation (3.11). The calculated value of is used to determine a^, etc.

From Figure A-2.1, $a_{zi} = a_{z1} + \sum_{j=2} \Delta a_{zj-1}$, (A-2.4)

The equilibrium equation (3.111) applied to the element i can be conveniently re-written as

A(Y I / $A_i + \Delta A_i$ { − (!zi) ΔA_i + (1 −{ − £ / Y }) Y

($K_{c2} M_{c2}(i) + K_{si} \Delta A_{s1}(i) + K_{c1} \Delta A_{c1}(i)$) } (A-2.5)

vhere

K_{si} = (μ_m cosα_s − sinα_s) = constant 1 (A-2.6)

K_{c1} = (μ_m cosα_c − sinα_c) = constant 2 (A-2.7)

K_{c2} = (μ_m cosα+sinα) = constant 3 (A-2.8)

Example:

Starting at $Z_{i=1}$ = 0 where the conditions of stress are known fz1 / Y = 0), the change of stress over element i=1 can be determined;

A(!f i) = {,(0)AA i + (1 _(0))

^ s ^ + Kcl AAcl(1) + KC2 AAC2(1»

which yields A ($\frac{\sigma_{z1}}{Y}$).

But (rf) = (J5i) + = A (^)

Therefore,

^ (A^AA$_2$) {-Zf<> +

(Ks1 Ms1(2) +Kc1 AAc1(2) +KC2 MC2(2))

which yields A($\frac{\sigma_{z2}}{Y}$) etc.

The mean pressure at the die-tube (or plug-tube) interface can be calculated from the total normal force for elements i=1, 2, ____ NL divided by the total die-tube surface area. For the element (i), the normal force NF^Ci) at the die-tube interface is given by:

$$NF_1(i) = P_{mi}(AA_{c2}(i)) \qquad (A-2.9)$$

$$V = (1 -(!5i)) \qquad (A-2.10)$$

Therefore, the total normal force for elements i=1, 2, 3, NL is

NF, NL-1 . a .
£ ^ ("f)> AA^i) (A-2.11)

The dimensionless pressure ratio becomes

& = ! V^Y
E4A$_{o2}$(i)

a ,
E (1 - H|i)}M$_{c2}$(i)

ZAA$_{c2}$(i)

a ,
Z (-~~f±) AA~~ $_2$~~(i)~~
= 1 _ {____1 9£ ; (A-2.12)
ZAA$_{c2}$(i)

The expression for the mean pressure at the plug-tube interface is

3. , E (A-2.13)
Z(AA$_{c1}$(i)+AA$_{s1}$(i))

A-3 COMPUTER PROGRAMMES

A-3.1 UPPER BOUND SOLUTION FOR POLYOONAL DRAWING

```
      TRACE 2
      MASTER UBFPTD
C      UPPER BOUND SOLUTION FQR POLYGONAL TUBE DRAWING
      DIMENSION PL(IO),A(10),AT(!0),ER(10),X(10),Y(IQ),XA(11,11),
     1YAd1, 11) ,ARLT3(10) ,ARSTB(10),ARLTACi10),ARSTA(10),XBCL(11,11),
     2Y8CL(11,11),X3CS(11,11),YBCS(11,11),KACL(11,11),fACL(11,11),
     3XAC5(11,11), YACS (11,11), KB(11,11),YB(11,11),RAS(11,11),
     4R8S (11,11), THETAS(11,11),DAS(11,11),PHISBA(11,11),ZS(11,11),
     5ZTS(11,11),ETAS(11,11) ,HETALC (11,11) ,RAL11,11),
     6RBL(11,11),0BL(11,11) ,DAL(U,11),PHILBA(U,11) ,ZL(11f11),
     7ZTL(11,11) ,PSIS( 11,11) ,HETASC(11,11),PSIL(11,11),
     IDBS(11,U) ,THETAL( 11,11),ETAL( 11,11)
      4RITE(2.10)
   10 FORMAT</5X,'UPPER BOUND SOLUTION FOR POLYGONAL TUBE DRAWING )
      t»RITE(2,20)
   20 FORMAT(5X,'SOLUTION FOR SQUARE HEXAGON AND OUODECASON)
C      STOCK OUTER QIAMETER=9OB,PftQOUCT OUTER OIAMETER=DOA GAUSE=TB
C      FRICTION COEFFICIENT=MU
      #RITE(2,30)
   30 FORMAT(5X, DOB,DOA AND TB ARE FIXED')
C      INPUT STATEMENTS
      READ(1,31)DOB,OOA,TB
   31 FORMAT(3F0.0)
      DI3=QGB-(2.0*T8)
      ROB-OOB/2.0
      ROA=DOA/2.0
      RIB=0tB/2.0
      PI=3.1415927
C      GENERATE NUMBER OF SIDES OF SECTION REQUIRED BY GENERATING BETA
      DO 100 I3ETA=15,45,15
      *RITE(2,40) IBETA
   40 FORMAT(5X, 'BETA5',14)
      BETA=PI*BETA/130.0
      C8ETA=COS(BETA)
      SBETA=SIN(BETA)
      T8ETA=TAN(BETA)
      TB2=T8ETA**2
      T84=T82»2
      TB8=TB4«2
      T828=1.0/TB2
      TB18=1.0/TBETA
      SPAR=CBETA*SBETA*P I / < 4.0*6ET A)
C      CALCULATE SECTION PARAMETERS I.E.AA,A8,AR,ETC
      HA=0i3
```

```
      AB=PIt|(ROB**2MRI8"2))
      AA*PI*RQA*t2-HA**2*SPAR
      R£3SQRT(ROft**2-(AA/PI))
      AR-AB/AA
      RED-1.0-1.0/AR
      RA=HA/2.0
      ¥RITE(2,42> HA,RE,TB,ftED
   42 FORMAT(21,4F10.5)
C     RADIUS OF INSCRIBED CIRCLE AT EW(RAI)
      RAI=HA》CBETA/2.0
C     SINGLE SYHHETRIC SECTION USED TO SAVE COMPUTER TI*E,DENOTED
C     HEREAFTER BY 'DOUBLE! SYMMETRIC
C     BAND THE INLET (DOUBLE)SYHIIETRIC INTO .1-1 EQUAL
C     SECTORS AND MP OUTLET rfITH N-2 HYPERBOLIC CURVES,(I,J)
C     DEFINES GENERAL INTERSECTION AND (I.DDENOTES THE ORIGIN
      M=10
      M=10
C     FIRST CURVE OF OUTLET CIRCULAR SECTION CORRESPONDS TO THE
C     DIE ,PL!I) REFERS TO THE POSITION OF HYPERBOLA VIRTUAL ORIGIN
C     ALONG LINE OF SYMMETRY AND A(I) IS THE FOCAL LENGTH
      TA=ROH-RA
      PL(I>=DOA/2
      PL(10)=0.0
C     TA IS THE THICKNESS OF SECTION ALONG TUBE DIAGONAL AND IS
C     DIVIDED INTO N-2 EQUAL LENGTHS
      DT=(TA*¥ROA*(<1.0/CBETA)-1.0>))/(N-2)
C     INCLUDED AREA OF THE DIE AT(I),ATi10) CORRESPONDS TO THE
C     ORIGIN
      AT(1)=0.0
      AT(10)=PI*(ROA《2)/(2.0*PI/BETA)
      ER(1)=ROB
      ER(10)=0.0
C            DETAILED HAPPIN6 STARTS HERE ittUUMtt
      DO 305 1=2,N-I
      PL(I)=(ROA/CBETA)-((I-1)*DT)
      A(I)~(i.0-I.0*I/N)*5.00
C     CALCULATE CO-ORDINATES AT INTERSECTION OF HYPERBOLA AND
C     LINE INCLINED TO(DOUBLE) BETA BY THE YA-AIIS
      IF(IBETA,EQ,45) GO TO 55
      T(I)=(-PL<I)》T84*SQRT(PL(I)**2》T88*(1.0-T84)*(A(I)**2*PL(I)*》2
     I*TB4)M/U.0-TB4)
      GO TO 56
   55 X(I)=(PHI)《2+A(I>**2)/I2.0*PL(I))
   56 Y(I)=TBETA*<-XiI><-PLH))
```

```
C      CO-ORDINATES OF INTERSECTION TO 5L3AL IA-YA AXES
       V=X(I)
       K»Y(I)
       *A<1,H)=«
       YA(I,N)=-VfPL(I)
C      AREA ENCLOSED 3Y HYPERBOLA 1 AND THE DIE I=DENOTED 3Y AT CI)
       ATU) = i2.0»T3&TAf((K/2.0US8RT(yu2*Am«2»T328)<-A(I)«2
      1*Q.5*T828*(AL06(W+SfIRT(H*»2*A(I)f*2»TB2B)))-A(I)"2*0.5*TB2B
      2*ALQ6(A(I)tRBIB))MBETA*DOA**2/4.0)*(VH2fT3ETA)-(PL(I)
      3TBETA)))
C      AREA ENCLOSED BY THE DIE AND THE CURVE REFERRED TO THE INLET
       A8T=AT(I)*AR
C      EQUIVALENT RADIUS AT INLET ER(I)
       ER(I)=SGRT(DO8»*2/4.0-ABT/BETA)
C      AREA OF THE BAND AT INLET ENCLOSED BY THE CIRCULAR ARC I t i-I
       ABAND=(ER(I-I)»2-ER(I>**2HBETA/2.0
C      DIVIDE THE AREA OF THE 3ANO INTO fI-1 EQUAL SECTORS AND ALSO
C      CALCULATE THE RADIAL MIDTH OF SAND
       A8CD=ABAND/(M-1)
       DR=€R(I-I)-&R(n
       DPHIJ=BETA/(H-1)
C      CALCULATE AREAS OF LARGE AND SHALL TRIANGLES AT INLET PLANE
       DD=0.5*OR«2*DPHIJ
       ARLT8(11=0.5*(ABCD*DD)
       AfiSTB(I)=0.5*(A8CO-OD)
C      EQUIVALENT TRIANGULAR AREAS AT EXIT PLANE
       ARLTA(I)=ARLT8(I)/AR
       AfiSTA(I)=ARSTB(I)/AS
C      INTERSECTION OF HYPERBOLA I AND YA-AIIS
       <A(I,I)=0.0
       IF(I3ETA.E9.45) GO TO 107
       YAR3=(PL(I)+SQRT(PL(I)"2-(1.0-TB4)*(PLiIJ"2-A(I)«2)))/
      HCBETAM1.0-TB4))
       YAR4=(PL(I)-SQRT(PL(I)**2-(1.0-TB4)*(PL (I)**2-A(1)»*2I))/
     · 1(C8&TA*(1.0-TB4))
       IF <YAfi3.LT.VAR4) SO TO 103
       YA(I,1)=YAR4
       GO TO 305
 103   YA(I,1)=YAR3
       60 TO 305
 107   YA(I,t)=PL(I)*A(I)
 305   CONTINUE
C      CURVE 1=1 IS A CIRCLE AND CO-ORDINATES OF INTERSECTION HITH
C      LINE INCLINED AT SETA TO YA-AHS CAN 3E FOUND
```

```
      YAU,M)=(DOA/2)《SSRTII.0/U.OfTB2)>
      KA(1,11>*fAU,ft)*T9£TA
      YA(1,1)=ROA
      XAtI,I)=0.0
      XAiI0,10)=0.0
      YAUO,10)=0.0
      HRITE(2,70>
   70 FORMAT(SX, LIHITIN6 CO-QftOIMATES AT EXIT PLANE ,11)
      iiRITE(2,7I) (XA(I,N),1=1,N)
      *RITE<2,71) <YAC1,H>,1*1,M>
   71 FORNAT(2X,10(2X^,6),/)
C     CO-ORDINATES OF TRIANGLES AT INLET
      OO 310 I=I,N-I
      DO 315 .3=I,11
      PH1J*(J-1)*BETA/(H-1)
      X8!I,J)=ER(I)*SIN(PHiJ)
      YB(I,J)=ER(D*COS(PHIJ)
  315 CONTINUE
  310 CONTINUE
C     LOCATE CENTRGIOS OF LARGE AND SHALL TRIANGLES AT INLET
      DO 320 1*1,(1-2
      DO 325 .j=I,H-I
      XBCL(If1,Jf1)a(X8(I,J)fX8(If1,J)fXB(I,Jf1))/3.0
      YBCL(1f1,Jf1)=<YB(I,J)fYB(If1fJ)fYB(I,Jf1))/3.0
      XBCSi!fI,JfI>=aBU*I,J)*<B(IfI,JM>《-XBiI,JfI))/3.0
      Y3C3(I+t,JfI)=(YB(IfI.JWBdM,MIfYB(I,Jft)>/3.0
  325 CONTINUE
  320 CONTINUE
      80 TO 503
C     CALL FOR A FRESH PAGE TO PRINT RESULTS
      WRITE(2,350)
  350 FORMAT<1HI)
C     PRINT CO-ORDINATES OF INLET TRIANGLES AND EQUIVALENT RADIUS
      WRITE(2,352)
  352 FORMAT(5X, VALUES OF XB,YB AT INLET PLANE AND EQUIVALENT
     IRADIUS ER'/)
      《RITE(2,353>
  353 FORMAT(2X, 1=',5X,'J=I',7X,'J=2',7X, J3',7X,'J=4',7X, 3=5 ,
     17X,'J=6',7X, J=7',7X,'J=8',7X,'J=9',7X, J=10',2X,'E9 RADIUS',
     2/)
      DO 370 1=1,N
      *RITE(2,355)KI,(XBiI,J),J=t《M),ERU)>)
      JjRITE(2,356)(YB(I,J),J=I,i1)
```

```
  355   FORNAT(2X,I2,10(2X,F8.4),2X,F9.4)
  356   FORHAT(7X,10(2X,F9.4>>
  370   CONTINUE
C        CENTftOIDS OF TRIANGLES AT INLET AND RESPECTIVE AREAS
        MRITE(2,3591
  359  FORMAT(//5X,'VALUES OF IBCS,YBCS,XBCL,Y8CL AND AREAS OF
       ITRIAN6LES',/)
        DO 375 1=2,N-I
        *RITE(2,3560>(I,(XBCS(IJ),J=2,?I),ARST8(H))
        MRITE(2,3561)(YBCS(I,J),J*2,!f)
        #RITE(2,3560)(I,(KBCL(IJ),J2,i1),ARLTI(I)))
        WRITE(2,3561)tYBCL(I,J),J=2,M)
  3560  FOR«AT(5X,I2,8X,?(2X,F8.4),2X,F8.4)
  3561  FQRf!ATi!5X,9t2X,F8.4))
  375   CONTINUE
C        NAPPING CORRESPONDING TRIANGLES AT EXIT PLANE
  503   AZERO=0.0
        DO 330 1=1,N-2
        DO 335 J=1,N-1
C        NAPPING LARGE TRIANGLES
        AREAL=AftLTA(IH)
        XI«A(I,J)
        YI-YA(I,J)
        X2XA(I+1,J)
        Y2*YA(H-I,J)
        IF(I.ST.I) SO TO 97
        IF(J.EQ.i) GO TO 72
        Df11(2.0*AREAL-(XI*Y2-YUX2))/(X2-XI)
        DK1=(Y1-Y2)/(X2-X1)
        X3R1»(COW1«DK1)*SQRT((SHt*OK11"2-U1.0^Wtl«*2)ttDHI**2
       1-ROA«2))))/<!.0*DKt«2)
        X3R2((DMfrDKI)-SQRT((DM*DK1)«2-€€I-O+DK1«2)*(DM»2
       I-ROA**2))))/It.0*OKIH2)
        Y3RI=CM-DK1*X3R1
        Y3R2=OM-DKi*X3R2
C        SELECT CO-ORDINATE OF THIRD VERTEX
        IFU3Ri.6T.X3R2) GO TO 75
        YA(I,J+1)=Y3R2
        (A(I,Jft)=X3R2
        30 TO 76
   75   YA(I,JH)*Y3RI
        XA(I,JM)=X3Ri
   76   GO TO 77
C       NAPPING THE INITIAL LARGE TRIANGLES BY SUBSTITUTING (
```

```
C      AND SOLVING FOR Y
   72  DHI=(2.0*AR&AL-(Y2《1-YUX2)>/(Y1-Y2)
       DKI》(X2-n>/m-Y2>
       Y3R1³(OH1*OK1)*SQRT{(DHIfOKI/1《-2-U1.0*OKU*2)*(DH1》*2
      1-ROA《2)))>/(1.<W)K1M2)
       Y3R2³((OHI*OKI)-SQRT((OHI*DKI)**2-<(I.0+DK1**2)*<OHI*《2
      i-RQA《2)>})/(1.0*OKI《2)
       X3R1=0《I-OK1》Y3《1
       X3R2=DH1-DKUY3R2
C       THIRD VERTEX OF TRIANGLE
       IFIY3R1.ST.Y3R2) 50 TO 78
       XA(I,.M)=X3R2
       YA(I,J+1)ˢY3R2
       SO TO 77
   73  XA<I,J+I)ˢX3RI
       YAiI,JfI)》Y3RI
       30 TO 77
C       HAPPING LARSE TRIANGLES ^HEftE THE THIRD VERTEX LIES ON
C       HYPERBOLA I
C       NAPPING LARGE TRIANGLES SY SUBSTITUTING < AND SOLVE FOR 1
   97  HH1=(2.0*AREAL-(X1*Y2-YI*X2))/(YI-Y2)
       HK1=(X2-X1)/(Y1-Y2)
       HCIˢPL(I)《2-T8I*HNt》*2
       HC2=-2.0*PL(I)+2.0*HK1*HHUTB2
       HC3³1.0-HK1》2》T82
       3QT=SQRT(HC2《*2-4.0*HC3(HC1-A(I)《2))
       Y3LI=(-HC2tSQT)/I2.0fHC3)
       Y3L2=(-HC2-SST)/(2.0*HC3)
       X3LI=ttHI-HKI*Y3LI
       X3L2=HN1-HK1*Y3L2
C       SELECT THE THIRD VERTEX
       IF(Y3LI.LT.Y3L2.AND.X3Li.5T.AZERO) SO TO 112
       XA(I,JH)*X312
       YAiI,J+I)=Y3L2
       50 TO 77
  112  XA(I,J+I)ˢX3U
       YAU,J+I)ˢY3LI
       GO TO 77
C       HAPPIN6 SHALL TRIANGLES AT INLET
  '11  XU=XAIIH,J>
       YU*YAU*I,J>
       X22=XA(I,J+1)
       Y22=<A(L,JH>
       AREAS=ARSTA(I+1)
```

```
      FNIs(2.OAREAS-(YIUX22-Y22》XIt)I/(X!i-X22>
      FK1=(Y22-Y11)/ (X11-X22)
      C3=FK1《2=TB2
      C2--2.O*FH1*FKI+2.O*FKI*PL(IH>
      CI=FMI》*2*PL (I+I)《2-2.O*PL(I)»FM
      SQT》SSRT(C2》2-4.Otf3*(Ct-A(!*I)**2I)
      X3SI-(-C2+SQT)/(2.O#C3)
      X3S2=<-C2-3QT>/(2.O+C3)
      Y3SI FNI-FKI*X3SI
      Y3S2=FIU-FKIfX3S2
C       SELECT THIRD VERTEX
      IF(X3S2.LT.X3S1.QR.X3S2.6T.AZERO)  80 TO 91
      XftU+t,J+I)=X3St
      YA(I*I,J+I) Y3SI
      50 TO 335
  91  XAU*I,JM)*X3S2
      YA(U*I,J*I)*Y3S2
 335  CONTINUE
 330  CONTINUE
C       LOCATING THE CENTROIOS OF THE HAPPED TRIANGLES AT EXIT PLANE
      DO 340 1=1,N-2
      DO 345 J=1,K-1
      XACL(I+M+1)=<XA(IfJ)*XA(I,J+IKXA<IM,J)>/3.0
      YACLUM J*I)=(*A<I,J)*YA(I,JM>*YA(I*M)>/3.0
      XACS(IMfJMMXA(M,J)*XA(I*1,J*1>*XA(I,J*1))/3.0
      YACSiM,JfI)=(YA(IM,J)+YA(Ifi,JfI)<'YA(I,JfI)>/3.0
 345  CONTINUE
 340  CONTINUE
      SO TO 504
C       CALL FOR A FRESH PASE TO PRINT RESULTS
      *RITE(2,349)
 349  FORMAT(1Hi)
C       PRINTOUT FOR EXIT PLANE
      *RITE(2,3565)
3565  FOPNAT(//5X,'VALUES OF XA,YA AND FOCAL DISTANCE A(I) OF
     IHYPERBOIA I',/)
      *RITE(2,353)
      A(10)=0.0
      AtU*ROA*(1.0/CBETA-i.0)
      DO 380 1=1,N
      *R!TE<2,355M(I,(XA(I,J=M>,A<1))>
      *RITE(2,356)(YA(M》,J M>
 380  CONTINUE
      《RITE(2,3570)
```

```
3570 FORMAT(//5X, VALUES OF IACS.YACS.XACIJACI AMD AREAS OF
     ITRIN6ALE3',/)
     DO 385 1=2, N-I
     *ftITE(2,3560()U,UCASU,J),J»2,H),ARSTAU)>>
     WfiITE(2,356IMYACS(I,J),J=2,M)
     KRtTE(2,3560)((I,(XACL(I,J),J=2,M),ARLTA(I)))
     HRITE(2,356I) (YACIiI,J),J=2,R)
385  CONTINUE
C     PER CENTA6E ERROR IN AREA OBTAINED FROM MAPPING AND ACTUAL
C     VALUE AA
     AS8=AA/(PI/BETA)
     ERRCR=((ASB-AT(N-I)I/ASB)*100.0
     WRITE(2,3571)ERROR
3571 FORMAT(//5X,'PERCENTAGE DIFFERENCE OF TOTAL (-SECTIONAL AREA
     Is',f8.4,//>
C     《*$*$**$ END OF CONFORiIAL MAPPING *$$W$ms
C   ttttt&ttt   UPPER BOUND SOLUTION NO* BEGINS  MfcttttM
504  WRITE(2,400)
400  FORMAT I//,5X,'i*ttfc  UPPER 3OUND SOLUTION BEGINS HERE  Itttit')
C     GENERATE THE DIE SEMI ANGLE
     DO 200 IALPHA=2,13,4
     ALPHA=<Pf/180.0)HALPHA
     TAD»TAN(ALPHA)
     DIEH-(RQB-ROA)/TAD
     ALPHAE=ATAN(RIB-ftE)/DIEH)
     ALFAEM180.0/PI)ALPHAS
C     CALCULATIONS OF THE RADIAL DISTANCE OF THE PARTICLES AND
C     DIFLECTIQN ANGLES PSI,XI,ETA,...ETC AND LENGTH OF FLOW PATH
     CAD=COS(ALPHA)
     SAD=SIN《ALPHA)
     TAE=TAN(ALPHAE)
     CAE=COS(ALPHAE?
     SAE=SIN(ALPHAE)
     RH08=OIEH»ROB/ICAD*(RGB-ROA)
C     CALCULATIONS FOR THE SHALL TRIANGLES AT EIIT(A) AND ENTRY(8)
     DO 405 I=2,N-I
     DO 410 d=2,M
     RAS(I,Ji=SQftT(KACS(I,J)》》2*YACS(I,J)"2)
     RBSii.J)=SQRT(I8CS(I,J)"2+YBCS(I,JI"2)
     THETAS(I,J)=ASIN(R8S(I,J)/RHQ8)
     PHIA=ATAN()(ACS(I,J>/YACS<I,J>>
     DB=RHO8Mi.O-CAO)
     BET2=2.0*BETA
     DBS(I,J)=RHOB*(COS(THETAS(I,J))-CADi
     DA=DB
```

```
      IF(PHIA.ST.BETA) 50 TO 402
      DAS(I,J)=0AHQ0A/(2.0*RAS(U)*CQ3<PHIA)1-1.0)
      80 TO 403
403I DAS(I,J)'Oft*(DOA/(2.0*RAS(I,J)*COS(BET2-PHIA))-1.0)
    i  PHI8=ATAN(X8CS(I,j)/Y5CS(I,J))
      PHISBA(I,Ji=PHIB-PHIA
      ZSIt,J)=D[EH*D8SiI,J)-DAS(I,J)
C        TOTAL LENGTH OF PLOW PATH IN DEFORMING ZONE
      ZT3(I,J)=S6RTC(XBC5(I,J)-XACS(1,J)>  YBC3Ct,J)-
     IYACSfI,J))*》2+ZS(I,J)**2)
      ZPS=SQRT((R3S(I,J)-RAS!I,J)*CQS<PHISBA(I,J)))§*2*
     IZS(!,J)》2)
      ETASiI,J)=ATAN(RA3(I,J)*SIM(PH1S8A(I,J)I/ZPS)
      HETASC(I,J)=ATAN((RBS(I,J>-RAS(I.J)*CGS(PHISBA([,J)
     I))/ZS(I,J)>
      PSIS(I,J)=A8S(HETALC(I,J)-THETAS11,J)>
410  CONTINUE
405  CONTINUE
C        CALCULATIONS FOR THE LARGE TRIAN6LE3 AT EKIT(A) AND ENTRY(8)
     ·00 415 1=2,N-I
      DO 420 J=2,.i
      RAL(I,J i=SQRT(KACL(I,J)**2+YACL(I,J)**2)
      R8L(I,J)=SfiRT(XBCL(I,J)《2+YBCL(I,J)《2)
      THETAL(I,J)=ASIN(RBL(I,J)/RHO8)
      DBL(I,J)=ROB*(COS(THETALiI,J))-CAD)
      PHIA=ATAN(XACL(I,J)/YACL(I,J)I
      IF<PHIA.ST.BETA) 50 TO 406
      DAL'.I,J)=DA*(OOA/(2.0*RAL(I,J)*COS(PHIft))-1.0)
      SO TO 407
406  DAL(I,J)=DA*<DOA/(2.0*RAL(I,J)*COSi8ET2-PHIA)-1.0)
407  PHIB-ATAN(XBCL(£,J>/Y8CL(I,J)>
      PHILBA(I,J)=PHI8-PHIA
      ZL'I,J)=DIEH*D3L!I,J)-DALiJ.I,J)
(        TOTAL LENGTH OF FLOW PATH IN DEFORMING ZONE
      ZTL(I,J)=S8RT((X8CL(I,J)-J(ACL(I,J))**2Mf8CL(I,J)-
     IYACLU,J))《2*ZL(I,J>《2)
      ZPL=SQRT{(RBL'I,J)-RAL(I,J)*CGSiPHILBA(I,J)I)*》2*
     IZL(I,J)**2)
      ETAL(I,J)=ATAN(RALU,J)《SIN{PHILBA(I,J>)/ZPL>
      HETALC(E,J>=ATAN(RBLi£,J>-RAL(I,J>》COS(PHILBA(E《J)))
     I/ZL(I,J)>
      PSIL<I,J>sA8S(HETALC11,J)-THETAL(I,J))
420  CONTINUE
415  CONTINUE
      SO TO 18
```

```
      WRITE(2,408>
  408 FORMAT(5X,"LENGTH OF FLOW PATH IN THE DEFQMIIN6 ZONE ITS
     I,ZTL',/)
      rfRITE(2,353)
      DO 425 I»2,N-I
      NRITE(2,411) (I, (ZTSU,J),J°2,H))
      WRITE(2,4t2)(ZTL(I,J),J=2,M)
  411 FORMAT*5X,I2,3X,?<3X,F8.*))
  412 FORMAT(15X,9(3X,F9.4>)
  425 CONTINUE
C      OPTIMIZATION OF SHEAR WORK IE VALUE OF T THAT MINIMIZES
C      SHEAR WORK FACTOR R(S)
   18 MR1TE(2,413)
  413 FORMAT(51,'PARAMETER T SHEAR FACTOR R(S)',/I
C      GENERATE T BETWEEN 0 AND 1
      DO 430 IT=1,10
      MTifI.I
      TP=I.0-T
      RS=0.0
      DO 460 I=2,N-I
      DO 465 j=2,H
C      VALUE OF RS FOR SMALL TRIANGULAR ELEMENTS
      AR&AS=ARST8-:n
      THETA=THETAS(I,J)
      ETA=ETAS(I,J)
      P3I=PSI5(I,J)
      RSSF=SQRT((COS<WHETA*TAN(ETA)/(COS(TPHHETA)HAN(PSI
     I)))**2+(-SIN(T*THETA)*COS(T*THETA)*TAN(PSI)《-CGS(T*TKETA
     2>*TAN(TP*THETA>>**2>
      RSS-(RSSF*(2.0»PI/8ETA)/A8)*AAftEAS/COS(T*THETA)
C      VALUE OF RS FOR SMALL TRIANGULAR ELEMENTS
      AREAL=ARLT9(Ii
      THETA=THETAL(I,J)
      ETA=ETAL!I,J)
      PSI=PSIL(I,J)
      RSIF=SQRT(ICOS(T*TKETA)tTAN(ETA)/(CQS(TP*TH£TA)*TAN(PSI
     1)))<2M-SINiT*THETA)^COS(T*THETA)»TAN(PSI)^COS(T*THETA
     2)<TAN(TP*THETA>)**2)
      RSL*(RSLF*(2.0*PI/BETA)/AB)*AREAI/CQS(T*TH&TA)
      RS=RS*RSL*RSS
  465 CONTINUE
  460 CONTINUE
      HRITE(2,414)T,RS
  414 FORMAT(9X|F5.,3,8X,F10.6)
      S5V-RS
```

```
      IF(IT.EQ.1)  60  TO  416
C1      SELECT  MINIMUM  SHEAR  FACTOR
      IF(RSV.LT.RSH)  60  TO  416
      60  TO  430
 416  RSN°RSV
      TM=T
 430  CONTINUE
      *RITE(2,4t7)TM,RSM
 417  FORMAT1//,5)(,  OPTIMAL  T=    F5.3,5X,  AND  MINIMUM  RS=',
     IF10.6//)
      T=TM
      RS=RSM
      TP=I.0-T
C       CALCULATE  SHAPE  FACTOR  FS  US IMS  OPTIMAL  T  FOR  INTERNAL
C       PGNER  OF  DEFORMATION
      C1=PI*SAD**2
      C2=RI8/SA0
      C3-PI*RIB**2
      RH08D0=RHOB**2CI-C3
      RHOA=RHOB*RQA/ROB
      FS=0.0
      00  435  1=2,N-I
      DO  440  J=2,M
C       VALUE  OF  FS  FOR  SMALL  TRIANGULAR  ELEMENTS
      AREAS=ARST8(I)
      THETA=THETAS(I,J)
      HETA=HETA3C(I,J)
      ETA=ETAS(I,J)
      ZDIE=ZS(I,J>
      PS1=PSIS(I,J)
      RAD=RAS(I,J)
      PHI=PHISBA<I,J)
      RHOE=(RHOB-ZS(I,J)]*COS(THETA)
C       DIVIDE  (RHOB-RHOA)  INTO  10  ELEMENTAL  LENGTHS
      ORHG='RHOA)/I0.0
      DO  445  IRHO=1,9
      RHO=RHOA*(DRHO*IRHO!
      RHOD='RHO-RHO8)*TAE/TAD
      RHOOD=CI*(RHQ《2-(C2*RHOD)《2)
      ft1=(2*CI*fiHO/RHODD)*(RHO-(C2+RHOD)*iRHQO/(RHO-RHOB)>)
      R2=2.0*RU*2
      R3=(-(1.0+TAN(PSI)》(-T》TAN(T》THETA)tTP*TAK(TP《THETfI)
     I+(1.0/(COS(PSI))))))《2
      R4=(1.0*RAD*COS(PHI)/((RHOB-RHOE)·COS(THETA)fSIN(THETA)
     I·COS(PSI>)HAN!PSI)/TANUHETA))《2
```

```
      R5= (-T AW <PSI) -ft I *TAN (PSI)-TtTAII (T*THETA)    (TP*
     ITHETA)))**2
      R6 (-U TAN(ETA)/TAN(PSI))* 1-1 J)/TAN(THETA) -T *TAN I T»
     ITHETA) +TAN(THETA) «-TPHANHP»THETA) *TAN(PST)))) " 2
      R7=(<TAN(ETA)/TAN(PSI))t11.0*R1))»2
      ROQTK=S9RT(R2fR3+R4*R5*R6*R7>
      ROQTKS=ROQTK*RHO*ORHO/RHODD
      FSS=RQGTKS*AREAS>CQS! THHETA) / COS (TP»THETA)
C      VALUE OF FS FOR LAPSE TRIANGULAR ELEMENTS
      AREAL=ARLT6(I)
      THETA=THETALtI,J)
      HETA=HETALC(I,J)
      ETA=£TAL(I,J)
      PSI=PSIL(I,J)
      ZDIE=ZL(I,J)
      PHI=PHIL3A(I,J)
      RAD=RAL(J,J)
      RHOE=( RHG8-ZL(I,J)) *CQS (THETA)
      S3= (=(1.0+TAN(PSI/•(-T »TANIT *THE TA)+TP*THETA)
     I*(t.0/<CQS(PSI>)>)))>«2
      S4= (1.0*RAD*COS(PHI)/((RHOB-RHQE)«CQSTITHETA)*SIN(THETA)
     I *COS (PS I)) *TAN (PS I) / TAN (THET A)) **2
      55*((-TAN(PSI)-R1*TAN(PSI)-T*TAN(T*THETA)*TP*TAN(TP*
     ITHETA)))«2
      S6=((TAN(ETA)/TAN(PSI))*(-1.0/TAN(THETA)-T*TAN(T»
     ITHETA) * TAN(THETA) *TP*TAN(TP«THETA)+TANIPSI)))«2
      S7 ((TAN(ETA)/TAN(PSI))*(1.0+fil)·)*»2
      RQGTK=SQRT(S2fS3<-S4*S5*S6*S7)
      RQQTKL=RGQTK*RHC*DRHO/RHODD
      FSL=ROOTKL*COS(T »THETA) *AR£AL/COS (TP »THETA)
      FS=FS+-FSL+F3S
  445 CONTINUE
  440 CONTINUE
    4 CONTINUE
      *RITE(2,441)FS
  441 FORMAT(5)1,'VALUE OF F(S)=   ¥F10.6,//)
      FS=FS*(PI/8ETA)/(RH08t*2»S6RT(3.0))
C      CALCULATE THE MEAN EQUIVALENT STRAIN(E3STH)
      E9STH=FS>(2.0/SfiRT(3.0))*RS
      *RITE(2,442)E3STN
  442 FORMAT<51, VALUE OF HEAN EQUIVALENT STRAIN*   ',fl0.S»
C      PRINT HEADING FOR FINAL TABLE OF RESULTS
      *RITE(2,443)
  443 FORMAT(7X,'ALPHA',2X,'AL?HAE',5X, RED',, 'NU',3K,'0SR'
     I,7X,'OPR')
```

```
      MITE(2,444)
 444  format(2x, $$$st$mm*t$m*m$sfmtmm*$tf$$s$)
      UA《3.0*25.4
      UB=UA/AR
      VOL=UB*A8
C      TO FIND FRICTION FACTORS II AND 12
      USBARI=UB》CAE《AL08(AR)/RED
      USBAR2<UB+UAJ»CAD/2.0
      D& R18*8ETA/(IH)
      0A32=iBETA/2.0)*CAD*(R08*RHOB-ROA*RHCA)
C      GENERATE COEFFICIENT OF FRICTION(0,0.02,.....0.II
      DO 450 ICOEFF=0.10,2
      CMU=ICOEFF*0.01
      Fli-O.O
      FI2=0.0
C      INTEGRATE EXPRESSIONS OVER PLUS-TUBE INTERFACE
      DO 455 J=I, 11-1
      THETA=THETAL·N-1,J+1>
      DOEu=Sfi?.T(iIA(N-I,jH)-j(A(N-I,J))《2MYA':N-I,JH)-
     1YA(N-1,J))《2)
      OASI=0.5*(DE*DDE!)IfZTL(N-I,J*i>
      FII=FII+DASIKCf!U*COS(THETA)-SIN!THETA)J
      FI2=FIH-DAS1
 455  CONTINUE
      FACT1D=(<C«U*CAO+5AD)《DAS2MFI1))/AA
      FACT20=((USBAR1/UB)*F12*(US8AR2/U8)*0AS2)*CNU/AB
      NS=PI/BETA
      FACT1=FACT1D*NS*2.0
      FACT2=FACT2D*NS*2.0
C      ASSUME A TYPICAL VALUE FOR THE *GRK HARDENING FACTOR
      YN=0.232i
      BFACT31.0/(i.O*YNI
C      HENCE DRAW STRESS RATIO AND DIE PRESSURE RATIO CAN
C      BE FOUND
      DSR=EQSTM/(I,0-BFACT*FACT2/FACTIi)
      DPR=EQSTH/iFACrI*U.0-8FACT*FACT2/FACTt))
      HRITE(2,456>IALPHA,ALFAE,KRED,CNLI,DSR,DPR
 456  FORMAT(2X,I8,F10.4,I3,3FI0.4i
 450  CONTINUE
 300  CONTINUE
 200  CONTINUE
 100  CONTINUE
      STOP
      END
      FINISH
```

A-3.2 LOWER BOUND SOLUTION FOR POLYGONAL DRAWING

```
      TRACE 2
      MASTER LBFPTD
C      LOWER BOUND SOLUTION FOR POLYGONAL TUBE DRAHIK6
C      PRCGRAM CALCULATES LOfcER BOUND BY NUMERICAL INTEGRATION
      KRITE(2,10)
  10  FORMAT(//,5K,'LONER BOUND SOLUTION FOR POLYGONAL TUBE DRAHIN6',//)
      «RITE(2.20
  20  FORMATI//,5X,'SOLUTION FOR SQUARE HE(A60N AND DUODECAGON',//>
C      STOCK OUTER O1AMETER=OG3 PRODUCT OUTER OIAMETER=OOA 3AU6E=TB
     t COEFF=MU
      WRITE(2,30)
  30  FORMAT(2X,'DOB,DOA AND TB ARE FIXED')
C      INPUT STATEMENTS
      READ(1,33)DOB,DOA,TB
  33  FORMAT(3F0.0)
      0IB=DOB-(2.0*TB)
      ROB=DOB/2.0
      ROA=DQA/2.0
      RIB=DI8/2.0
C      DIE ANGLE=ALPKA PLU6 EQUIVALENT AN6LE=ALPHAE DIMENSIONLESS STRESS
     I RATIO=DSR DIE PRESSURE RATIO=')Pfi
      PI=3.1415927
C      GENERATE NUMBER OF SIDES OF SECTION REQUIRED BY GENERATING BETA
      DO 100 18&TA$15,45,15
      WRITE(2,40)2BETA
  40  FOFMAr(2X,'BETA=',I6)
      BETA=P1^IBETA/100.0
      CBETA=COS(BETA)
      S8ETA=SIN(BETA)
C      CALCULATE SECTION PARAMETERS I.E.AA,AB,AR,HA,5PAfi,ETC
      HA=0I8
      AB=PHM(RQB》2HRiB**2))
      SPAR》C8ETA*S6ETA*Pi/(4.0tBETA)
      AA=PI*ROA**2-HA《2*SPAR
      Aft-AB/AA
      RED-1.0-1.0/Aft
      RE=SfifIT(RQA**2-(AA/PI))
      *RITE(2,43)HA,RE,TB,RED
  43  FGRMAT2X,4F 10.5
C      PRINT HEADING FOR FINAL TABLE OF RESULTS
      *RITE(2,50)
  50  FORMAT(7X,' ALPHA',2X,'ALPHAE',6X,'MU',IX,'DSR',
     17X,'DPR')
      《RITE(2,70)
  70  FORMAT (2X,   tt$$$t$f$$Sti$$U$ti$S$$$$ft$99t*$$iitSS$$$$tS$tf$$   >
```

```
C      GENERATE THE DIE SEMI-ANGLE
      DO 225 IALPHA=2,22,4
      ALPHA* (PI/180.0) HALPHA
      TAD=TAN(ALPHA)
      CAD=COS(ALPHA)
      5AD=SIN(ALPHA)
      DIEH=(RQ8-RQA)/TAO
      ALPHAE=TAN((RI9-RE)/DIEH)
      ALFAE=(130.0/PIi *ALPHAE
      TAE=ThN(ALPHAE>
C      CALCULATE CONICAL ANO FLAT SURFACE ANGLES
      ALPHAC=ATAN(DI3-HA)/(2.')*DIEH))
      ALPHAS=ATAN( iOI9-(HA》C&ETA)) /(2.0*DIEH))
C      CONSTANTS FOR THE ELLIPSE
      CAC=COSIALPHAC)     '
      CAS=COS(ALPHAS)
      SAC=SIN(ALPHAC)
      SAS=SIM<ALPHAS)
      TAC=TAN(ALPHAC)
      TAS=TAN(ALPHAS)
      8=RIB* (1.0/SIN(ALPHAC+ALPHAS)) *S&RT( (CAC) **2-<CAS) 《2
      A-RIB* <CAC/SIN(ALPHAOALPHAS))
C      NUMERICAL INTEGRATION OF THE DRAW STRESS
C      ACCUMULATIVE SURFACE AREA OF DIE 13 9SURFA
      DSURFA=0.0
C      FOR NO BACKPULL THE NORMAL STRESS AT INLET PLANE IS ZERO
      DSR=0.0
C      EVALUATE FRICTION CONSTANTS KS1,KC1 AND KC2
      DO 425 KCQEFF=0,t0,2
      COEFF=KCOEFF/100.0
      S1=(COEFF*CAS)-3AS
      CI=(COEFFtCAC)-SAC
      C2*(COEFF《CAO)*3AO
C      DIVIDE DIE LENGTH INTO 50 E3UAL LENGTHS
      NL=5I
C      ACCUMULATE PRODUCT OF DSRI AND DIE SURFACE AREA
      DSRSF=0.0
      DZ=DIEH/(NL-1)
      A11=0.5*8ETAMRO8-R18)KRQ8*-RI&)
      DO 500 I=2,NL,1
      ZI=(M)*OZ
      RIL=RQ8-(ZItTAD)
      RIS=RI8-(ZI*TAC)
C      Y VALUE ON THE ELLIPSE
      YI=8*S6RT(2.0*A*ZI*CAS-(ZI**2))/(A*CAS)
```

```
C       INLCUDED ANGLE FOR THE CONICAL AND FLAT SURFACE ALONG Z-AXIS
        AHBOAS°ATAN((YI/R(S)/§QfIT(I.d-((Y[/RIS)t*2))>
        AMBDAC=BETA-AM8DAS
        CAMS=COS!AHBDAS)
        SAMS=SIN(AMBDASI
C       AREA AT SECTION ZONE
        AI=0.5*(RIL《2)*BETA-(0.5*(RIS"2)KICAI1S*SA《)>AHBOAC)
C       CHANGE Of CROSS-SECTIONAL AREA OVER ELEMENT I
        P1=(CAMStSAMS)·AHBDAC
        P2°A>CAMS*CAS*RIS
        P3=RIS*((A*CAS)-ZI)
        P4=2.0*A*ZUCAS-(ZI《2)
        P6=<A《BOAS《-ANBI>AC)》RIL》TAD
        P7=(SAHS《2》*B/P2
        DAI=(RIS*((P1《TAC)MIP7)K(P3/SQRTIP4))MP4《TAC))))-P6)《DZ
        80 TO 76
   75   DAI=AI-A11
C       CALCULATE SURFACE AREA OF ELEMENTS
   76   DAStI-(YI*DZ>/CAS
        DACII=(RIS*AMSOACtOZ)/CAC
        DAC2I=(RIL*BETA*DZ)/CAD
C       ACCUMULATE SURFACE AREA OF DIE
        DSURFA=DSURFA+DAC21
        PSURFA=OSURFA+DAC11<-DAS11
C       OMENSIONLESS STRESS RATIO
        SKI=(SUDA3II)*<CUQACIIi《-(C2*DAC2I)
        D3RI=(1.0/ (AI*DAI))*((-9SR*DAiM(1.0-DSR)*(SKI))>
        DSR3F=DSRSFMDSRI*&AC2I)
C       STRESS ON THE SECOND FACE BECOMES STRESS FOR FACE ONE OF
C       ELEMENT I+I
        DSR=DSR*DSRI
        AII-AI
  500   CONTINUE
        DPR=1.O-IOSRSF/OSURFA)
        NRITE (2,600)IALPHA,ALFAE,COEFF,DSR,DPR
  600   FQRHAT《2X,I9,F10.4,3Ft0.4)
  425   CONTINUE
  225   CONTINUE
  100   CONTINUE
        KRITE(2,800>
  S00   FORMAT(//v2X,'END OF LOWER BOUND SOLUTION")
        STOP
        END
        FINISH
```

A-3.3 UPPER BOUND SOLUTION FOR AXISYVMETRIC DRAWING

```
      MASTER UBFAO
C       UPPER BOUND SOLUTION FOR CORRESPONDING AXISVMMETRIC CASE
        KRITE(2,15>
   15  FGRMAT(//,2X, UPPER BOUND SOLUTION FOR AXISYNHETRIC DRAWING',//)
£       DIMENSIONS FOR INCOMIN6 TUBE AND PROCESSED PRODUCT
c       TUBE QD IS D01 GAUGE(TI) PRODUCT OD IS 002 M FRICT FACTER FACT
        D0 1=0.0296
        D02=0.0254
        T1=0.004064
        PI=3.1415927
        ROI=001/2.0
        R02=DG2/2.0
        RI1=RQ1-TI
§       PRINT HEADING FOR FINAL TABLE OF RESULTS
        HRITE(2.10)
   20  FORMAT(//,5X,'IALPHAD',4X, ALPHAP',5X, RED',4^,'1U'DSR',
      I7X,'DPR')
C       GENERATE THE DIE AND PLUG SEMIANGLE
        DO 30 IALPHA=4,16,4
        DO 40 <RED=5,50,5
        DO 45 IFACT=2,10,2
        FACT=IFACT/100.0
        ALPHAO=(PI》'130.0)*IAL?HA
        TAD=TAN(ALPHAD)
        CAD=CQS(ALPHAD)
C       CALCULATE GEOMETRICAL PARAMETERS AI A2 AR DIEH RED
        DIEH=(R01-tfG2)/TAD
        AR=100.0/(100.0-KRED)
        AI=PI*t(RGI《2)-iRU**2))
        A2=A1/AR
        RI2=S8RT<(R02**2)-(A2/PI))
        ALPHAP=ATAN(<RII-RI2)/DIEH>
        ALFAPO°(180.0/PI)*ALPHAP
        CAP=COS(ALPHAP>
        TAO=TAN(ALPHAD)
        IF IRI2.6T.RII.OR.RI2.GT.RQ2) GO TO 40
        IF (ALPHAP.ST.ALPHAD) 30 TO 40
C       NCK SOLVE THE DRAM STRESS EQUATION
        HI=ROI-ftli
        H2*fiQI》2-RII《2
        H3=R02-RI2
        H4=R02《2-RI2**2
        H5=<R0t《3-RI2《3)/3.0
        H6=(R02883-RI2H3)/3.0
```

```
      H7》(RQ2*TADMR12*TAP)
      H8='RQ1*TAD)-(R11*!AP)
      H9=(RII*TAD)-(ROI*TAP)
      HI(MRI2HADMRO2tTAf>
      FI*(RQ1《-RIU/(IHI2*R[2)
      F2°((1.0/(tCAO)《*2))·(!.')/UCAP)w2>)I
      H*=ALQ6(H2/H4)M(1.0/6.0)*ALOG<(H2/H41M(H7/H9)《2)1)
      S《Is(2.0/SQRT(3.0)》(H2″2i)*((H5»(-He)>HR01*R11»H1*H9))
      SH2》(2.0/SQRT(3.0)》(H4《2I)K(H6*(-H7»)MRO2*RI2»«3tH1O))
      FW°(FACT/SQRT(3.0))*(ALQ6(H1/H3)/(TAD-TAP)-(A106(F1)/(TAD*
     1TAP)))*F2
      DSR=HH+SM1+SH2+FM
      DPR°1.0-OSR
C      PRINT THE RESULTS
      WRITE(2.50)IALPHA,ALFAPO,KRED,FACT,BSR,DPR
   50 FQRMAT(2X,I3,F10.4,I8,3F10.4)
   45 CONTINUE
   40 CGNTINUE
   30 CONTINUE
      WRITE(2,60)
   60 FORMAT(5X,'END OF UPPER 3OUNO SOLUTION')
      STOP
      END
      FINISH
```

A-3.4 LOVER BOUND SOLUTION FOR AXISYMMETRIC DRAWING

```
      TRACE 2
      MASTER L8FAO
      *R1TE(2,10)
 10   FORMAT(//,5X,'LOWER BOUND SOLUTION FOR AXISYNMETRIC DRAN1N6',//)
C      DIMENSIONS FOR INCOMIN6 TU8E ANO PROCESSED PROOUCT
C      STOCK OUTER RADIUS IS ROB PRODUCT O R IS KOA MU IS COEFF
C      SAU6E=TI STOCK INNER RADIU5=RI8 PRODUCT INNER RADIUS=RIA
      RQB=0.0143
      RQA=0.0127
      TH16=0.375*0.0254
      R18=RQ8-THI8
      PI=3.1415927
      WRITE(2,20)
 20   FORMAT(//,5X,'ALPHAD",5X, RED',4X, MU',3X,'DSR',
     17X,'DPR')
      DO 30 IALPHA=4,20,4
      DO 40 KRED=15,50,2
      DO 45 ICOEFF=2,LO,2
      COEFF³ICOEFF/I00.0
      ALPHAD=(P1/130.0)*IALPHA
      QIEH》(RQB-RQA)/TAN(ALPHAD)
      AR-100.0/(100.0-KRED)
      A9=PI*((ROB**2)-iRI3**2))
      AA=AB/AR
      RI ASSORT((ROA**2)-IAA/PI))
      ALPHAP=ATAN((RI8-RIA)/DIEH)
      ALFAPO®(180.0/P t)*ALPHAP
      THIA=ROA-RIA
      IF (RIA.3T.R18.OR.RIA.ST.ROA) 50 TO 40
      IF (ALPHAP.ST.ALPHAD) SO TO 40
C      CALCULATE DRAW STRESS RATIO ANO DIE PRESSURE RATIO
      B= (2.0tCOEFF)/<TAN(ALPHAD)-TAN(ALPHAP))
      DSR°((1.0+8)/8)*II.0-UTHIA/THI8)**B>)
      DRPM.0-DSR
      IWITE (2,50) I ALPHA, ALFAPD,KRED, COEFF. DSR. DPS
 50   FORNATI2X,I8,Ft0.4,I8,3F10,4)
 45   CONTINUE
 40   CONTINUE
 30   CONTINUE
      WRITE(2,60)
 60   FORMAT(5X, END OF LOWER BOUND SOLUTION)
      STOP
      END
      FINISH
```

TABULATED SAMPLE SOLUTIONS OF THE UPPER AND
LOWER BOUND FOR POLYGONAL AND AXISYiWETRIC
DRAWING

TABLE A-4.1.1 THE CPPER AND LOWER BOUND SOLUTIONS FOR THE DRAWING OF HEXAGONAL TUBE FROM ROUND THROUGH A CYLINDRICAL DIE ON A POLYGONAL PLUG

INPUT TUBE SIZE: 28.6 mm O.D. x 9.52 mm THICKNESS
REDUCTION OF AREA: 21.61%
OUTPUT TUBE SIZE 25.4 mm O.D.

	/-v	Upper bound			Lower bound	
0) rt 1 I) •r-t Sbi MO c a 3	M-d 3 w rH (J) a. a C t-i UW hO 3 § > I ffl	a (V ;d a 1) o -H -U a i ^ £ O	Mean draw stress/yielci stress (σ_{za}/Y_m)	.Vfean die pressure/ yield stress (p/Y) tn	Mean draw stress/yield stress (σ_{za}/Y_m)	Mean die pressure/ yield stress
2	0.54	0.02 0.04 0.06 0.08 0.10	2.0661 2.3101 2.4587 2.5648 2.6484	3.9779 2.8578 2.2407 1.8501 1.5809	0.6077 0.9416 1.1501 1.2298 1.2309	0.9964 0.9978 0.9990 0.9997 1.0000
6	1.63	0.02 0.04 0.06 0.08 0.10	1.0401 1.1411 1.2194 1.2833 1.3374	3.1860 2.7135 2.3696 2.1083 1.9031	0.5314 0.8204 1.0749 1.2701 1.3971	0.9971 0.9981 0.9987 0.9992 0.9996
LO	2.73	0.02 0.04 0.06 0.08 0.10	0.3062 0.8531 0.3936 0.9306 0.9647	2.9125 2.7252 2.5635 2.4226 2.2987	0.5147 0.7879 1.0426 1.2614 1.4333	0.9973 0.9982 0.9987 0.9991 0.9994
L4	3.86	0.02 0.04 0.06 0.08 0.10	2.1694 2.3269 2.4614 2.5789 2.6837	7.4811 6.7690 6.1917 5.7145 5.3137	0.5073 0.7728 1.0260 1.2538 1.4467	0.9974 0.9982 0.9987 0.9991 0.9994
18	5.02	0.02 0.04 0.06 0.08 0.10	2.4043 2.5088 2.6064 2.6983 2.7853	8.7732 8.3968 8.0570 7.7488 7.4681	0.5031 0.7641 1.0159 1.2484 1.4533	0.9974 0.9983 0.9987 0.9991 0.9993

TABLE A-4.1.2 THE UPPER AND LOWER BOUND SOLUTIONS FOR THE DRAWING OF HEXAGONAL TUBE FROM ROM) THROUGH A CYLINDRICAL DIE CN A POLTOCNAL PLUG

INPUT TUBE SIZE: 26.99 mm O.D. x 8.89 mm THICKNESS
REDUCTION OF AREA: 10.66%
OUTPUT TUBE SIZE: 25.4xrm O.D.

			Upper bound		Lower bound	
Q) r SP T" ffl an •iHV QC	3 li→ D as D l CrV^ j M ils f g i-3'gg . a ᴓ	C a> •H a. O •H C «H O «H -H 8 o	Mean draw stress/yield stress (a_{za}/Y_m)	Mean die pressure/ yield stress	Mean drav stress/yiel<i stress (a_{za}/Y_m)	Mean die pressure/ yield stress (p/Y_m)
2	1.05	0.02 0.04 0.06 0.08 0.10	3.2388 3.6601 3.9212 4.1097 4.2595	13.0959 9.5102 7.5060 6.2271 5.3409	0.3088 0.5424 0.7636 0.9369 1.0498	0.9980 0.9984 0.9989 0.9993 0.9996
6	3.16	0.02 0.04 0.06 0.08 0.10	0.5355 0.5920 0.6367 0.6738 0.7055	3.4268 2.9569 2.6078 2.3385 2.1245	0.2541 0.4136 0.5793 0.7396 0.S848	0.9986 0.9989 0.9992 0.9994 0.9995
10	5.29	0.02 0.04 0.06 0.08 0.10	0.4945 0.5328 0.5663 0.5962 0.6233	3.4965 3.2183 2.9860 2.7891 2.6202	0.2427 0.3841 0.53C9 0.6767 0.8158	0.9987 0.9991 0.9993 0.9994 0.9995
14	7.46	0.02 0.04 0.06 0.08 0.10	0.5024 0.5313 0.5582 0.5833 0.6070	3.6041 3.4441 3.3002 3.1702 3.0522	0.2376 0.3710 0.5066 0.6463 0.7801	0.9987 0.9991 0.9993 0.9994 0.9996
18	9.68	0.02 0.04 0.06 0.08 0.10	1.3719 1.4254 1.4767 1.5261 1.5737	10.7605 10.4497 10.1618 9.8943 9.6454	0.2348 0.3635 0.4956 0.6282 0.7583	0.9988 0.9991 0.9993 0.9995 0.9996

TABLE A-4.1.1 THE CPPER AND LOWER BOUND SOLUTIONS FOR THE DRAWING OF HEXAGONAL TUBE FROM ROUND THROUGH A CYLINDRICAL DIE ON A POLYGONAL PLUG

INPUT TUBE SIZE: 26.99 mm O.D. x 8.89 mm THICKNESS
REDUCTION OF AREA: 8.15%
OUTPUT TUBE SIZE: 25.4 mm O.D.

			Upper bound		Lower bound	
[illegible]	[illegible]	[illegible]	Mean draw stress/yield stress (σ_{za}/Y_m)	Mean die pressure/ yield stress (p/Y_m)	Mean draw stress/yield stress (σ_{za}/Y_m)	Mean die pressure/ yield stress
2	2.34	0.02	3.9176	16.4255	0.2550	0.9983
		0.04	4.4468	11.9934	0.4709	0.9986
		0.06	4.7769	9.4961	0.6847	0.9989
		0.08	5.0157	7.8949	0.8602	0.9993
		0.10	5.2056	6.7820	0.9814	0.9996
6	7.02	0.02	2.2232	14.6811	0.1986	1 0.9989
		0.04	2.4637	12.7423	0.3336	0.9991
		0.06	2.6554	11.2872	0.4792	0.9993
		0.08	2.8148	10.1558	0.6250	0.9994
		0.10	2.9520	9.2517	0.7617	0.9995
10	11.66	0.02	2.3528	17.0116	0.1868	0.9990
		0.04	2.5361	15.7551	0.3C23	0.9992
		0.06	2.6980	14.6926	0.4259	0.9994
		0.08	2.8433	13.7831	0.5522	0.9995
		0.10	2.9755	12.9962	0.6760	0.9996
14	16.27	o.ce	3.5528	26.3100	0.1816	0.9990
		0.04	3.7628	25.1762	0.2883	0.9993
		0.06	3.9584	24.1542	0.4013	0.9994
		0.08	4.1416	23.2285	0.5172	0.9995
		0.10	4.3144	22.3868	0.6324	0.9996
18	20.83	0.02	3.5060	27.6629	0.1787	0.9991
		0.04	3.6813	26.6545	0.2804	0.9993
		0.06	3.8469	25.7351	0.3871	0.9995
		0.08	4.0041	24.8939	0.4964	0.9996
		0.10	4.1542	24.1218	0.6058	0.9996

TABLE A-4.1.1 THE CPPER AND LOWER BOUND SOLUTIONS FOR THE DRAWING OF HEXAGONAL TUBE FROM ROUND THROUGH A CYLINDRICAL DIE ON A POLYGONAL PLUG

INPUT TUBE SIZE: 26.99 rnn O.D. x 7.93 mm THICKNESS
REDUCTION OF AREA: 10.24%
OUTPUT TUBE SIZE: 25.4 mm O.D.

		Upper bound		Lower bound	
[illegible]	[illegible]	Mean draw stress/yield stress (σ_{za}/Y_m)	Mean die pressure/ yield stress	Mean draw stress/yield stress (σ_{za}/Y_m)	Mean die pressure/ yield stress
2 1.27	0.02 0.04 0.06 0.08 0.10	2.8058 3.1259 3.3152 3.4507 3.5594	10.8644 7.4976 5.7596 4.6996 3.9863	0.3090 0.5506 0.7754 0.9453 1.0498	0.9980 0.9984 0.9989 0.9993 0.9996
6 3.81	0.02 0.04 0.06 0.08 0.10	0.4839 0.5347 0.5727 0.6031 0.6287	3.1570 2.6138 2.2384 1.9637 1.7542	0.2478 0.4083 0.5757 0.7369 0.8814	0.9986 0.9989 0.9992 0.9994 0.9995
10 6.37	0.02 0.04 0.06 0.08 0.10	0.6869 0.7423 0.7886 0.8286 0.8640	5.0665 4.5139 4.0796 3.7297 3.4418	0.2349 0.3752 0.5216 0.6671 0.8054	0.9987 0.9991 0.9993 0.9994 0.9995
14 8.87	0.02 0.04 0.06 0.08 0.10	0.7468 0.7927 0.8337 0.8710 0.9053	5.6508 5.2568 4.9212 4.6322 4.3808	0.2283 0.3604 0.4965 0.6329 0.7654	0.9988 0.9991 0.9993 0.9995 0.9996
18 11.63	0.02 0.04 0.06 0.08 0.10	0.7300 0.7644 0.7966 0.8270 0.8557	5.4422 5.2103 5.0012 4.8119 4.6397	0.2261 0.3519 0.4818 0.6125 0.7407	0.9988 0.9992 0.9993 0.9995 0.9996
22 14.35	0.02 0.04 0.06 0.08 0.10	3.1558 3.2763 3.3920 3.5032 3.6105	9.4421 8.8023 8.2062 7.6498 7.1295	0.2240 0.2240 0.4722 0.5989 0.7239	0.9988 0.9992 0.9994 0.9995 0.9996

TABLE A-4.1.7 THE UPPER AND LOWER BOUND SOUUTIOTS FOR THE DRAWING OF OCTAOCNAL TUBE FRCM ROUND THROUGH A CYLINDRICAL DIE ON A POLYGONAL PLUG

INPUT TUBE SIZE: 31.75 mm O.D. x 9.52 mm THICKNESS
REDUCTION OF AREA: 39.56%
OJTFUT TUBE SIZE: 25.4 mm O D.

		Lower bound	
Mean draw stress/yield stress	Mean die pressure/ yield stress	Mean draw stress/yield stress	I Mean die pressure/ yield stress
		1.0980	0.9941
		1.3702	0.9982
		1.3654	1.0000
		1.2859	1.0003
		1.2226	1.0002
		1.0511	0.9946
		1.4762	0.9972
		1.7089	0.9988
		1.7642	0.9998
		1.7097	1.0002
		1.0389	0.9947
		1.4979	0.9969
		1.8244	0.9984
		1.9991	0.9993
		2.0419	0.9999
		1.0333	0.9948
		1.5071	0.9968
		1.8812	0.9981
		2.1300	0.9990
		2.2541	0.9996
		1.0301	0.9948
		1.5122	0.9968
		1.9151	0.9980
		2.2132	0.9988
		2.3989	0.9994
		1.0279	0.9948
		1.5155	0.9968
		1.9378	0.9979
		2.2710	0.9987
		2.5041	0.9992

TABLE A-4.1.1 THE CPPER AND LOWER BOUND SOLUTIONS FOR THE DRAWING OF HEXAGONAL TUBE FROM ROUND THROUGH A CYLINDRICAL DIE ON A POLYGONAL PLUG

INPUT TUBE SIZE: 31.75 mn O.D. x 9.52 mm THICKNESS
REDUCTION OF AREA: 35.94%
OUTPUT TUBE SIZE: 25.4 mm OS).

r		Upper bound		Lower bound	
[illegible]	[illegible]	Mean draw stress/yield stress (σ_{za}/Y)	Mean die pressure/ yield stress (p/Y)	Mean draw stress/yield stress	Mean die pressure/ yield stress (p/Y)
2 0.81	0.02	5.9384	5.2951	1.0071	0.9944
	0.04	6.4796	3.5707	1.2958	0.9980
	0.06	6.7877	2.7065	1.3187	0.9999
	0.08	7.0030	2.1877	1.2551	1.0G03
	0.10	7.1726	1.8418	1.1989	1.0002
1 6 2.43	0.02	2.2836	3.4704	0.9411	0.9951
	0.04	2.4819	2.8015	1.3432	0.9973
	0.06	2.6242	2.3560	1.5803	0.9988
	0.08	2.7349	2.0383	1.6564	0.9997
	0.10	2.8260	1.8004	1.6259	1.0001
11O 4.08	0.02	1.7829	3.o463	0.9246	0.9952
	0.04	1.9053	2.7233	1.3474	0.9972
	0.06	2.0032	2.4059	1.6597	0.9984
	0.08	2.0848	2.1590	1.8400	0.9993
	0.10	2.1551	1.9617	1.9009	0.9998
J14 5.76	0.02	2.3474	4.4302	0.9171	0.9953
	0.04	2.4748	3.9861	1.3482	0.9971
	0.06	2.5833	3.6289	1.6973	0.9982
	0.08	2.6780	3.3354	1.9394	0.9990
	0.10	2.7625	3.0903	2.0718	0.9996
18 7.48	0.02	3.3003	6.4454	0.9127	0.9954
	0.04	3.4435	5.9495	1.3483	0.9971
	0.06	3.5706	5.5312	1.7192	0.9981
	0.08	3.6853	5.1740	2.0016	0.9989
	0.10	3.7903	4.8653	2.1866	0.9994
22 9.28	0.02	5.9063	11.7439	0.9099	0.9954
	0.04	6.1130	11.0431	1.3482	0.9971
	0.06	6.3023	10.4310	1.7337	0.9981
	0.08	6.4774	9.8918	2.0444	0.9987
	0.10	6.6409	9.4136	2.2692	0.9992

TABLE A-4.1.7 THE UPPER AND LOWER BOUND SOUUTIOTS FOR THE DRAWING OF OCTAOCNAL TUBE FRCM ROUND THROUGH A CYLINDRICAL DIE ON A POLYGONAL PLUG

INPUT TUBE SIZE: 37.75 mm O.D. x 9.52 am THICKNESS
REDUCTION OF AREA: 40.96%
OUTPUT TUEE SIZE: 25.4 mm O.D.

			Upper bound		Lower bound	
[illegible]	[illegible]	[illegible]	Mean draw stress/yield stress (σ_{za}/Y_m)	Mean die pressure/ yield stress (p/Y_m)	Mean draw stress/yield stress (σ_{za}/Y_m)	Mean die pressure/ yield stress (p/Y_m)
2	0.20	0.02	2.4639	1.9868	1.1341	0.9940
		0.04	2.6750	1.3357	1.3992	0.9982
		0.06	2.7946	1.0107	1.3834	1.00C1
		0.08	2.8780	0.8159	1.2977	1.0003
		0.10	2.9436	0.6862	1.2319	1.0002
6	0.62	0.02	0.8747	1.2001	1.0951	0.9944
		0.04	0.9463	0.9650	1.5290	0.9971
		0.06	0.9974	0.8094	1.7594	0.9988
		0.08	1.0370	0.6988	1.8062	0.9998
		0.10	1.0695	0.6162	1.7420	1.0002
10	1.03	0.02	0.7882	1.2627	1.0848	0.9945
		0.04	0.8306	1.0871	1.5581	0.9968
		0.06	0.8805	0.9565	1.8897	0.9983
		0.08	0.9143	0.8556	2.0617	0.9993
		0.10	0.9434	0.7753	2.0969	0.9999
14	1.46	0.02	0.7574	1.3125	1.0800	0.9946
		0.04	0.7971	1.1725	1.5708	0.9967
		0.06	0.8305	1.0612	1.9545	0.9981
		0.08	0.8595	0.9708	2.2055	0.9990
		0.10	0.8852	0.8959	2.3258	0.9996
18	1.90	0.02	0.7445	1.3567	1.0772	0.9946
		0.04	0.7763	1.2410	1.5779	0.9967
		0.06	0.8042	1.1451	1.9933	0.9979
		0.08	0.8291	1.G643	2.2973	0.9988
		0.10	0.8518	0.9953	2.4828	0.9994
22	2.37	0.02	0.7388	1.3976	1.0754	0.9946
		0.04	0.7648	1.3002	1.5826	0.9966
		0.06	0.7883	1.2168	2.0194	0.9978
		0.08	0.8C09	1.1447	2.3613	0.9986
		0.10	0.8298	1.0817	2.5972	0.9992

TABLE A-4.1.8 THE tPPER AND LOWER BOUND SOLUTIONS FOR THE DRAWING OF OCTAGONAL TUBE FRCM ROUND THROUGH A CYLINDRICAL DIE ON A POLYGONAL PLUG

INPUT TUBE SIZE: 26.99 inn O.D. x 8.89 mm THICKNESS
REDUCTION OF AREA: 11.63%
CUIPUT TUBE SIZE: 25.4 run O.D.

[illegible]	[illegible]	[illegible]	Upper bound: Mean draw stress/yield stress « W V	Upper bound: Mean die pressure/ yield stress <P/*m> m	Lower bound: Mean dray/ stress/yield stress « W	Lower bound: LMean die pressure/ yield stress < p / V
	0.59	0.02	1.9488	7.7633	0.3300	0.9979
		0.04	2.2017	5.0491	0.5704	0.9984
		0.06	2.3587	4.4634	0.7942	0.9989
		0.08	2.4721	3.7053	0.9666	0.9993
		0.10	2.5621	3.1793	1.0762	0.9996
	1.78	0.02	0.5471	3.4408	0.2760	0.9985
		0.04	0.6044	2.9708	0.4451	0.9989
		0.06	0.6498	2.6214	0.6185	0.9991
		0.08	0.6874	2.3515	0.7844	0.9993
		0.10	0.7196	2.1369	0.9329	0.9995
1O	2.99	0.02	0.4234	2.9498	0.2646	0.9986
		0.04	0.4560	2.7135	0.4163	0.9990
		0.06	0.4845	2.5163	0.5721	0.9992
		0.08	0.5100	2.3493	0.7255	0.9994
		0.10	0.5330	2.2063	0.8705	0.9995
14	4.22	0.02	0.4928	3.4992	0.2597	0.9986
		0.04	0.5211	3.3397	0.4035	0.9990
		0.06	0.5475	3.1966	0.5507	0.9993
		0.08	0.5721	3.0676	0.6969	0.9994
		O.1O	0.5952	2.9509	0.8380	0.9995
18	5.501	0.02	0.7526	5.2569	0.2569	0.9987
		0.04	0.7856	5.1423	0.3961	0.9991
		0.06	0.8174	5.0336	0.5383	0.9993
		0.08	0.8480	4.9306	0.6800	0.9994
		0.10	0.8776	4.8327	0.8181	0.9995

TABLE A-4.1.9 THE UPPER A>D LOWER BOUND SOLUTIONS FOR THE DRAWING OF SQUARE TUBE FROM ROUND THKXXH A CYLINDRICAL DIE ON A POLYGONAL PLUG

LWT TUBE SIZE: 26.99 rm O.D. x 7.62 mn THICKNESS
REDUCTION OF AREA: 5.61%
OJTPtrr TUBE SIZE: 25.4 mn O.D.

			Upper bound		Lower bound	
[illegible]	[illegible]	[illegible]	Mean draw stress/yield stress (σ_{za}/Y_m)	Mean die pressure/ yield stress ($\bar{p}/Y$)	Mean **draw** stress/yield stress (σ_{za}/Y_m)	Mean die pressure/ yield stress ($\bar{p}/Y$)
2	2.99	0.02	14.9998	60.6583	0.2160	0.9984
		0.04	16.7400	41.5045	0.4324	0.9986
		0.06	17.7631	31.7552	0.6498	0.9989
		0.08	18.4973	25.8551	0.8258	0.9993
		0.10	19.0892	21.9046	0.9438	0.9996
6	8.92	0.02	2.9367	20.3027	0.1487	0.9991
		0.04	3.2575	16.7174	0.2679	0.9992
		0.06	3.4957	14.2646	0.4030	0.9993
		0.08	3.6858	12.4826	0.5424	0.9994
		0.10	3.8455	11.1307	0.6752	0.9996
10	14.75	0.02	3.4550	26.9145	0.1345	0.9992
		0.04	3.7438	23.9277	0.2297	0.9994
		0.06	3.9846	21.5898	0.3369	0.9995
		0.08	4.1917	19.7116	0.4504	0.9995
		0.10	4.3746	18.1711	0.5646	0.9996
14	20.42	0.02	3.6085	28.9524	0.1283	0.9993
		0.04	3.8394	26.8472	0.2126	0.9994
		0.06	4.0449	25.0647	0.3062	0.9995
		0.08	4.2308	23.5371	0.4056	0.9996
		0.10	4.4011	22.2143	0.5072	0.9997
18	25.89	0.02	1.7363	14.5340	0.1248	0.9993
		0.04	1.8280	13.7299	0.2028	0.9995
		0.06	1.9123	13.0245	0.2884	0.9996
		0.08	1.9904	12.4012	0.3790	0.9996
		0.10	2.0634	11.8469	0.4721	0.9997
22	31.11	0.02	6.1123	57.1004	0.1226	0.9993
		0.04	6.4033	53.9408	0.1965	0.9995
		0.06	6.6714	51.1712	0.2766	0.9996
		0.08	6.9208	48.7251	0.3612	0.9997
		0.10	7.1550	46.5507	0.4483	0.9997

TABLE A-4.1.10 TOE UPPER AND LOWER BOUND SOLUTION FOR THE DRAWING OF HEXAGONAL TUBE FRCM ROUND THRCUCH A CYLINDRICAL DIE ON A POLYGONAL PLUG

INPUT TUBE SIZE: 26.99 mm O.D. x 7.62 mm THICKNESS
REDUCTION OF AREA: 10.06%
OUTPUT TUBE SIZE: 25.4 mm O.D.

			Upper bound		Lower bound	
[illegible]	[illegible]	[illegible]	Mean draw stress/yielci stress (a za/V	Mean die pressure/ yield stress m	Vie an draw stress/yield stress (a za/Y m)	.Mean die pressure/ yield stress <p>V
1 2	1.34	0.02 0.04 0.06 0.08 0.10	28.8523 31.9847 33.8099 35.1168 36.1707	110.0514 74.5862 56.7769 46.0763 38.9433	0.3089 0.5534 0.7795 0.9479 1.0492	1 0.9980 0.9984 0.9989 0.9993 0.9997
6	4.03	0.02 0.04 0.06 0.08 0.10	0.4803 0.5305 0.5673 0.5964 0.6208	3.1629 2.5766 2.1824 1.8995 1.6868	0.2452 0.4G60 0.5740 0.7356 0.8797	0.9986 0.9989 0.9992 0.9994 0.9995
10	6.73	0.02 0.04 0.06 0.08 0.10	0.5961 0.6449 0.6850 0.7191 0.7491	4.4833 3.9419 3.5265 3.1979 2.9318	0.2317 0.3715 0.5177 0.6631 0.8011	0.9987 0.9991 0.9993 0.9994 0.9995
14	9.48	0.02 0.04 0.06 0.08 0.10	0.7169 0.7620 0.8018 0.8376 0.8702	5.5640 5.1190 4.4341 4.1653	0.2258 0.3560 0.4915 0.6274 0.7593	0.9988 0.9991 0.9993 0.9995 0.9996
18	1.2.27	0.02 0.04 0.06 0.08 0.10	0.7696 0.8069 0.8415 0.8738 0.9041	5.9033 5.5993 5.3304 5.0910 4.8767	0.2225 0.3471 0.4762 0.6061 0.7335	0.9988 0.9992 0.9994 0.9995 0.9996

TABLE A-4.1.11 THE UPPER AND LOWER BOUND SOLUTIONS POR THE DRAWING OF OCTAGONAL TLBE FROM ROUND THROUGH A CYLLVDRICAL DIE ON A POLYGONAL PLUG

INPUT TLBE SIZE: 26.99 mm O.D. x 7.62 mm THICKNESS
REDUCTION OF AREA: 11.78%
OUTPUT TUBE SI2Z: 25.4 mm

			Upper bound		Lover bound	
[illegible]	Equivalent plug semi-angle α_e (degrees)	[illegible]	Mean draw stress/yield stress <°za/V	Mean die pressure/ yield stress	Mean draw stress/yield stress (σ_{za}/Y_m)	Mean die pressure/ yield stress
2	0.76	0.C2 0.04 0.06 0.08 0.10	1.8572 2.0586 2.1763 2.2605 2.3282	6.9106 4.7019 3.5858 2.9129 2.4634	0.3458 0.6013 0.8303 0.9953 1.0900	0.9976 0.9983 0.9989 0.9993 0.9997
6	2.26	0.02 0.04 0.C6 0.08 0.10	4.3332 4.7807 5.1096 5.3702 5.5884	27.6833 22.6025 19.1729 16.7043 14.8441	0.2836 0.4609 0.6418 0.8119 0.9602	0.9984 0.9988 0.9991 0.9993 0.9995
10	3.81	0.02 0.04 0.06 0.08 0.10	0.5139 0.5555 0.5897 0.6188 0.6443	3.7612 3.3068 2.9582 2.6824 2.4590	0.2706 0.4280 0.5896 0.7475 0.8947	0.9985 0.9989 0.9992 0.9994 0.9995
14	5.38	0.02 0.04 0.06 0.08 0,10	0.5190 0.5515 0.5001 0.6058 0.6291	3.9477 3.6256 3.3579 3.1321 2.9392	0.2648 0.4132 0.5652 0.7156 0.8594	0.9986 0.9990 0.9992 0.9994 0.9995
18	7.00	0.02 0.04 0.06 0.08 0.10	3.2430 3.4008 3.5463 3.6813 3.8090	24.5271 23.2122 22.0548 21.0287 20.1135	0.2615 0.4047 0.5510 0.6965 0.8374	0.9986 0.9990 0.9993 0.9994 0.9995

TABLE A-4.1.12 THE UPPER AND LOWER BOUND SOUTH (US FOR AXISYMMETTUC TUBE DRAWING

INPUT TUBE SIZE: 28.6 mm O.D. x 9.525 nm THICKNESS
REDUCTION OF AREA: VARYING FRCM 15% TO 40%
CUTFUT TUBE SIZE: 25.4 am O.D.

•8		3	Upper bound		Lower bound	
			Mean draw stress/yield stress	Mean die pressure/ yield stress	Mean draw stress/ yield stress (σ_{za}/Y_m)	Jean die pressure/ yield stress (p/Y_m)
7.4450	15	0.0200	0.1322	0.8678	0.1339	0.8661
7.445C	15	0.0400	0.1144	0.8856	0.2284	0.7716
7.445C	15	0.0600	0.0966	0.9034	0.3126	0.6874
7.4450	15	0.0000	0.0788	0.9212	0.3878	0.6122
7.4450	15	0.1000	0.0610	0.9390	0.4548	0.5452
6.0631	20	0.0200	0.2175	0.7825	0.2070	0.7930
6.0531	20	0.0400	0.2142	0.7858	0.3006	0.6995
6.0531	20	0.0600	0.2108	0.7892	0.3834	0.6166
6.0531	20	0.0800	0.2075	0.7925	0.4569	0.5431
6.0531	20	0.1C00	0.2042	0.7958	0.5220	0.4780
4.6962	25	0.0200	0.3077	0.6923	0.2833	0.7167
4.6962	25	0.0400	0.3192	0.6808	0.3755	0.6245
4.6962	25	0.0600	0.3308	0.6692	0.4567	0.5433
4.6962	25	0.0800	0.3424	0.6576	0.5283	0.4717
4.6962	25	0.1000	0.3540	0.6460	0.5912	0.4088
3.3729	30	0.0200	0.4036	0.5964	0.3632	0.6368
3.3729	30	0.0400	0.4306	0.5694	0.4538	0.5462
3.3729	30	0.0600	0.4576	0.5424	0.5330	0.4670
3.3729	30	0.0800	0.4846	0.5154	0.6023	0.3977
3.3729	30	0.1000	0.5116	0.4884	0.6627	0.3373
2.0816	35	0.0200	0.5061	0.4939	0.4474	0.5526
2.0816	35	0.0400	0.5492	0.4508	0.5360	0.4640
2.0816	35	0.0600	0.4576	0.5424	0.5330	0.4670
2.0816	35	0.0800	0.4846	0.5154	0.6023	0.3977
2.0816	35	0.1000	0.5116	0.4884	0.6627	0.3373

TABLE A-4.1.12 TOE UPPER AND LOWER BOUND SOLLTTIONS FOR AXISYWWmiC TUBE DRAWLNG

CONT'D.

8	0.8213	40	0.0300	0.6164	0.3836	0.5366	0.4634
8	0.8213	40	0.0400	0.6765	0.3235	0.6227	0.3773
8	0.8213	40	0.0000	0.7365	0.2635	0.6966	0.3034
8	0.8213	40	0.0000	0.7965	0.2035	0.7599	0.2401
8	0.8213	40	0.1000	0.8565	0.1435	0.8140	0.1800
12	11.1797	15	0.0200	0.1380	0.8620	0.0994	0.9006
12	11.1797	15	0.0400	0.1250	0.8741	0.*I655	0.8345
12	11.1797	15	0.0000	0.1139	0.8861	0.2269	0.7731
12	11.1797	15	0.0800	0.1018	0.8982	0.2838	0.7162
12	11.1797	15	0.1000	0.0898	0.9102	0.3365	0.6635
12	9.1114	20	0.0200	0.2185	0.7815	0.1727	0.8273
12	9.1114	20	0.0400	0.2163	0.7837	0.2384	0.7616
12	9.1114	20	0.0000	0.2141	0.7859	0.2991	0.7009
12	9.1114	20	0.0800	0.2118	0.7882	0.3551	0.5932
12	9.1114	20	0.1000	0.2096	0.7904	0.4068	0.5932
12	7.0823	25	0.0200	0.3009	0.6961	0.2493	0.7507
12	7.0823	25	0.0400	0.3116	0.6884	0.3143	0.6857
12	7.0823	25	0.0000	0.3194	0.6806	0.3741	0.6259
12	7.0823	25	0.0800	0.3272	0.6728	0.4291	0.5709
12	7.0823	25	0.1000	0.3350	0.6650	0.4796	0.5204
12	5.0936	30	0.0200	0.3947	0.6053	0.3296	0.6704
12	5.0936	30	0.0400	0.4128	0.5872	0.3937	0.6063
12	5.0936	30	0.0600	0.4309	0.5691	0.4524	0.5476
12	5.0936	30	0.0800	0.4490	0.5510	0.5061	0.4939
12	5.0936	30	0.1000	0.4671	0.5329	0.5552	0.4448
12	3.1465	35	0.0200	0.4919	0.5081	0.4143	0.5857
12	3.1465	35	0.0400	0.5208	0.4792	0.4773	0.5227
12	3.1465	35	0.0600	0.5497	0.4503	0.5868	0.4132
12	3.1465	35	0.0800	0.5785	0.4215	0.6342	0.3658
12	3.1465	35	0.1000	0.6074	0.3926	0.5042	0.4957
12	1.2420	40	0.0200	0.5966	0.4034	0.5043	0.4957
12	1.2420	40	0.0400	0.6368	0.3632	0.5658	0.4342
12	1.2420	40	0.0600	0.6770	0.3230	0.6214	0.3786
12	1.2320	40	0.0800	0.7172	0.2828	0.6717	0.3283
12	1.2320	40	0.1000	0.7574	0.2426	0.7170	0.2830
16	14.9288	15	0.0200	0.1408	0.8592	0.0814	0.9186
16	14.9288	15	0.0400	0.1316	0.8684	0.1319	0.8681
16	14.9288	15	0.0000	0.1224	0.8776	0.1797	0.8203
16	14.9288	15	0.0800	0.1131	0.8869	0.2248	0.7752
16	14.9288	15	0.1000	0.1039	0.8961	0.2675	0.7325

TABLE A−4.1.12 TOE UPPER AND LOWER BOUND 90LUTC0NS FOR AXISYVMETRIC TUBE DRAWING

CONT'D.

16	12.2061	20	0.0200	0.2191	0.7809	0.1549	0.8451
16	12.2081	20	0.0400	0.2174	0.7826	0.2051	0.7949
16	12.2081	20	0.0600	0.2157	0.7843	0.2524	0.7476
16	12.2081	20	0.0800	0.2140	0.7860	0.2970	0.7030
16	12.2081	20	0.1000	0.2123	0.7877	0.3391	0.6600
16	9.5148	25	0.0200	0.3020	0.6980	0.2316	0.7684
16	9.5148	25	0.0400	0.3079	0.6921	0.2813	0.7187
16	9.5148	25	0.0600	0.3J38	0.6862	0.3281	0.6719
16	9.5148	25	0.0800	0.3197	0.6803	0.3721	0.6279
16	9.5148	25	0.1000	0.3256	0.6744	0.4134	0.5866
16	6.8567	30	0.0200	0.3903	0.6097	0.3121	0.6879
16	6.8567	30	0.0400	0.4040	0.5900	0.3613	0.6387
16	6.8567	30	0.0600	0.4177	0.5823	0.4073	0.5927
16	6.8567	30	0.0800	0.4314	0.5686	0.4505	0.5495
16	6.8567	30	0.1000	0.4451	0.5549	0.4908	0.5092
16	4.2412	35	0.0200	0.4848	0.5152	0.3971	0.6029
16	4.2412	35	0.0400	0.5067	0.4933	0.4455	0.5545
16	4.2412	35	0.0600	0.5285	0.4715	0.4906	0.5094
16	4.2412	35	0.0800	0.5503	0.4497	0.5327	0.4673
16	4.2412	35	0.1000	0.5721	0.4279	0.5720	0.4280
16	1.6753	40	0.0200	0.5867	0.4133	0.4873	0.5127
16	1.6753	40	0.0400	0.6171	0.3829	0.5347	0.4653
16	1.6753	40	0.0000	0.6474	0.3526	0.5787	0.4213
16	1.6753	40	0.0800	0.6778	0.3222	0.6196	0.3804
16	1.6753	40	0.1000	0.7081	0.2919	0.6574	0.3426

A-5 EQUATIONS FOR EQUIVALENT AXISYMMETRIC DRAWING

The corresponding upper bound solution for tube axisymnetrtc drawing {13} is as follows:-

$$\frac{\sigma}{Y_m} \quad \text{Un} \quad \frac{R^2 - R^2.}{R_{oa} - R_{ia}} \quad \frac{i}{\sigma} \quad \frac{R^2. - R^2..}{K_{oa} - K_{ia}} \qquad (3-U2)$$

$$\frac{R\_J* \tan a - R_{ia} \tan 8}{R_{ob} \tan m - R_{ib} \tan B} \;)\} \quad + \quad \frac{Q}{1}{/3} \quad iR db - *lb)^2$$

$$\{ \frac{(R^\wedge - R^\wedge_{ib})}{3} \quad (R_{ib} \tan 8 - R_{ob} \tan a) \; \cdot$$

$$+ \frac{2}{/3} \quad \frac{1}{(R^2_{oa} - R^2_{ia})} \; f) \; o \quad \{ \; \frac{\circ}{3} \quad (R_{i*} \tan 0 - R_{oa} \tan a)$$

$$+ R_{oa} R_{ia} (R_{oa} - R_{ian})(R_{ia} \tan x \;\text{"}\; R_{oa} \tan 6)\}$$

$$\frac{V_{ob} - y}{R - R.} \; , \quad - \quad \ln(! * 3b) \quad a\_\_ + R.$$

$$+ \frac{m_2}{\sqrt{3}} \sec\theta \left\{ \frac{\ln\left(\frac{R_{ob}-R_{ib}}{R_{oa}-R_{ia}}\right)}{\tan\alpha-\tan\theta} \quad \frac{\ln\left(\frac{R_{ob}+R_{ib}}{R_{oa}+R_{oa}}\right)}{\tan\alpha+\tan\theta} \right\}$$

where m_1 and m_2 are constant friction factors on the die-tube and plug-tube interfaces respectively.

α is the mean die semi-angle

θ is the mean plug semi-angle

R_{ob} is inlet tube external radius

R_{ib} is inlet tube bore radius

R_{oa} is outlet tube external radius

R_{ia} is outlet tube bore radius

The corresponding lower bound solution for tube axi-symnetric drawing (6) is as follcws:-

$$\frac{\sigma_a}{Y_m} = \frac{1+B^*}{B^*}\left(1-\left(\frac{t}{*}\right)^{B^*}\right) \qquad (3.113)$$

where $B^* = \frac{\mu_1+\mu_2}{\tan\alpha-\tan\theta}$

μ_1 and μ_2 are the mean coefficients of friction on the die-tube and plug-tube interfaces respectively, a is the mean die semi-angle,

8 is the mean plug semi-angle,

t^ is inlet tube wall thickness,

t_a is outlet tube wall thickness.

The die or plug pressure in both cases is

$$\frac{p}{Y_m} = 1 - \frac{\sigma_a}{Y_m} \tag{3.114}$$